TECHNICAL REPORT STANDARD TITLE PAGE

1. Report No. TX - 99 1735 - 2	2. Government Accession No.	3. Recipient's Catalog No.
4. Title and Subtitle Quality Management of Asphalt-Concrete Layers Using Wave Propagation Techniques		**5. Report Date** July 1999
		6. Performing Organization Code
7. Authors J. Rojas, S. Nazarian, V. Tandon, and D. Yuan		**8. Performing Organization Report No.** Research Report 1735-2
9. Performing Organization Name and Address Center for Highway Materials Research The University of Texas at El Paso El Paso, Texas 79968-0516		**10. Work Unit No.**
		11. Contract or Grant No. Study No. 0-1735
12. Sponsoring Agency Name and Address Texas Department of Transportation P.O. Box 5051 Austin, Texas 78763		**13. Type of Report and Period Covered** Summary Report 4/97 - 7/99
		14. Sponsoring Agency Code

15. Supplementary Notes
Research Performed in Cooperation with TxDOT
Research Study Title: Development of Structural Field Testing of Flexible Pavement Layers

16. Abstract
Highway agencies spend significant amounts of money and time coring and in-situ testing flexible pavements to implement a rigorous quality control/quality assurance program. The quality of the asphalt concrete (AC) pavement is assessed through field inspections, laboratory testing of pavement cores, thickness determinations, and compacted density measurements. To successfully implement a mechanistic pavement design procedure or to develop realistic performance-based specifications, a method of monitoring the modulus of a laid-down AC layer is needed.

The modulus of an AC layer can be either indirectly predicted by using physical and volumetric properties of the mixture, which are measured in the laboratory, or obtained directly from field testing. Seismic nondestructive testing methods can potentially offer an efficient, economical, reliable, and repeatable way of measuring the modulus of AC layers. In addition, seismic methods are the only means of measuring the same moduli in the field and in the laboratory.

In this study, a laboratory method and a field seismic method for determining the modulus of AC layers are introduced, and their instrumentation and theoretical aspects are presented. The impacts of the gradation, asphalt viscosity (asphalt grade), void in total mix, temperature, and thickness of the AC layer on the modulus are introduced. The preliminary protocol proposed for quality management of AC, based on seismic methods, is included.

17. Key Words	18. Distribution Statement		
Quality Control/Quality Assurance, Asphalt Concrete Layer, Seismic Nondestructive Testing	No restrictions. This document is available to the public through the National Technical Information Service, 5285 Port Royal Road, Springfield, Virginia 22161		
19. Security Classified (of this report) Unclassified	**20. Security Classified (of this page)** Unclassified	**21. No. of Pages** 63	**22. Price**

Form DOT F 1700.7 (8-69)

Quality Management of Asphalt-Concrete Layers Using Wave Propagation Techniques

by

Jaime Rojas, MSCE
Soheil Nazarian, Ph.D., P.E.
Vivek Tandon, Ph.D.
and
Deren Yuan, Ph.D.

Research Project 0-1735

Conducted for

Texas Department of Transportation

Research Report 1735-2

July 1999

The Center for Highway Materials Research
The University of Texas at El Paso
El Paso, TX 79968-0516

The contents of this report reflect the view of the authors, who are responsible for the facts and the accuracy of the data presented herein. The contents do not necessarily reflect the official views or policies of the Texas Department of Transportation or the Federal Highway Administration. This report does not constitute a standard, specification, or regulation.

The material contained in this report is experimental in nature and is published for informational purposes only. Any discrepancies with official views or policies of the Texas Department of Transportation or the Federal Highway Administration should be discussed with the appropriate Austin Division prior to implementation of the procedures or results.

NOT INTENDED FOR CONSTRUCTION, BIDDING, OR PERMIT PURPOSES

Jaime Rojas, MSCE
Soheil Nazarian, Ph.D., P.E. (69263)
Vivek Tandon, Ph.D.
Deren Yuan, Ph.D.

Acknowledgments

The authors would like to express their sincere appreciation to Steve Smith of the TXDOT Odessa District for his ever-present support. We would also like to thank the constructive advice from the Project Advisory Team consisting of Roger Cisneros, Lisa Lukefahr, Mike Murphy, Dale Rand, and Dingyi Yang.

We would also like to thank the hardworking people from districts that generously offered their time. Especially, we would like to thank Raymond Guerra of El Paso District and K.C. Evans of Odessa District for arranging the logistics for the field tests.

The authors would also like to thank undergraduates who worked on this project. Specifically, the recognition is extended to Javier Dominguez and Cijifredo Zuniga for their enthusiasm in performing all the necessary tests for this project and their help in the preparation of this report.

Abstract

The benefits of implementing a rigorous quality control/quality assurance (QC/QA) program have become more obvious to many highway agencies and contractors. Highway agencies spend significant amounts of money and time coring to implement this concept. The quality of the asphalt concrete (AC) pavement is assessed through field inspection, laboratory testing of pavement cores, thickness determination, and compacted density measurements.

One of the primary parameters considered in the design of flexible pavements is the modulus of the AC layer. Unfortunately, current quality-management programs are typically not based on this parameter. To successfully implement a mechanistic pavement design procedure or to develop realistic performance-based specifications, a method of monitoring the modulus of a laid-down AC layer is needed. As a result, more quantitative feedback about the pavement structure may be provided to the pavement engineer.

The modulus of an AC layer can be either indirectly predicted by using physical and volumetric properties of the mixture, which are measured in the laboratory, or obtained directly from field testing. Seismic nondestructive testing (NDT) methods can potentially offer an efficient, economical, reliable, and repeatable way of measuring the modulus of AC layers. In addition, seismic methods are the only means of measuring the same moduli in the field and in the laboratory.

In this study, a laboratory method and a field seismic method for determining the modulus of AC layers are introduced, and their instrumentation and theoretical aspects are presented. The impacts of the gradation, asphalt viscosity (asphalt grade), void in total mix (VTM), temperature, and thickness of the AC layer on the modulus are introduced. The preliminary protocol proposed for quality management of AC based on seismic methods is included, and issues yet to be resolved are discussed. Two case studies are also included to demonstrate the potential uses of the methods in "real-life" projects.

In general, it was found that the relationship between the modulus and mix properties established in the laboratory and the seismic moduli measured directly on cores and nondestructively on the pavement models compared closely. In conclusion, this study showed that an economical quality management program for AC pavements, based on the seismic methods presented, might be established.

Implementation Statement

The main goal of this project is to develop the tools and protocols that are needed to conduct quality control and quality assurance associated with different pavement layers. For the asphalt concrete layer, this goal is achieved. However, the equipment and protocols should be evaluated by TxDOT personnel within their districts and divisions.

The necessary tools have been acquired for up to four districts or divisions to implement the developed procedures on a limited basis. The equipment and protocols will be shortly distributed to Odessa District, El Paso District, Abilene District and Bituminous Section of Construction Division. The feedback received from that group will be used to improve the equipment and to mainstream the testing protocols.

A pilot two-day training workshop has been developed to ensure that all the technical and nontechnical concerns of the users are understood and addressed. In addition, one-on-one training sessions should be arranged for review of the procedures and for teaching more advanced uses of the devices and new procedures and information that we learn about the devices.

Table of Contents

Page No.

Acknowledgements vii
Abstract ix
Implementation Statement. xi
Table of Contents xiii
List of Tables xv
List of Figures xvii

CHAPTER 1 INTRODUCTION
1.1 Problem Statement 1
1.2 Objective and Approach 1
1.3 Organization 2

CHAPTER 2 PRINCIPLES RELATED TO IMPLEMENTING A QUALITY MANAGEMENT PROGRAM
2.1 Mechanistic Pavement Design 3
2.2 Factors Influencing Modulus 4
2.3 Methods for Measuring AC Modulus 6
2.3.1 Resilient Modulus (ASTM-D 4123-82) 7
2.3.2 Flexural Test 9
2.3.3 Deflection Based Test (FWD)... 10
2.4 Asphalt Concrete QC/QA Specifications 11
2.4.1 AASHTO QC/QA Specifications 11
2.4.2 Summary of State QC/QA Specifications 12

CHAPTER 3 QUALITY MANAGEMENT WITH SEISMIC METHODS
3.1 Historical Background 15
3.2 V-Meter 16
3.3 Portable Seismic Pavement Analyzer (PSPA) 18

CHAPTER 4 MATERIALS, EXPERIMENTAL SETUP, AND TESTING PROCEDURES
4.1 Introduction 27
4.2 Laboratory Testing 27
4.2.1 Materials.. 27

4.2.2 Briquette Preparation.. 30
4.2.3 Seismic Experimental Setup 30
4.2.4 Temperature Study Experimental Setup 32
4.2.5 Testing Procedures....34
4.3 Seismic Field Testing....34
4.3.1 Testing Procedures....36

CHAPTER 5 RESULTS AND DISCUSSION
5.1 Introduction....39
5.2 Results from Seismic Laboratory Method 39
5.2.1 Influence of Voids in Total Mix 39
5.2.2 Impact of Gradation 40
5.2.3 Impact of Viscosity 42
5.3 Influence of Temperature....44
5.3.1 Influence of Gradation 45
5.3.2 Influence of Asphalt Viscosity....47
5.4 Results from Seismic Field Method....47
5.4.1 Influence of Gradation 49
5.4.2 Influence of Voids in Total Mix 50
5.4.3 Influence of AC Layer Properties 51
5.5 Case Studies....54
5.5.1 El Paso Case Study 54
5.5.2 Odessa Case Study....54

CHAPTER 6 CONCLUSIONS AND RECOMMENDATIONS
6.1 Conclusions....59
6.2 Recommendations for Future Research 60

REFERENCES.... 61

APPENDIX A: Wave Propagation Theory
APPENDIX B: Mix Design
APPENDIX C: Quality Assurance Laboratory/ Field Testing Procedures
APPENDIX D: Phase I Laboratory Room Temperature Study Data
APPENDIX E: Phase II Laboratory Temperature Study Data
APPENDIX F: Pavement Model/ Field Data

List of Tables

Table No.	Description	Page No.
2.1	Testing and Inspection of AC	12
2.2	Summary of 16 State QC/QA Asphalt Concrete Specifications	14
3.1	Example Calculation for Laboratory Seismic Test	18
3.2	Testing Techniques Utilized in the PSPA	19
3.3	Example Calculation for Field Tests	26
4.1	Mixture Properties	28
4.2	Briquette Preparation Procedure	31
4.3	Phase I and Phase II Test Matrix	34
4.4	Summary of Pavement Models	36
5.1	Variation in Modulus with VTM for Three Different Mixtures	41
5.2	Variations in Modulus with VTM for Three Asphalt Grades	43
5.3	Impact of Gradation on Modulus – Temperature Relationship at 4% VTM	46
5.4	Impact of Gradation on Modulus – Temperature Relationship at 8% VTM	46
5.5	Impact of Viscosity on Modulus – Temperature Relationship at 4% VTM	48
5.6	Impact of Viscosity on Modulus – Temperature Relationship at 8% VTM	48
5.7	Comparison of Field and Laboratory Tests Moduli	49
5.8	Comparison of Laboratory and Field Modulus Measured on Specimens with Different VTM's	50
5.9	Comparison of Field and Laboratory Moduli on ACP Models with Different Thickness	52
5.10	Comparison of Field and Laboratory Moduli for El Paso Case Study	55

List of Figures

Figure No.	Description	Page
2.1	Three Layer Pavement Model	4
2.2	Stress-Strain Curve for Pavement Materials	5
2.3	Variation in Modulus with Frequency and Temperature	6
2.4	Resilient Modulus Test Setup	8
2.5	Time Relationships for Repeated-Load Indirect Tension Test	8
2.6	Repeated Flexure Apparatus for Determining Stiffness and Fatigue Characteristics	10
2.7	Schematic of Falling Weight Deflectometer	10
3.1	Schematic of the V-Meter	16
3.2	Picture and Schematic of the PSPA	20
3.3	Typical Time-Domain Records Collected by PSPA	21
3.4	Typical Analysis Used in USW Method	23
3.5	Typical PSPA Time Domain Record	25
4.1	Mix Gradations	29
4.2	Picture of Laboratory Setup	32
4.3	Picture of Temperature Study Experimental Setup	33
4.4	Temperature Monitoring Setup	33
4.5	Schematic of Pavement Models	35
4.6	Picture of Field Test Experimental Setup	37
5.1	Typical Variation in Young's Modulus with VTM	40
5.2	Variation in Modulus with VTM for Three Different Mixtures	41
5.3	Typical Variation in Young's Modulus with VTM	43
5.4	Typical Variation in Young's Modulus with Temperature	45
5.5	Variation in Measured and Predicted Modulus with VTM	51
5.6	Typical ACP Model No. 2 Core	52
5.7	Variation in Modulus for ACP Model No. 2	53
5.8	Variation in Young's Modulus with VTM for Odessa Material	56
5.9	Variation in Young's Moduli for Odessa ACP	56
5.10	Comparison of Modulus – VTM Relationship Obtained from Cores and AC Briquettes	57

Chapter 1

Introduction

1.1 Problem Statement

State highway agencies and contractors have started implementing quality control/quality assurance programs to improve the quality of laid-down asphalt concrete (AC) pavements. Highway agencies spend significant amounts of money and time coring to properly implement this concept. The quality of the AC pavement is assessed through field inspection, laboratory testing of pavement cores, thickness determination, and density measurements (via-nuclear density gauge).

One of the primary parameters considered in the design of flexible pavements is the modulus of the AC layer. Unfortunately, current quality management programs are not based on this engineering property. Instead, field compliance measures are mainly based on evaluating the density (Russell et al., 1998). To successfully implement a mechanistic pavement design procedure or to develop realistic performance based specifications, a method of monitoring the modulus of laid-down AC layers is needed. In that manner, more quantitative information about the pavement structure may be provided to the design engineer.

1.2 Objective and Approach

The main objective of this study is to present an economical quality management program based on seismic methods to determine the modulus of AC layers. More importantly, the goals are to understand the parameters that affect the seismic modulus.

In this thesis, a seismic laboratory method and a field method were employed. In the laboratory, tests were performed using a seismic device to generate compression waves through AC briquettes. The modulus of the AC briquette was then calculated using the travel time, length, and mass density of the briquette.

Using this approach, the impact of different mix properties on the modulus was studied. The parameters investigated were the gradation, viscosity of the asphalt (asphalt grade), voids in total mix (VTM), and temperature.

In the field study, the Portable Seismic Pavement Analyzer (PSPA) developed by Baker et al. (1995) was utilized. The PSPA uses seismic testing methods to determine the quality of pavements.

The PSPA was used on six pavement models constructed in the laboratory. The pavement models varied in gradation, VTM content, and layer thickness. The limitations and sensitivity of PSPA measurements in a controlled environment were evaluated. The pavement models were then cored to compare the laboratory seismic moduli measured directly on cores with those determined with the PSPA. Finally, two case studies using the proposed seismic methods were performed on AC pavements in Texas.

1.3 Organization

The problem statement, objective and approaches of this investigation are presented in this chapter.

Chapter Two contains a review of the principles related to implementing a quality management program. A brief discussion on mechanistic pavement design, current definitions and influencing factors on modulus, methods of measuring AC modulus, and current QC/QA specifications for AC construction are also presented.

A brief review of the historical background of quality management with seismic methods is presented in Chapter Three. Also, this chapter includes sections on the descriptions of the seismic devices, data collection, and analysis used in the study.

The laboratory and pavement model materials, experimental setups, and testing procedures are presented in Chapter Four. Chapter Five contains the results and discussions from the laboratory tests and the results from the pavement model study. Chapter Six contains conclusions and recommendations for future research.

Chapter 2

Principles Related to Implementing a Quality Management Program

In order to establish a practical quality management program based on seismic methods for asphalt concrete layers, current methods of pavement design, measuring AC moduli (stiffness), and quality control/quality assurance (QC/QA) must be reviewed. Current mechanistic approaches for predicting the remaining life of AC pavements are presented in the first section. In section two, an attempt is made to define the current terminology used to distinguish measured moduli with different methods and an explanation of the parameters that impact AC modulus. In the third section, current practical methods for measuring AC modulus are presented. Current QC/QA specifications for AC construction are discussed in the fourth and final section.

2.1 Mechanistic Pavement Design

Current mechanistic flexible pavement design procedures are based on modeling a pavement system as an elastic multi-layered and/or viscoelastic system. The remaining life of flexible pavements is mainly based on predicting the strains or stresses at the interfaces of different layers. For instance, if one models a pavement as a three-layer system composed of an asphalt concrete layer, a base course, and a subgrade layer (Figure 2.1), the two main strains considered are the tensile strain at the bottom of the AC layer and the compressive strain on top of the subgrade.

The fatigue cracking damage to the pavement is mainly due to the tensile strain at the bottom of the AC layer and to the modulus of the AC layer (Finn et al., 1977). The rutting is a function of the compressive strain on top of the subgrade (Shook et al., 1982). The general form for most

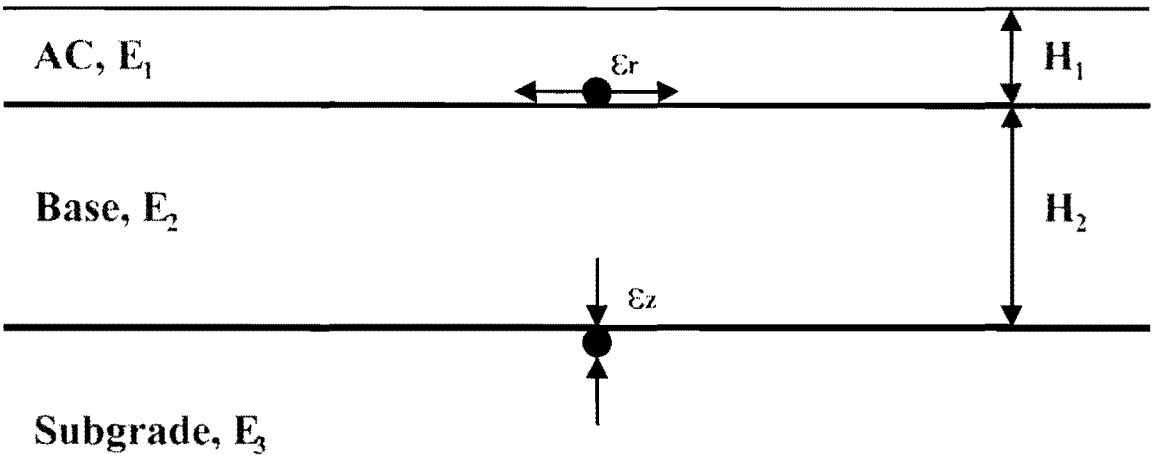

Figure 2.1 –Three Layer Pavement Model

distress models, which are used to estimate the fatigue damage and the rutting failure, may be expressed as Equations 2.1 and 2.2 (Ayres and Witczak, 1998)

$$N_F = K_1 (\varepsilon_t)^{K2} (E_{AC})^{K3} \tag{2.1}$$

$$N_R = K_4 (\varepsilon_c)^{K5} \tag{2.2}$$

where N_F is the number of equivalent single axle loads (ESAL), ε_t is the tensile strain at the bottom of the AC layer, and E_{AC} is the modulus of the AC layer. Therefore, one of the most important parameters in a mechanistic design procedure is the strains and the modulus of the AC. The strains developed within a pavement system are strongly related to the moduli of different layers. As a result, moduli of all layers should be determined accurately.

2.2 Factors Influencing Modulus

The modulus (stiffness) is the relationship between stress and strain. The behavior of most pavement materials may be represented by the stress-strain curve given in Figure 2.2 (Nazarian et al., 1998). The initial tangent modulus, E_{max}, is the slope of the linear portion of the curve passing through the origin. In that state of stress, the material is said to be elastic and to obey Hooke's law (i.e., stress, σ, is proportional to strain, ε)

$$\sigma = E\,\varepsilon. \tag{2.3}$$

Parameter E is the modulus. The initial tangent modulus is associated with tests performed at small strains such as seismic methods. The strength of a material, σ_{max}, is the horizontal line asymptotic to the curve. The secant modulus, E_1, E_2, or E_3, is the slope of the line connecting the

origin to any point. The secant modulus is strongly affected by the magnitude of the strain experienced by the material. This modulus normally corresponds to the laboratory resilient modulus.

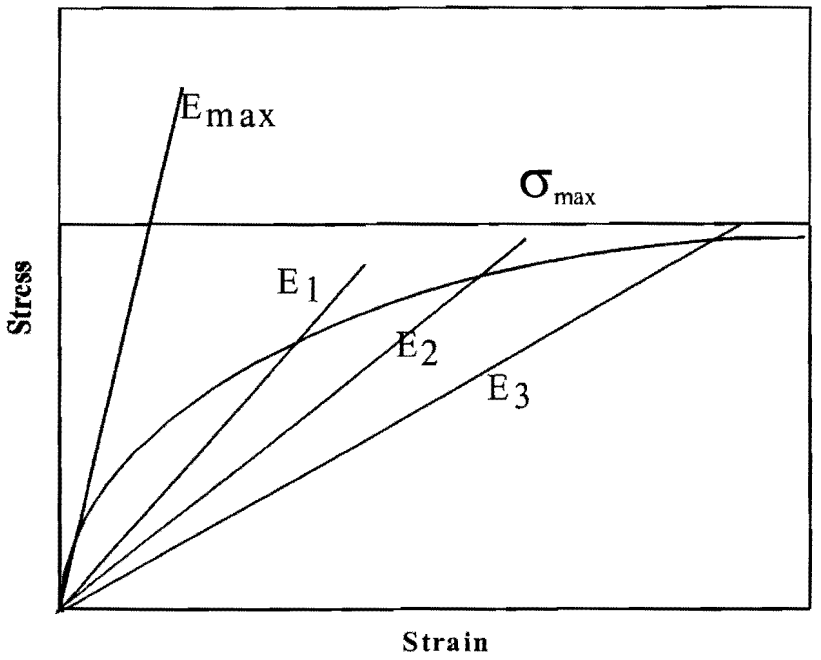

Figure 2.2 –Stress-Strain Curve for Pavement Materials

Different terms, related to modulus, that are also used in pavement design are the Dynamic Modulus, E^*, and Creep Compliance Stiffness, S(t) (Daniel and Kim, 1998). These moduli represent the stress/strain relationship as a function of time of loading, which is associated with the rheological behavior of asphalt mixtures. The dynamic modulus is measured with repeated-load laboratory tests. This method yields a complex modulus containing a real part (representing the elastic stiffness) and an imaginary part (that characterizes the internal damping of the material).

The creep compliance, D(t), is typically calculated by dividing the strain by the applied stress from creep tests (at any temperature and time). A common approximation used to convert the creep compliance to stiffness, S(t), is to simply invert the creep compliance (Daniel and Kim, 1998).

Baladi and Harichandran (1989) conducted a comparative study on test methods for determining the fundamental engineering properties required for design of AC pavements. The test methods evaluated in that study included triaxial tests (constant and repeated cyclic loads), cyclic flexural tests, Marshall tests, indirect tension tests (constant and variable cyclic loads), and creep tests. Baladi and Harichandran concluded that: (1) the repeatability of the test results was poor, (2) the

material properties obtained from different tests were substantially different, and (3) the results from indirect tensile tests were the most promising, although not consistent. This is not to say that tests which model the viscoelastic behavior of AC mixtures are not needed, but the degree of sophistication of laboratory and field tests should be balanced based on the importance and significance of the project.

Several parameters affect the modulus of AC mixtures. AC mixtures are dependent on the time of loading and temperature (Roberts et al., 1996). The time of loading is the rate or frequency of loading. Actual traffic has a dominant frequency of about 10 to 30 Hz. Based on a study of measuring the stiffness of AC with seismic methods, Aouad et al. (1993) demonstrated the importance of frequency and temperature. Figure 2.3 shows that estimated seismic moduli at a particular temperature should be reduced by a frequency adjustment factor. Several other researchers have studied the effects of temperature and rate of loading on modulus, but a unique temperature adjustment relationship has not been established.

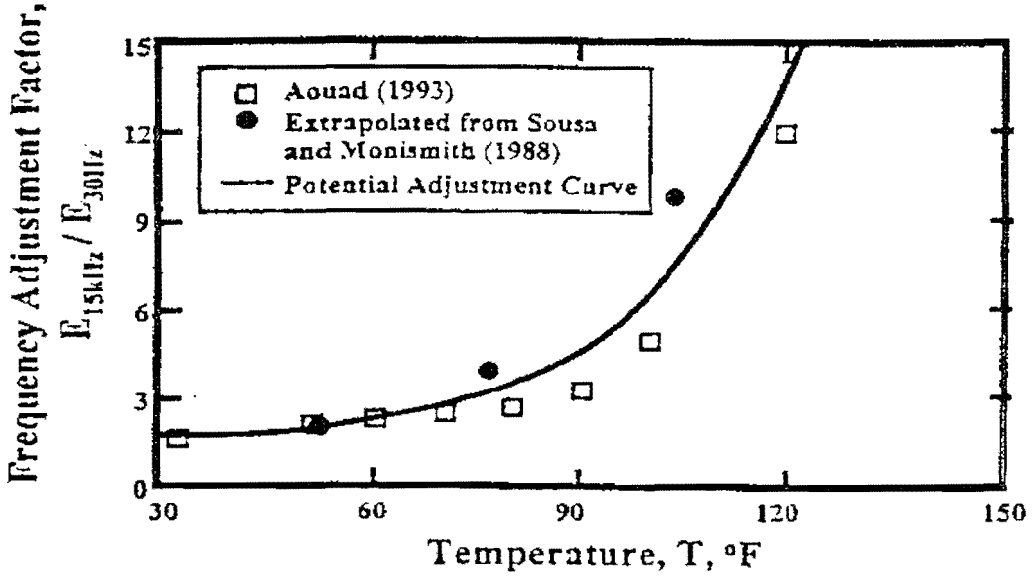

Figure 2.3 –Variation in Modulus with Frequency and Temperature (after Aouad et al., 1993)

2.3 Methods for Measuring AC Modulus

Several laboratory and field test methods for measuring the modulus (stiffness) of asphalt-concrete mixes are available to pavement engineers. The tests range from modeling the viscoelastic behavior of AC mixtures to indirect (nomograph based) methods. In this section, only the most common and practical test methods will be reviewed. This approach is taking into consideration the fact that the proposed quality management program could be practical for daily monitoring of laid-down AC pavements and may be combined with more comprehensive tests depending on the project at hand. The following tests are the most commonly used:

1) Resilient Modulus (Indirect Tension Test-ASTM- D 4123)
2) Flexural Stiffness Test
3) Deflection Based Tests –Falling Weight Deflectometer (FWD)

2.3.1 Resilient Modulus (ASTM-D 4123-82)

The resilient modulus is the current state of practice for measuring the modulus of AC mixtures. This test may be performed either axially or diametrically. A schematic of a resilient modulus test setup is shown in Figure 2.4.

A typical load and deformation versus time relationship, for a repeated-load indirect tension test, is shown in Figure 2.5. This test setup is recommended by the American Society for Testing and Materials (ASTM D 4123). The testing procedure consists of subjecting an AC briquette or core to a cyclic haversine deviatoric stress applied for 0.1 seconds followed by a 0.4 or 0.9 second rest period. Furthermore, the tests are performed at three temperatures 5, 25, and 40 ^{0}C. The deformations are measured using linear variable differential transducers (LVDT's) or other devices. The average recoverable horizontal and vertical deformations, over at least 3 cycles, are measured. The resilient modulus of elasticity, E_{RT}, may be calculated as follows:

$$E_{RT} = P(\nu_{RT} + 0.27)/ t\,\Delta H \qquad (2.4)$$

where
E_{RT} = resilient modulus of elasticity,
P = applied load,
t = sample thickness,
ν_{RT} = Poisson's ratio, and
ΔH = total horizontal deformation.

This test is popular with most pavement engineers because it models the actual pulse generated by a vehicle loading, which is about 0.1 to 0.4 seconds (Shah, 1993). These tests require a preconditioning period before the actual resilient modulus may be determined. The preconditioning period requires a minimum of 50 to 200 cycles of loading, or until the deformations are stable. The tests are then performed at the recommended loading frequencies at each temperature. The specimens have to be maintained at a controlled test temperature for 24 hours prior to testing. The test is also repeated for each loading frequency by rotating the specimen 90 degrees. At a workshop on resilient modulus testing held at Oregon State University in 1989, there was a strong consensus amongst pavement engineers that the testing procedure is rather time-consuming and that the results were not very repeatable (Shah, 1993).

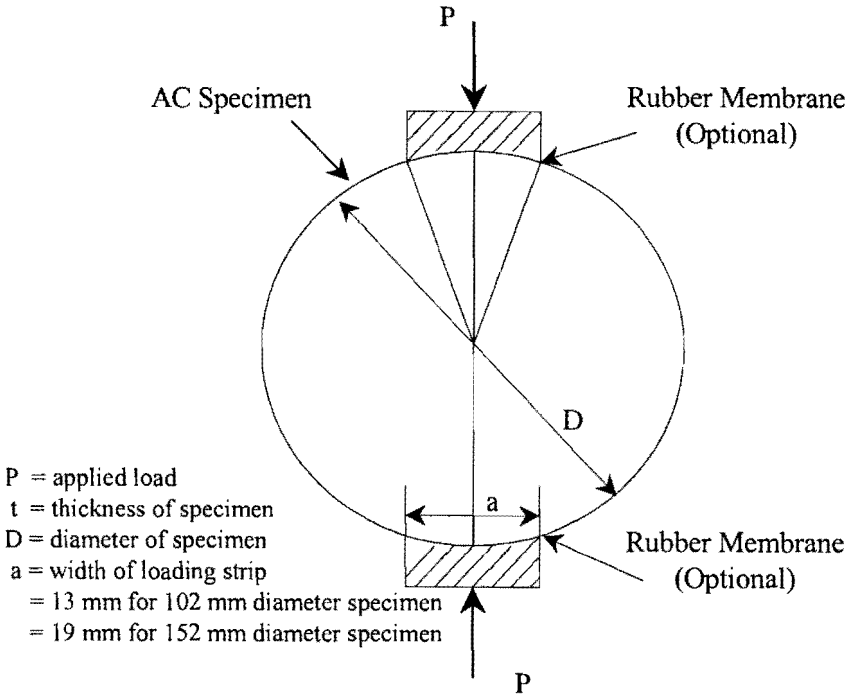

Figure 2.4 –Resilient Modulus Tests Setup

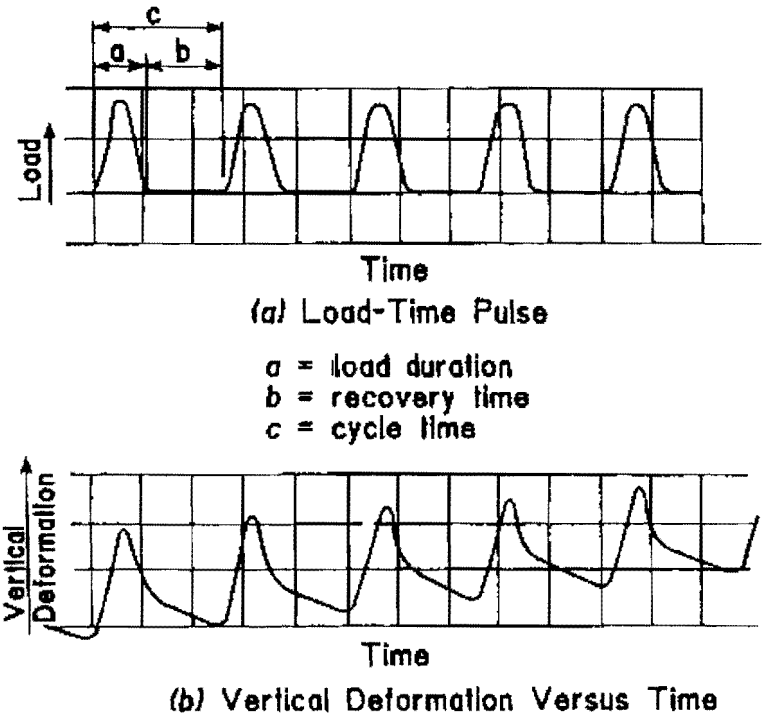

Figure 2.5 -Time Relationships for Repeated-Load Indirect Tension Test (after Roberts et al., 1996)

2.3.2 Flexural Test

Different types of flexural tests to evaluate the fatigue properties and modulus of AC mixtures have been developed. A typical testing apparatus is shown in Figure 2.6 (Kennedy et al., 1975). These tests are typically performed on AC beam specimens that are loaded repeatedly with a haversine pulse under a third-point loading configuration. The load is applied for 0.1 seconds followed by a 0.4-second rest period. The deflection of the beam caused by the loading is measured with LVDT's. The stresses, strains, and moduli are calculated after about 200 load applications.

The equation to calculate the modulus, which may be derived using beam theory, is as follows:

$$E_s = Pa\,(3L^2 - 4a^2)/(48I\,\Delta) \qquad (2.5)$$

where

E_s = Flexural Stiffness Modulus (psi),
P = repeated load (lbf),
L = reaction span length (in.),
a = distance between support and the first applied load (in.),
I = moment of inertia of the beam (in.^{4}), and
Δ = deflection at the center (in.).

The test may be performed either in a load-controlled or a strain-controlled mode. In the load-controlled mode, a constant repeated stress is applied to the specimen until failure occurs. For small stresses, the time to conduct this test on one specimen may be long (Roberts et al., 1996). The strain-controlled mode is performed by maintaining a constant deflection with increasing cycles. In that mode, it may be difficult to define failure during the test. Tangella et al. (1990) suggest that the test method is costly, time consuming, and requires specialized equipment. Furthermore, unlike within the pavement structure, the state of stress is uniaxial.

2.3.3 Deflection Based Tests (FWD)

The FWD measures the response (surface deflections) of a pavement from an applied impulse load. A schematic of a falling weight deflectometer is shown in Figure 2.7. The impulse load is created by dropping a weight of 50 kg to 300 kg from a height of 20 mm to 400 mm. By varying the drop height and weight, a peak load from 6 kN to 100 kN may be developed. The load is applied on the pavement through a 300-mm diameter plate. The duration of the pulse is about 20 to 80 msec. The deflections at the surface of the pavement are measured through seven geophones, which automatically lower onto the pavement.

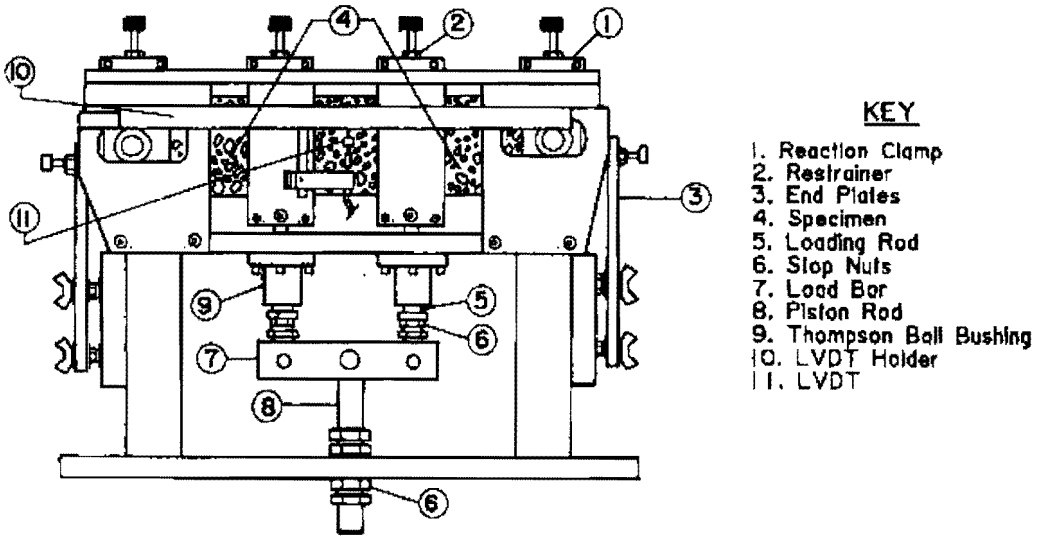

Figure 2.6 –Repeated Flexure Apparatus for Determining Stiffness and Fatigue Characteristics (after Kennedy et al., 1975)

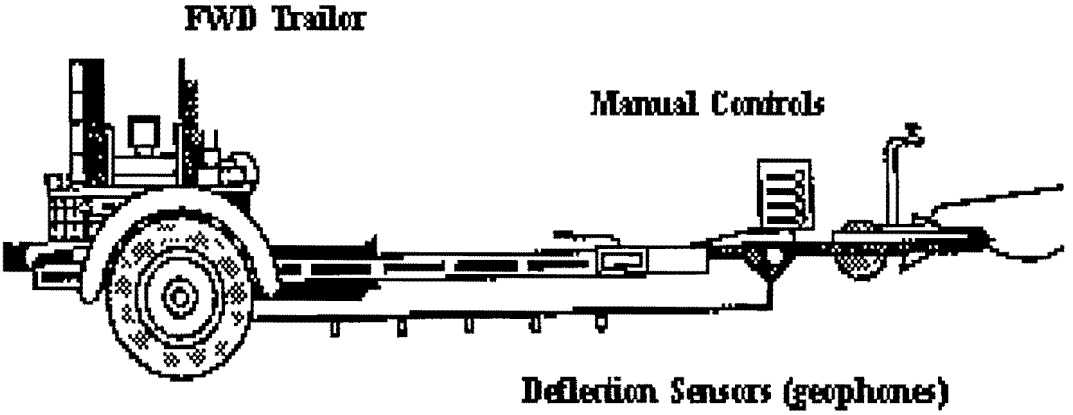

Figure 2.7 –Schematic of Falling Weight Deflectometer

To analyze the measured load and deflections, the pavement is modeled as a multi-layered linear elastic system. The measured deflections are compared to predicted deflections generated with a computer program that performs a linear elastic analysis. The modulus of each layer is obtained when the measured and predicted deflections compare well. The analysis is mainly conducted by comparing the measured and predicted deflections until they compare well, which is known as deflection basin-fitting.

The main advantages to the FWD are that tests are conducted in the field and that the method is practical for daily use. However, several combinations of moduli and layer thickness may generate predicted deflections that match measured deflections. Furthermore, many studies have shown that with the current configuration of the receivers in the FWD it may be difficult to accurately determine the modulus of the top layer in the pavement.

2.4 Asphalt Concrete QC/QA Specifications

State highway agencies and contractors have been implementing quality control/quality assurance (QC/QA) programs to improve the quality of laid-down AC pavements. Under most state specifications, the contractor has the responsibility of quality control, and the state agencies have the responsibility of quality assurance. Quality Assurance is defined, by the AASHTO QC/QA guide, as the activities having to do with making sure that the quality of a product is what it should be (AASHTO, R-10-92I). These specifications provide rewards or penalties based on statistical quality analysis of end result quality characteristics such as mix properties, pavement density, and smoothness of the pavement. In the following subsections, summaries of the AASHTO quality assurance specifications and state QC/QA programs are presented, as well as a discussion on a key consideration relevant to quality assurance testing and to the design of AC pavements.

2.4.1 AASHTO QC/QA Specifications

AASHTO published its quality assurance specifications in 1996 to provide state agencies with the framework, definitions, and guidelines for implementing QA programs. The guide provides detailed specifications for QC/QA testing and inspection methods (see Table 2.1). The table defines the AASHTO recommendations about the frequency of QC testing at each construction phase, while the agency is left to decide its QA testing frequency. The QA section on asphalt concrete pavements (QA-401) contains subsections on materials, quality control, basis of acceptance and payment. In general, these sections define the material composition specifications, job mix formula (JMF), contractor requirements, type of tests, testing frequency, specification limits, and payment adjustments.

Table 2.1–Testing and Inspection of AC (after Russell et al., 1998)

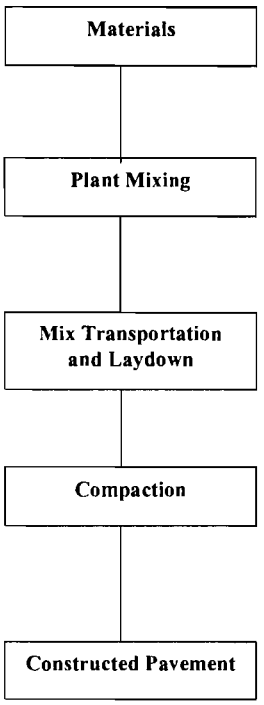

Testing and Inspection Property	AASHTO[1] QC	Acceptance
Aggregate Gradation	1 per 500 tons for Plant Setup, then 1 per 1,000 tons	--
Aggregate Properties	1 per 1,000 tons or C	--
Asphalt Binder Properties	--	--
Aggregate Gradation	1 per 1,000 tons	A
Asphalt Content	1 per 500 tons	A
Volumetric Properties	1 per 1,000 tons	A
Temperature of Mix	1 per hour	--
Temperature of Base or Air	As Needed	--
Tack/ Prime	Load or Half Day	--
Pavement Application Rate	As Needed	--
Density	1 per 500 tons	A
Temperature of Mat	1 per hour	--
Thickness	C	--
Smoothness (Ride)	C	0.1 Lane-Mile
Agency Acceptance	--	--

C = As needed to control operations
A = To be determined by agency
-- = No frequency given in specifications

The payment adjustment is related to the mixture properties, pavement density, and ride quality. Furthermore, the guide provides an appendix on Quality Level Analysis (QLA), which is the recommended statistical procedure. QLA provides a method for estimating the "percent within limits" (PWL) of each lot or sub-lot of material, product, item of construction, or completed construction that may be expected to be within specified tolerances. The PWL is that amount of material or workmanship that has been determined by statistical methods to be within the pre-established characteristic boundary(ies) of the material and may be used to determine acceptance (AASHTO, 1996).

2.4.2 Summary of State QC/QA Specifications

A survey by Benson (1996) detailed QC/QA specifications for asphalt concrete practiced by sixteen states (Table 2.2). Many attributes are similar from state to state. In general all states

include some method of pay adjustment in their specifications, though they vary in the material properties specified, statistical parameters used, and methods for multiple pay adjustments (Benson, 1996).

In order to determine pay adjustments, compliance measures are performed based on statistical quality analysis of end result quality characteristics (e.g., mix properties, pavement density, and smoothness of the pavement). There are five different compliance measures being used by most state agencies including: (1) average, (2) quality level analysis (QLA), (3) average absolute deviation (AAD), (4) moving average (MA), and (5) range.

The average method simply takes the arithmetic average of test results within a lot or sub-lot. In the QLA method, the average and standard deviation of tests results for a lot are evaluated. The AAD determines the average of absolute deviations from a reference density. The MA measures the arithmetic moving average of several consecutive tests against the target value. In the range method, the arithmetic range is used to determine the quality pavement.

Currently, QLA is the most rigorous approach to measuring compliance because it may be used to estimate the percentage of the lots falling within lower and/or upper specification limits. This is thought to be more beneficial for the agencies and contractors, since they have the ability to quantify risk levels during acceptance (Russell et al., 1998).

The review of current QC/QA programs for AC contains one key issue that is relevant to the initial pavement design and analysis. QC/QA should be viewed as an integral part of the pavement design and analysis process. Most AC pavement analyses are based on the assumption that pavement layers are linear elastic or linear viscoelastic.In such analyses, materials should be characterized based on parameters, such as modulus and Poisson's ratio. However, a review of current QC/QA testing methods for acceptance shows that these parameters are not considered. At a minimum, the modulus of laid-down AC pavement should be considered and measured to provide feedback to the pavement engineer as per his pavement design assumptions. Instead, the acceptance criteria for laid-down AC pavements are based on measuring adequate density. Furthermore, highway agencies and contractors are primarily using nuclear density gages to measure in-place pavement density, but they have experienced differing results between core samples and nuclear readings (Schmitt et al., 1997). This has raised many concerns for agencies and contractors.

In response to this key issue, implementation of methods to measure more engineering based parameters during QC/QA programs should be considered. Although, most states are just beginning their QC/QA programs, this type of change would need qualified personnel, experience, and the tools to measure these properties. Instead, a gradual change should be considered, with feasibility studies at the quality assurance level, which is mainly performed by state agencies.

Table 2.2 –Summary of 16 State QC/QA Asphalt Concrete Specifications (after Benson, 1996)

State	QC Plan Required	Contractor Provides Mix Design	Pay Adjustment	Compliance Measures	Contractor's Tests Used for Acceptance	Contractor's Technician Certified by	Split Samples Used for Verification	Independent Samples Used for Verification	Dispute Resolution System
Alabama	yes	yes	yes	Avg. |Dev.|[a]	yes	DOT	yes	no	yes
Arizona	yes	yes	yes	QLA[b]	no	NCET[c]	no	no	yes
Colorado	yes	yes	yes	QLA	no	NCET	yes	no	yes
Georgia	yes	no	yes	Avg. |Dev.| and Range	no	DOT	no	no	no
Indiana	yes	yes	yes	Avg. and Range	no	DOT	no	no	yes
Louisiana	no	yes	yes	Avg.	no	DOT	no	no	no
Michigan	no	yes	yes	Avg. and Avg. |Dev.|	yes	Pending	yes	no	yes
New York	yes	yes	yes	Avg. and Range	yes	Pending	yes	yes	yes
Oregon	yes	yes	yes	QLA	no	DOT	yes	no	no
Pennsylvania	yes	yes	yes	Avg. or QLA	yes	DOT	no	yes	yes
Texas	no	yes	yes	Avg and Avg. |Dev.|	yes	DOT	yes	no	yes
Utah	yes	no	yes	QLA	no	NCET	no	no	yes
Virginia	yes	yes	yes	QLA	yes	DOT	yes	no	yes
Washington	no	no	yes	QLA	no	Pending	no	no	yes
West Virginia	yes	yes	yes	Moving Avg. or QLA	yes	DOT	no	yes	yes
Wisconsin	no	yes	yes	Moving Avg.	yes	DOT	yes	yes	yes

[a] Average of the absolute value of deviations from the target value.
[b] Quality Level Analysis used to estimate the percent within or outside of specification limits.
[c] National Institute for Certification in Engineering Technologies. Some states allow equivalent certifications.

Chapter 3

Quality Management with Seismic Methods

Seismic nondestructive testing (NDT) methods can potentially offer an efficient, economical, reliable, and repeatable way of measuring the modulus of AC layers. This chapter presents a brief historical background on the use of seismic methods in quality control and in determining the in-situ modulus of pavement layers. In addition, sections describing the seismic testing devices used in the study are contained in this chapter. A review of wave propagation theory relevant to the proposed methods is presented in Appendix A.

3.1 Historical Background

The ultrasonic pulse velocity methods were first used to evaluate the quality of concrete over 50 years ago (Naik and Malhorta,1991). These methods have been implemented in the laboratory as well as in the field. Also, these methods offer the ability to detect internal structural changes, cracking, changes due to freezing and thawing, and measurement of the elastic modulus (Naik and Malhorta, 1991). Nazarian et al. (1996, 1997) developed seismic methods for quality control of Portland Cement Concrete (PCC) that measure the in-situ modulus, Poisson's ratio, and the thickness of slabs. One impact of that study was that the measured moduli in the field and laboratory were repeatable.

The Spectral Analysis of Surface Waves (SASW) tests have been used to determine the modulus and thickness of AC pavement layers (Aouad et al., 1993). The SASW method is based upon the theory of stress wave propagation in layered media. The dispersive characteristics of measured surface waves are used for determining the modulus and thickness of the pavements.

The major groundwork for the SASW method has been developed in the last 15 years. Nazarian and Stokoe (1986,1987) developed the experimental and theoretical aspects of the SASW method as applied to geotechnical and pavement engineering. Nazarian et al. (1995) developed an experimental and theoretical approach using the SASW method to determine the moduli of pavements.

The Portable Seismic Pavement Analyzer (PSPA) was developed by Baker et al. (1995) for monitoring PCC pavements. The device has been used in the QC of PCC pavements. The quality is determined by measuring Young's and shear moduli in the PCC pavement, using the ultrasonic surface wave method and the ultrasonic body wave method. The device is practical for day to day use, and tests are rapid and repeatable. Understanding this potential, the implementation of these seismic methods in the QC/QA of AC pavements is desirable.

3.2 V-Meter

A schematic of the V-Meter is shown in Figure 3.1. The V-Meter is a seismic device that is designed for both laboratory and field-testing. The device is fully portable and is simple to operate.

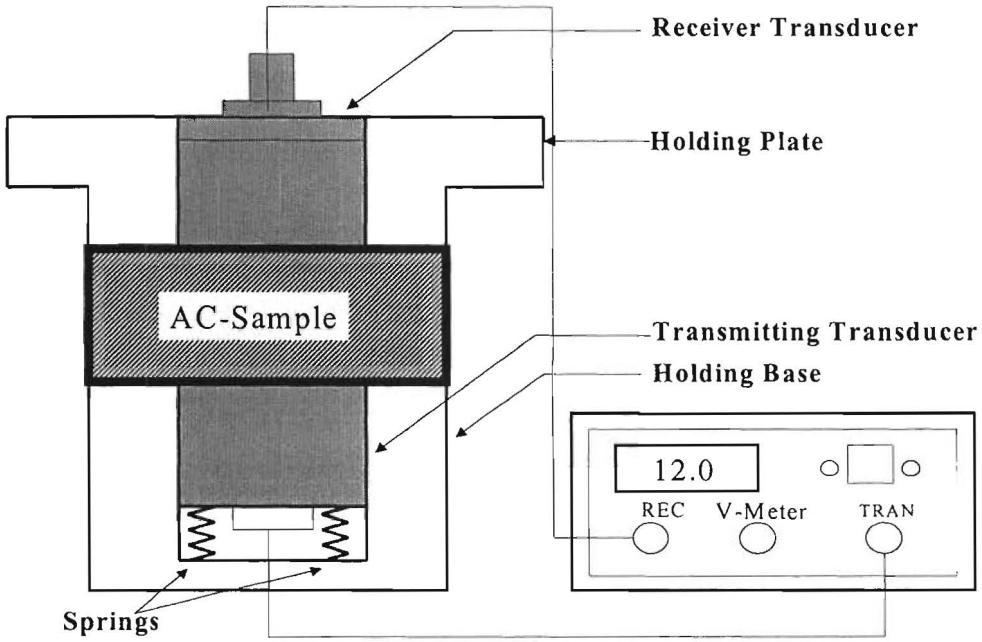

Figure 3.1 – Schematic of the V-Meter

This method is based on measuring the propagation of pulses or seismic waves through materials. The V-Meter generates seismic waves by a built-in pulse generator, which transforms an electrical pulse to a mechanical vibration through a transducer. The seismic wave arrival time is recorded by a receiver, which is connected to an internal clock. The internal clock has the capability of automatically measuring and displaying the travel time of the waves. The transducers have a central frequency of 54 kHz, and the transmitting time is displayed in μsec with an accuracy of ± 0.1μsec.

Using the wave arrival time, t_V, the constrained modulus, M_V, may be fundamentally calculated as:

$$M_V = \rho V_P^2 = \rho (L / t_V)^2 \qquad (3.1)$$

This equation may be simplified to:

$$M_V = 4\ m\ L / \pi\ d^2\ t_V^2 \qquad (3.2)$$

where
m = mass of the AC briquette,
L = average length of the briquette, and
d = average diameter of the briquette.

Young's Modulus may be determined from:

$$E_V = M_V\ [\ (1-2\nu)\ (1+\nu)/(1-\nu)\ ] \qquad (3.3)$$

The data reduction for the seismic test is rather simple. Knowing the average length, average diameter, mass of the AC briquette, and the travel time measured by the V-Meter, the modulus can be determined. An example calculation is presented in Table 3.1.

3.3 Portable Seismic Pavement Analyzer (PSPA)

As mentioned before, the Portable Seismic Pavement Analyzer (PSPA) was developed by Baker et al. (1995) for monitoring PCC pavements. Three different seismic testing techniques are utilized. These tests are:

1. Ultrasonic Body Wave (UBW) method,
2. Ultrasonic Surface Wave (USW) method,
3. Impact Echo (IE) method.

These tests are utilized to determine the thickness and quality of pavements. The parameters calculated from the raw data are summarized in Table 3.2. In the following discussion, only the ultrasonic surface wave and the ultrasonic body wave methods will be covered because they are the two main methods used in the study.

Table 3.1- Example Calculation for Laboratory Seismic Test

Given:

Average AC briquette length	100 mm
Average briquette diameter	101 mm
Briquette mass	1.68 kg
V-Meter travel time	30.5μsec
Poisson's Ratio	0.33

Solution:

Calculating the constrained modulus from Equation 3.2

$$M_V = [(4 \times 1.68 \times 100)/ [(\pi \times (101)^2 \times (30.5 \times 10^{-6})^2)] \times (1 \times 10^{-6})$$

$$= 22.5 \text{ GPa.}$$

Calculating Young's modulus from Equation 3.3

$$E_V = 22.5[(1-2(0.33))\ (1+0.33)/\ (1-0.33)]$$

$$= 15.2 \text{ GPa.}$$

Table 3.2 - Testing Techniques Utilized in the PSPA

TESTING TECHNIQUES	PARAMETERS MEASURED
Ultrasonic Surface Wave	Young's Modulus of top paving layer
Ultrasonic Body Wave	Shear Modulus of top paving layer
Impact Echo	Thickness of paving layer or Depth to delaminated layer

A picture and a schematic of the PSPA are shown in Figure 3.2. The PSPA is controlled by a computer, which is connected to the hand-carried transducer unit through a cable that carries power to the accelerometers and the hammer. The cable also returns the measured signals to the data acquisition board in the computer. The main components of the PSPA are the two accelerometers (A and B) and an electrical solenoid, used as a high-frequency source (C). The internal components consist of an amplifier board and a solenoid firing board. The main structural member, holding the transducers and source, is a thick steel plate mounted on the base of the box holding the electronics. Rubber vibration isolators decouple the accelerometers (A and B) from the steel plate, and the source is directly mounted on the plate.

Upon placing the PSPA at a given test location and initiating the testing sequence through the computer, the high-frequency source is activated. The source is fired four to seven times. For the last three impacts of the source, the output voltages of the load cell and receivers are saved and averaged (stacked) in the frequency domain. The other prerecorded impacts are used to adjust the gains of the pre-amplifiers. The gains are set in such a manner that the output of the sensors is optimized.

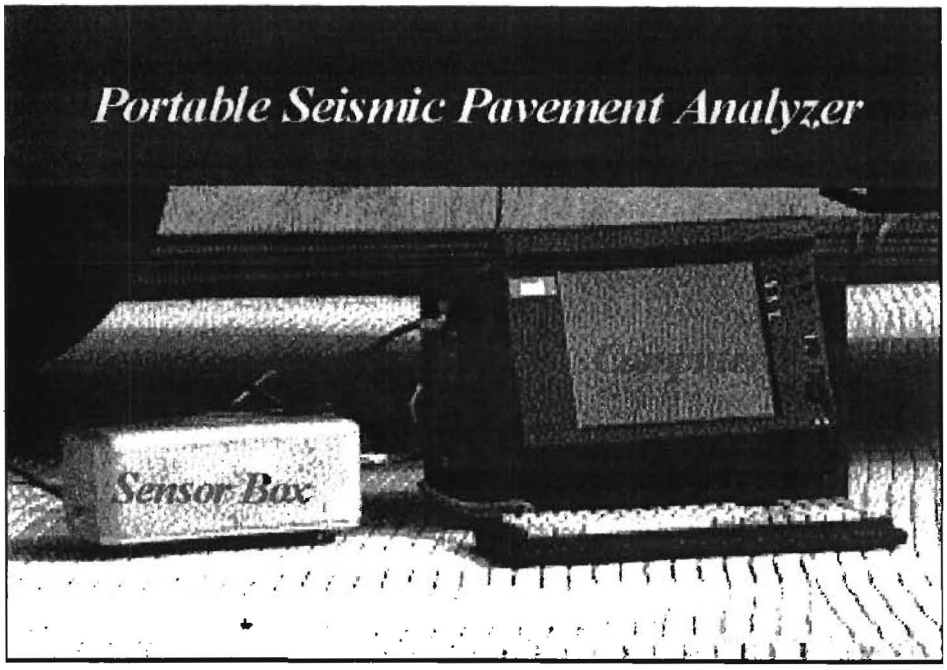

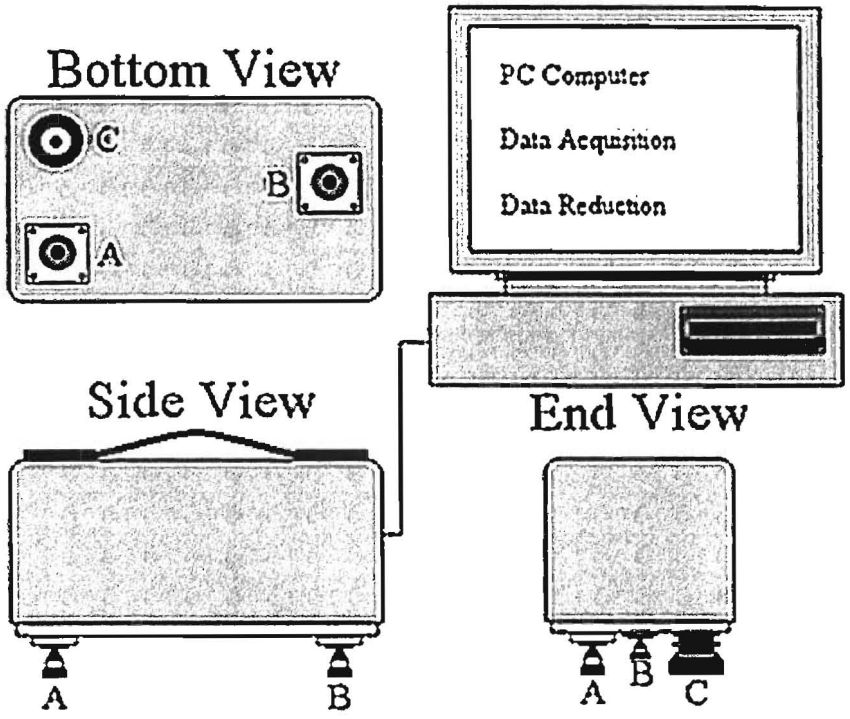

Figure 3.2 – Picture and Schematic of the PSPA

Typical outputs of the two accelerometers for tested AC pavement are shown in Figure 3.3. Naturally, as the distance from the source increases, the amplitude of the signal decreases. To ensure that an adequate signal-to-noise ratio is achieved in all channels, the signals are all normalized to a maximum amplitude of one, as shown in Figure 3.3. In this manner, the main features of the signals can be easily inspected.

The ultrasonic surface wave (USW) method is an offshoot of the SASW method. The major distinction between these two methods is that, with the USW method, the properties of the top paving layer can be easily and directly determined without the need for a complex inversion algorithm.

To perform the test, a disturbance (through high frequency source C) is applied to the ground surface to generate stress waves, which propagate mostly as surface waves of various wavelengths. The waves are monitored and captured with a data acquisition system (through the receivers A and B). The signals, as depicted in Figure 3.3, may be denoted as a(t) and b(t). The signals are transformed to the frequency domain [A(f) and B(f)] through the use of a Fast Fourier Transform algorithm. The transformed signals, A(f) and B(f), are used to calculate the cross power spectrum between the two receivers, denoted as G_{AB}.

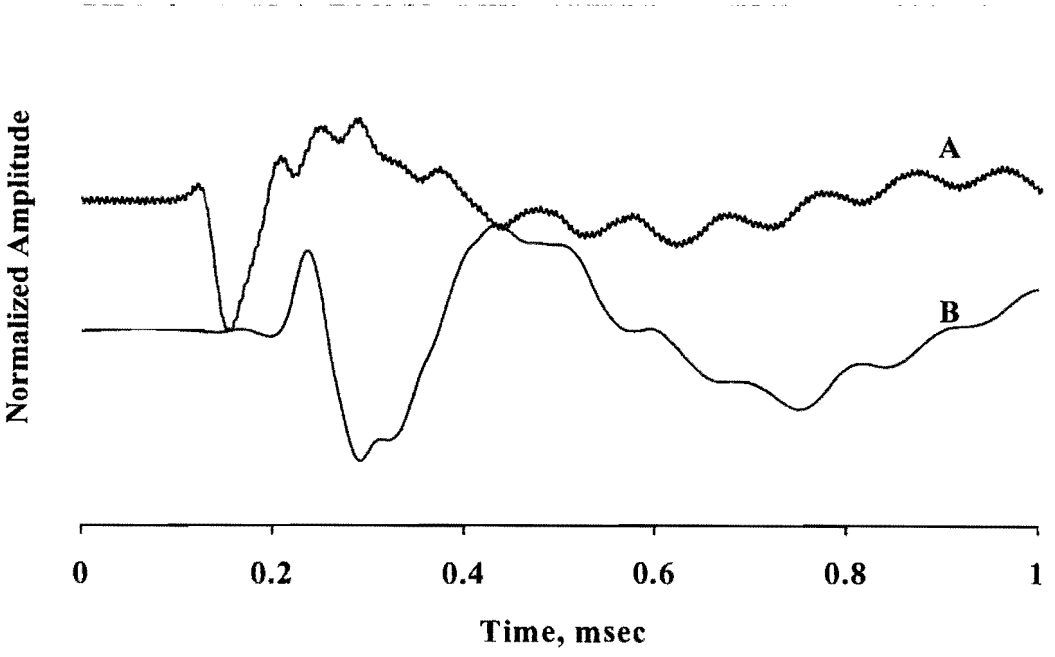

Figure 3.3 – Typical Time-Domain Records Collected by the PSPA

The cross-power spectrum, shown in Figure 3.4a, depicts the phase information for the time records as a function of frequency. The phase may be calculated using the following equation:

$$\phi(f) = \tan^{-1}[\mathrm{Im}(G_{AB})/\mathrm{Re}(G_{AB})] \quad (3.4)$$

where $\mathrm{Im}(G_{AB})$ represents the imaginary part of the cross power spectrum at each frequency and $\mathrm{Re}(G_{AB})$ represents the real part.

In the next step, the phase is "unwrapped;" that is, an appropriate number of cycles are added to each phase. The unwrapped phase spectrum for the "wrapped" phase spectrum is shown in Figure 3.4b. The slope of the line is more or less constant with frequency.

The dispersion curve, which is the relationship between the velocity of propagation of surface waves, V_R, and the wavelength, λ, is determined from the unwrapped phase spectrum. For a phase, ϕ, at any frequency, f, this relationship can be written as

$$V_R = D/[\,\phi/360f\,] \quad (3.5)$$

$$\lambda = D/[\phi/360], \quad (3.6)$$

where D is the distance between the receivers. A dispersion curve for a two-layer system, consisting of an 80-mm AC layer over a 200-mm base course (soil) is shown in Figure 3.4c. The figure shows that the phase velocity is about 1300 m/s for the AC. The dispersive characteristic of phase velocity may be used to approximate the thickness of different layers and changes in material properties.

In the analysis of AC layer, the velocity of propagation, V_R, is determined by performing a least-squares linear regression over the raw data of the high-frequency region of the wrapped phase spectrum and obtaining the slope of the best-fit line. The average velocity of propagation of the top layer is estimated by constraining the wavelengths to the thickness of the top layer. As a result Young's modulus of the top layer, E_{PSPA}, can be very easily determined from:

$$E_{PSPA} = 2\,\rho\,C^2\,V_R^2(1+\nu), \quad (3.7)$$

where

ρ = mass density of the AC layer,
C = a constant based on Poisson's ratio to convert Rayleigh wave velocity to shear wave velocity (see Appendix A),
V_R = the average surface wave velocity of the AC layer,
ν = Poisson's Ratio.

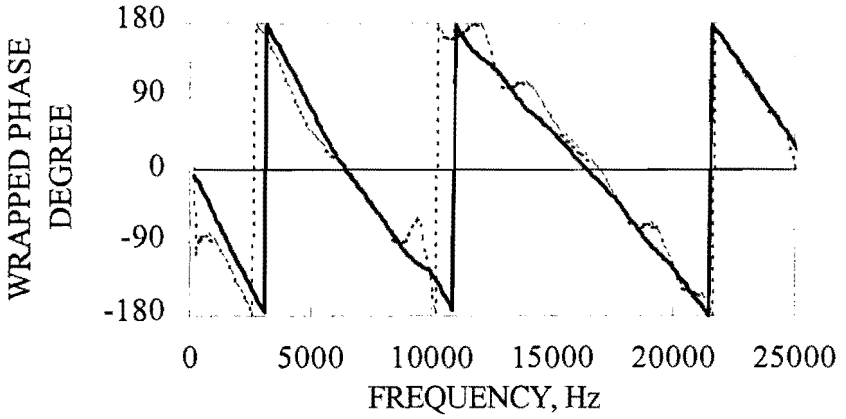

a.) Cross Power Spectrum

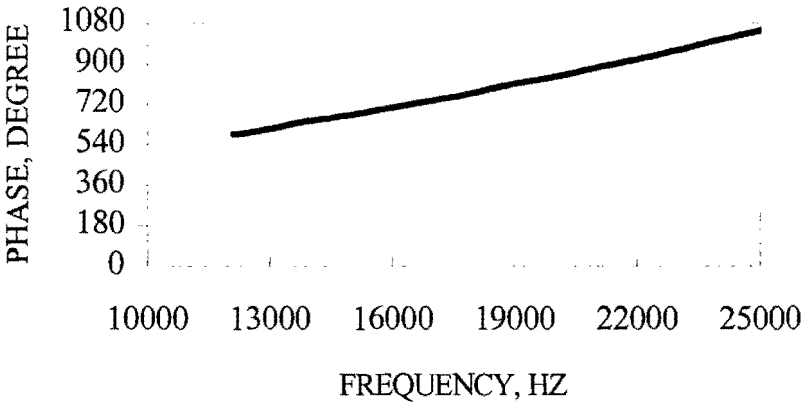

b.) Unwrapped Phase

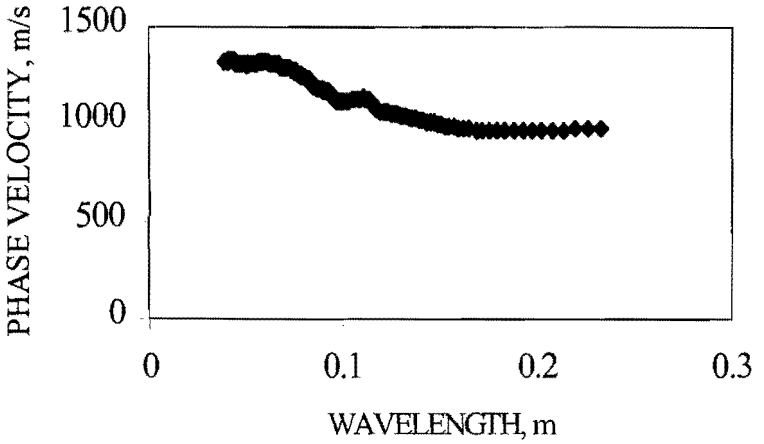

c.) Dispersion Curve

Figure 3.4 - Typical Analysis Used in USW Method

Equation 3.7 may be used to compare the estimated Young's modulus with those determined using the seismic laboratory method on cores.

The data reduction and analysis time is significantly reduced because the PSPA software has the capability of automatically generating the wrapped phase transfer function and the dispersion curve. Furthermore, the data analysis may be performed in the field.

In the ultrasonic body wave method, the time histories are used to find the travel times of body waves. A typical time domain record for a tested AC pavement from the PSPA is shown in Figure 3.5. The velocity of propagation, V, is found by dividing the distance between the two receivers, D, by the difference in arrival time of a specific wave, Δt. In general the velocity of propagation for any three waves [compression, V_P; shear wave, V_S; or surface wave (Rayleigh) wave, V_R] may be found through the following expression

$$V = D/\Delta t. \tag{3.8}$$

The velocities can then be converted to moduli as discussed in Appendix A.

Miller and Pursey (1995) found that when the surface of a medium is disturbed the generated stress waves propagate mostly with Rayleigh wave energy and, to a lesser extent, shear and compression wave energies. As such, body wave energy present in a seismic record, generated using the setup shown in Figure 3.2, is small. However, compression waves travel faster than any other type of seismic waves and are detected first on seismic records. Several automated techniques for determining the arrival of compression waves are available. A method suggested by Willis and Toksoz (1990) has been implemented in the PSPA.

In this study, the ultrasonic surface wave method was mainly used to determine the modulus of AC layers, while the ultrasonic body wave method was used for estimating the Poisson's ratio of the AC layer. This was accomplished by using the PSPA time histories. In the time domain records, the P-wave or S-wave travel times were determined. Poisson's ratio was then estimated with the use of Figures A.5 and A.6.

The data reduction process for the field tests is easy, since the PSPA is automated. The main step in the data analysis is to fit the raw data of the wrapped transfer function with the curve-fitting program and to generate the dispersion curve for the AC layer. An example calculation pavement model is shown in Table 3.3.

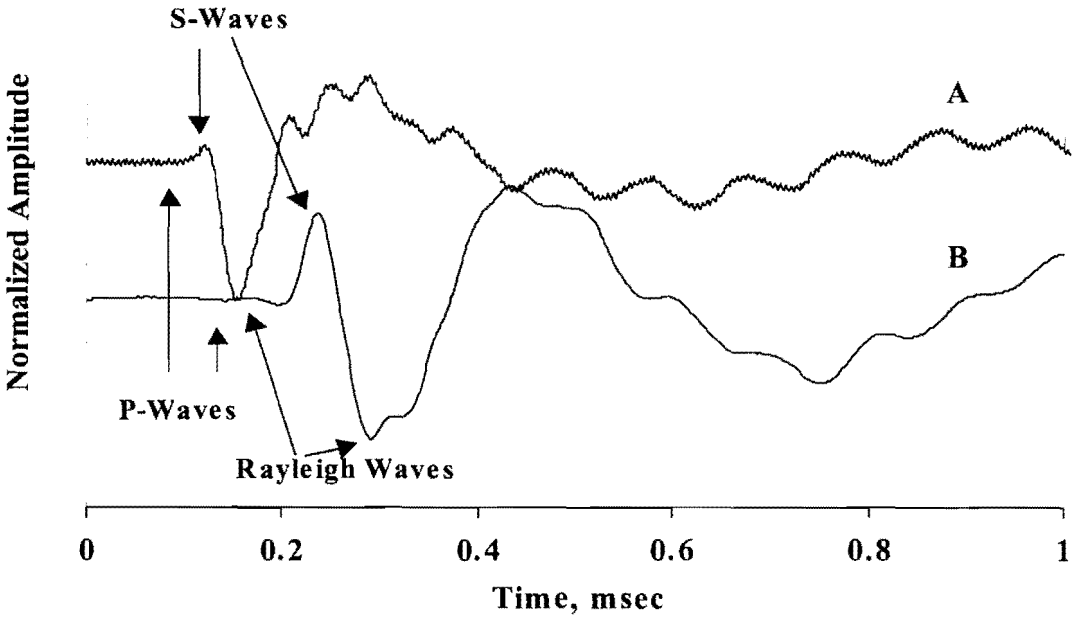

Figure 3.5 - Typical PSPA Time Domain Record

Table 3.3- Example Calculation for Field Tests

Given:

Receiver spacing — D =152 mm

Depth of Pavement — h = 76 mm

Mass density of AC layer (determined from AC cores) — $\rho = 2200\ kg/m^3$

Average Compression Wave travel time (determined from time-domain data) — $t_P = 48.3 \mu sec$

Solution:

Average AC layer Surface Wave Velocity: $V_R = 1313$ m/s

Compression Wave Velocity: $V_P = D/ t_P = .152 / 48.3 = 3147$ m/s (Eq. 3.8)

Ratio Between Surface Wave Velocity to P-Wave Velocity: $V_R/ V_P = 1313 / 3147 = 0.417$

Using Figure A.6 and $V_R/ V_P = 0.42$
Poisson's Ratio: $\nu = .38$

Using Figure A.5 and $\nu = .38$: $V_R/ V_S = 0.94$

Constant C (Constant for Converting Surface Wave Velocity to S-Wave Velocity): $C = 1/ (V_R/ V_S) = 1/ 0.94 = 1.1$

Young's Modulus using Equation 3.6:

$$E_{PSPA} = 2 \rho C^2 V_R^2(1+\nu) = [2*2200*(1.1)^2*(1313)^2 (1+0.38)](1x10^{-9})$$

$$= 12.7 \text{ GPa}$$

Chapter 4

Materials, Experimental Setup, and Testing Procedures

4.1 Introduction

This chapter contains an overview of the laboratory and field seismic tests and the procedures carried out to study the parameters that affect seismic modulus of asphalt concrete pavements. The laboratory tests are separated into two phases. In the first phase, the sensitivity of seismic modulus to mix properties at room temperature was studied. The influence of temperature was studied during the second phase. After the laboratory evaluation, field tests were carried out using the PSPA. Six pavement models with varied gradation, VTM, and layer thickness were prepared and tested for verification purposes. A description of the materials, preparation of laboratory briquettes, laboratory experimental setups, and testing procedures are also presented. The final section contains a description of field test setup and testing procedures.

4.2 Laboratory Testing

The laboratory tests were performed using a V-Meter to generate compression waves through AC briquettes. The seismic modulus of the AC briquette was calculated using the travel times, length, and mass density of the briquette.

Using this approach, the sensitivity of seismic modulus to AC mix properties was studied. The parameters investigated were the gradation, viscosity of the asphalt, voids in total mix (VTM), and temperature.

4.2.1 Materials

Three local asphalt concrete mixtures were used in the study. The mixtures are called Types B, C, and D under Texas Department of Transportation (TXDOT) specifications. A typical job mix formulae that complied with the master grading specified by TXDOT standards was used for each mix design. The Jobe Concrete Company in El Paso provided the job mix

formulae and aggregates for the mixes. Three types of asphalt grades obtained from the Chevron refinery in El Paso were used in the study.

A summary of the mixture properties is shown in Table 4.1, and the gradations of three mixes are shown in Figure 4.1. More comprehensive information about each mix type may be found in Appendix B.

Table 4.1- Mixture Properties

Mix Type	Type-B (Coarse)	Type-C (Medium)	Type-D (Fine)
Asphalt Grade	AC-20	AC-20	AC-20
Asphalt Content	4.0%	4.5%	5.0%
Aggregate Type	Limestone	Dolomite	Limestone
Percent Coarse Aggregate	63%	60%	60%
Percent Screenings	25%	28%	30%
Percent Sand	12%	12%	10%

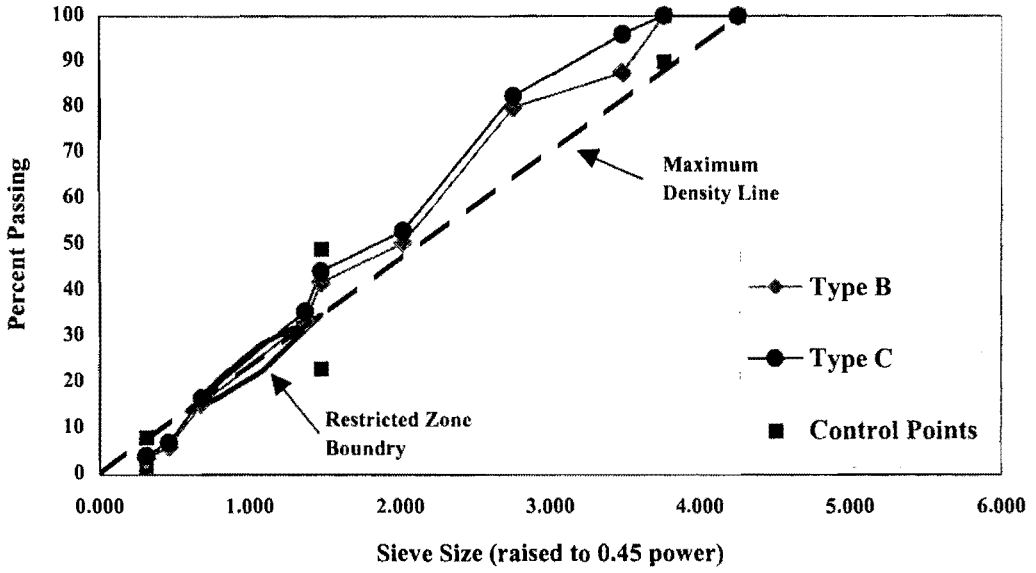

a) Type B and C

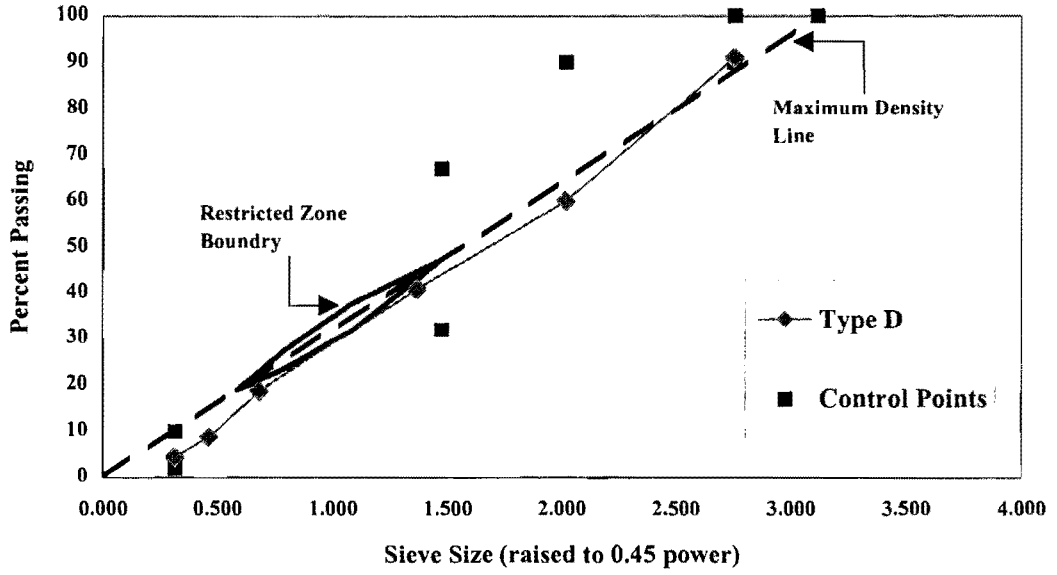

b) Type D

Figure 4.1– Mix Gradations

4.2.2 Briquette Preparation

A Strategic Highway Research Program (SHRP) gyratory compactor was used to prepare the briquettes. The briquette preparation process was the same in Phase I and in Phase II. An outline of the briquette preparation procedure is presented in Table 4.2. A comprehensive protocol for laboratory preparation and testing of AC briquettes is provided in Appendix B.

4.2.3 Seismic Experimental Setup

A picture of the test setup is shown in Figure 4.2. As indicated in Section 3.2, a V-Meter was used to generate compression waves through an AC briquette. As shown in Figures 4.2, apart from the V-meter, the test setup contains a spring supporting system, holding plate, loading bar, and a calibration bar. The spring supporting system is located in the holding base to support the receiving transducer and to ensure that there is appropriate pressure and contact between the AC briquette and the transducer. The holding plate and the loading bar are located in the top portion on the testing setup. The sole purpose of the holding plate is to align the transmitting transducer with the receiving transducer and to apply pressure. The loading bar is 50 mm in diameter and 75 mm in length; it accommodates the transducer cable through a 15-mm diameter hole and is placed on top of the transmitting transducer. The loading bar allows the operator to apply pressure to the transmitting transducer to ensure full coupling between the AC briquette and the transducer. The calibration bar, which is supplied with the V-Meter, is used to calibrate the V-Meter before each set of AC briquettes is tested. The holding device is designed to conveniently test AC briquettes at high temperatures. This test setup allows the operator to perform a test in under a minute.

Table 4.2- Briquette Preparation Procedure

Step	Procedure
1	**Sample asphalt binder in accordance with AASHTO-T40** - Determine the ranges of mixing and compaction temperatures for AC mix from the temperature-viscosity plot: (Measure Viscosity at Temp. 135,160,180 °C) 1.) Mixing temperatures should be selected to provide a viscosity of 170 ± 20 centistokes 2.) Compaction temperatures should be selected to provide a viscosity of 280 ± 30 centistokes.
2	**Sample aggregates in accordance to AASHTO-T2**
3	**Prepare the asphalt concrete mixtures in accordance to AASHTO-TP4.** - Mixture should be sufficient for two-specimens of final compacted dimensions equal to 100 ± 2 mm in diameter by 100 ± 4 mm in length (length depends on gyrations)
4	**Subject AC mixtures to short-term aging in accordance with PP2 (SHRP 1025)**
5	**Compact AC mixture in accordance to AASHTO-TP4.** - Prepare several AC briquettes with VTM between 2 to 12 percent.
6	**Cool AC briquettes for 24 to 48 hours at room temperature (25 ± 3°C).**
7	**Measure the diameter and length of AC briquettes at three locations.** - Make measurements at top, middle, and bottom of briquette. - Or use ASTM D3549 - Record average diameter and length (± 0.1 mm).
8	**Perform Seismic Tests with V-Meter.** - Perform tests as described in Appendix C.
9	**Determine VTM and Rice Specific Gravity of AC briquettes and mixture.** - Perform tests in accordance to ASTM D 3203 and ASTM D 2041.

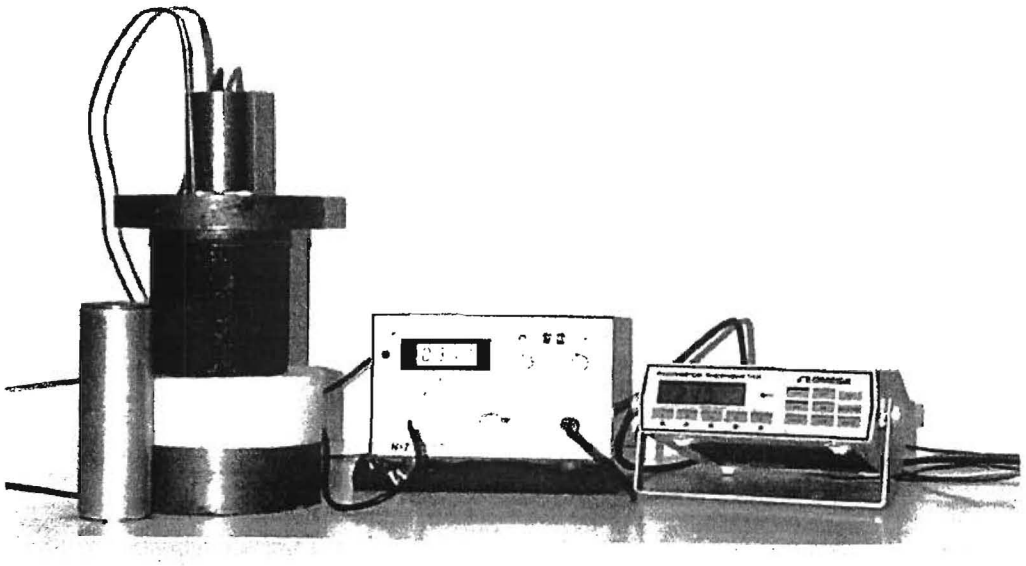

Figure 4.2 –Picture of Laboratory Setup

4.2.4 Temperature Study Experimental Setup

The seismic test setup for the temperature study was the same as the test setup described in Section 4.2.3, with the exception that the AC briquette was placed in a temperature controlled chamber before testing (Figure 4.3). The temperature chamber has an operating range of -50^0C to 150^0C.

An AC briquette was subjected to a sequence of temperatures (-5^0C, 5^0C, 15^0C, 25^0C, 35^0C, and 45^0C) for a four hour period at each temperature. However, for six AC briquettes, the temperature was first increased from -5^0C to 45^0C and then decreased from 45^0C to -5^0C. At the end of each temperature period, the internal briquette temperature was measured, and a seismic test was performed on the briquette.

The internal briquette temperature was monitored through a second AC briquette, as shown in Figure 4.4. A thermocouple, insulated with silicone at the exposed surface, was placed at the center of the briquette to monitor the temperature.

This approach was taken to determine the modulus-temperature relationships, which are extremely important for the implementation of a practical modulus-based QA/QC program.

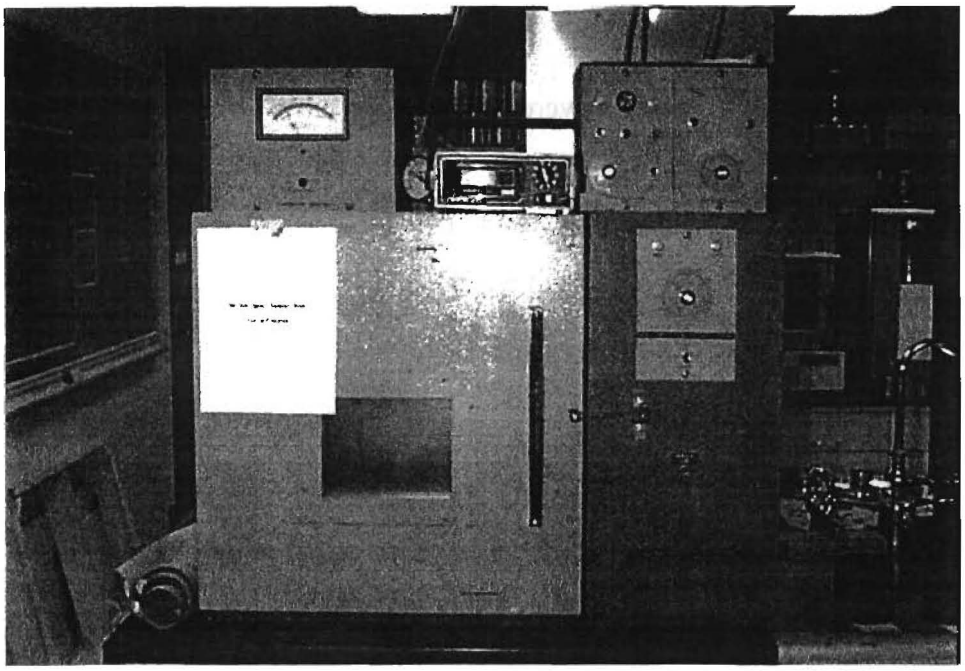

Figure 4.3 –Picture of Temperature Study Experimental Setup

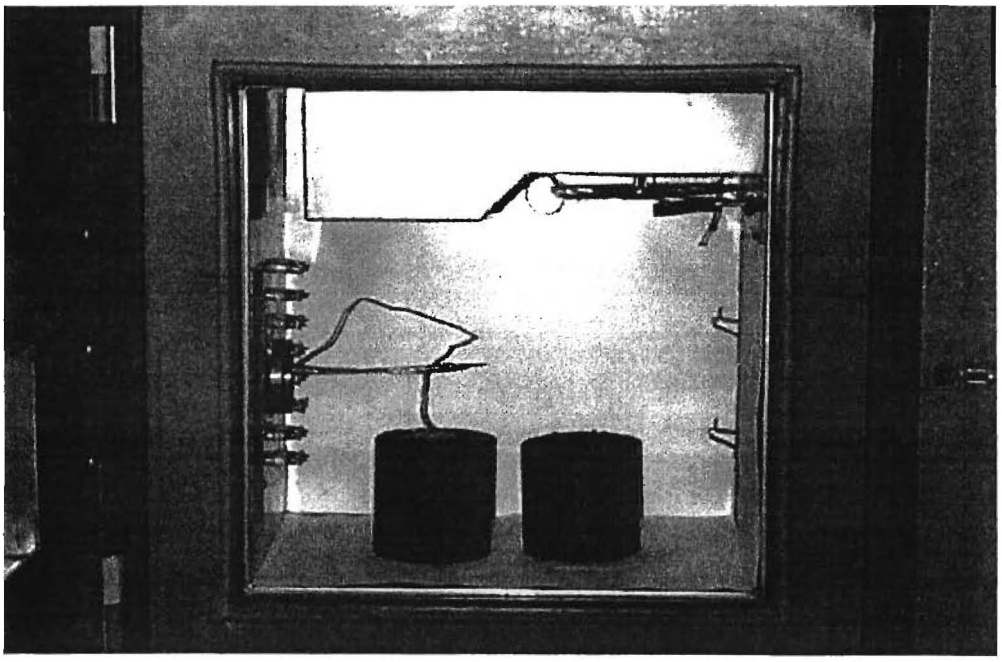

Figure 4.4 –Temperature Monitoring Setup

4.2.5 Testing Procedures

The test matrix for Phase I and Phase II is shown in Table 4.3. In Phase I, 14 briquettes with VTM ranging from 2 to 12 percent were prepared for each of the six mix types described in Table 4.3.

In the first three mixes, the asphalt grade was kept constant, but the gradation was changed. For the last three mixes, the gradation was kept constant and the asphalt grade was varied. This procedure was used to investigate the sensitivity of seismic modulus to aggregate gradation and asphalt grade. After 24 hours, the seismic modulus for each briquette was measured using the V-meter.

Table 4.3- Phase I and II Test Matrix

Mix Type	Asphalt Content %	Max. Sieve Size mm (in.)	Asphalt Grade
B (Coarse)	4.0	25.0 (1.0")	AC-20
C (Medium)	4.5	22.0 (0.9")	AC-20
D (Fine)	5.0	12.5 (0.5")	AC-20
D (Fine)	5.0	12.5 (0.5")	AC-30
D (Fine)	5.0	12.5 (0.5")	AC-20
D (Fine)	5.0	12.5 (0.5")	AC-10

Similarly, in Phase II, seismic tests were performed on mixtures with different gradation and viscosity of asphalt. However, a total of seventeen briquettes, about ten at a 4 % VTM and seven at an 8 % VTM (nominal), were prepared and tested at different temperatures.

4.3 Seismic Field Testing

The experimental setup for field study was a controlled process from pavement model construction to PSPA testing. The pavement models were constructed in wooden boxes with a wall thickness of 20 mm and inner dimensions of 600 mm (width) x 850 mm (length) x 350 mm (depth). The boxes were lined with 6-mil plastic sheeting to prevent moisture loss and deterioration of the wood.

To simulate an actual pavement section, a three-layer pavement system was constructed in each model. A cross-sectional schematic of one of the pavement models is shown in Figure 4.5. In each model, a 75-mm layer of sand was placed at the bottom, followed by a 200-mm layer of base course with average dry density of 20 kN/m^3. In addition, a thin layer of emulsion was placed on top of the base course layer 24 hours prior to placing the AC layer, to provide bonding between the two layers.

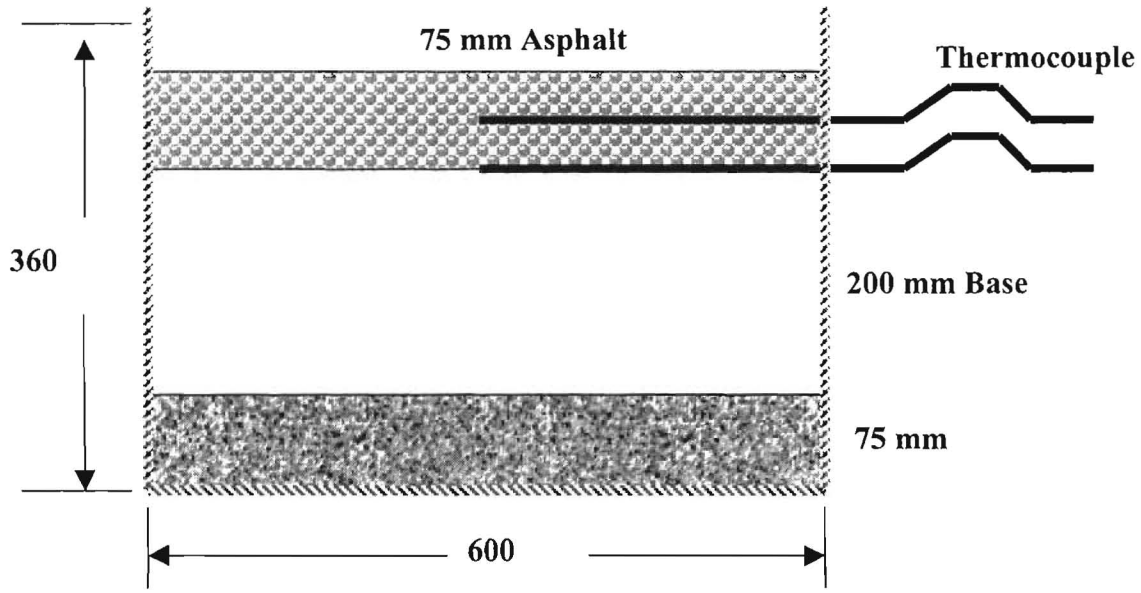

Figure 4.5 –Schematic of Pavement Models

The AC layer was constructed under a controlled process. First, a pre-weighted amount of asphalt concrete was heated to 150 ^{0}C for a four hour period and mixed every hour during this period. Then, the asphalt concrete was placed on top of the base course layer in 25-mm lifts. Once the mix was spread evenly on the surface of the base, it was initially tampered with a hot manual foot compactor and, finally, with a mechanical vibratory compactor. Each time, the same process was followed until the AC material was compacted to a marked reference line on the box to control the thickness of the pavement mat. During the compaction process, care was taken to monitor the pavement temperature through two thermocouples, which were placed at the bottom of the AC layer and at mid-depth. Furthermore, the surface temperature of the AC layer was also monitored with a temperature probe.

The AC layer properties for the six pavement models are shown in Table 4.4. The table is separated into three sections. For the first three models, the depth of the AC pavement was kept constant, but the gradation was changed. For the next three models, their gradation was kept constant, and the pavement depth was varied. In the last section of the table, two pavement models with different mix types and pavement depths greater than 150 mm were constructed.

This approach was taken to evaluate the limitations and sensitivity of PSPA measurements in a controlled environment.

4.3.1 Testing Procedures

A picture of the field tests experimental setup is shown in Figure 4.6. The pavement models were tested at room temperature using the PSPA at 5 to 13 points. The points were generally located in the central area of the pavement surface with a clearance of 125 to 150 mm all around the edges of the box to avoid wall reflections. Three to five consecutive measurements were taken at and around each point. The pavement temperature was also monitored during testing through the embedded thermocouples.

Once the PSPA data collection was complete, the pavement models were cored at the test points. The disturbed end of the AC cores was finished with a cutting saw and was allowed to air dry for a period of 48 hours. The direct wave travel-time of each of the AC cores was then measured in the laboratory with the V-Meter. The air void content was also measured.

Table 4.4- Summary of Pavement Models

Pavement Model	Mix Type (%)	Pavement Nominal Depth (mm)
11a*	B (Coarse)	75
2	C (Medium)	75
1	D (Fine)	75
5	D (Fine)	50
4	D (Fine)	65
1	D (Fine)	75
11b*	B (Coarse)	180
7	D (Fine)	150

* Pavement model was repaved

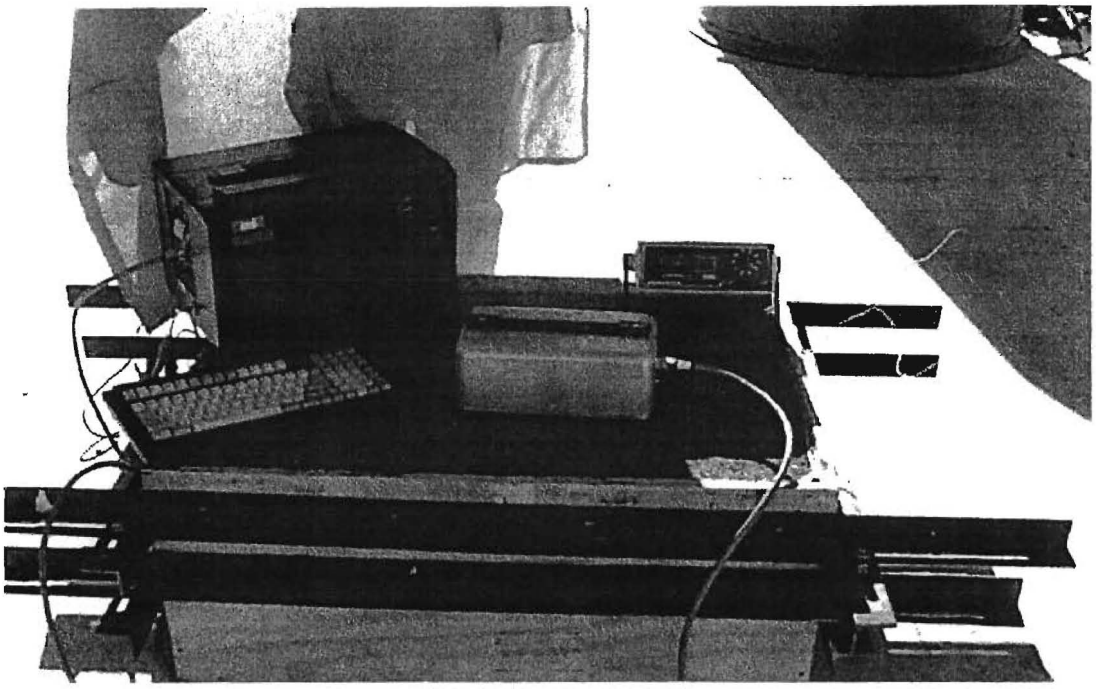

Figure 4.6 –Picture of Field Test Experimental Setup

Chapter 5

Results and Discussion

5.1 Introduction

The results from the seismic laboratory and field tests are presented in this chapter. In addition, two case studies that demonstrate the use of these methods are also discussed. The results from Phase I laboratory study are presented first, followed by the results from Phase II (temperature study). In section four, the results from the field study are discussed. Finally, the two case studies are presented in section five.

5.2 Results from Seismic Laboratory Method

As mentioned before, the objective of the seismic laboratory study was to investigate the impact of parameters such as the gradation, viscosity of the asphalt, voids in total mix (VTM), and temperature on seismic modulus.

5.2.1 Influence of Voids in Total Mix

The main objective of this task was to establish a relationship between the modulus of asphalt concrete briquettes and the VTM of the specimens. To achieve this objective, about fourteen specimens with a VTM range of 2 to 12 percent were prepared and tested for three different standard mixtures used by TXDOT.

A typical variation in modulus with VTM for one mixture is shown in Figure 5.1. A linear trend can be observed between the modulus and VTM. This trend indicates that the modulus is inversely proportional to VTM. As the VTM increases, the modulus decreases. The least-squares best-fit line to the measured data is also included in Figure 5.1. A good agreement between the measured and fitted results is observed. The correlation coefficient (R^2-value) is about 0.90, indicating that the fitted data describes the measured data reasonably well.

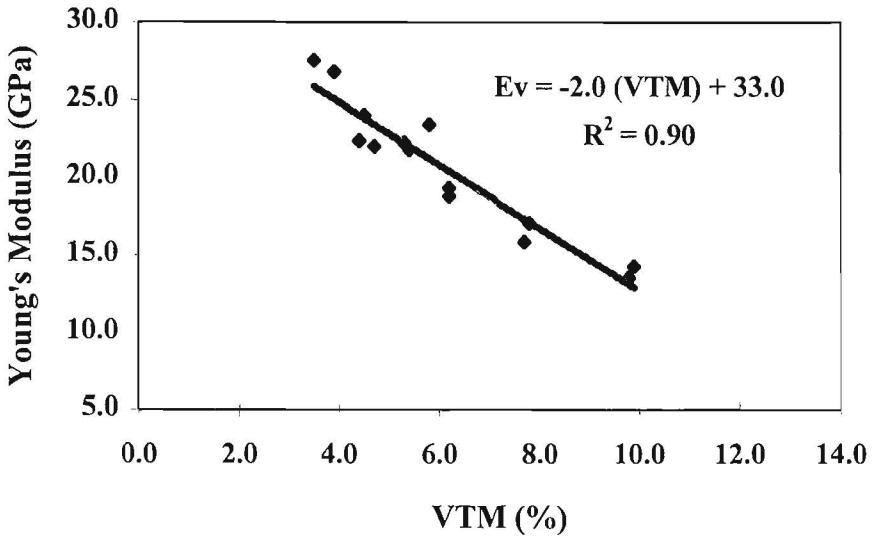

Figure 5.1-Typical Variation in Young's Modulus with VTM

The data used to establish the relationship between the modulus and VTM for each mix is included in Appendix E for closer observation. The results from the three mixtures are summarized in Table 5.1. The R^2-values in all cases are above 0.90, indicating that the relationship between the modulus and VTM can be considered linear with a reasonably good approximation and independent of the gradation (mixture type).

5.2.2 Impact of Gradation

The variations in modulus with VTM for the three mixtures tested are summarized in Table 5.1 and shown in Figure 5.2. The intercepts of the lines, which correspond to the moduli at the theoretical maximum density, become larger as the mixture becomes coarser. For type B mix, the coarsest mixture, the intercept is about 33 GPa, whereas for Type D (fine) mix, the intercept is about 27 GPa.

Table 5.1-Variation in Modulus with VTM for Three Different Mixtures

Mix Type	Binder Grade	Slope (GPa/%)	Intercept (GPa)	R^2	Young's Modulus at 4 % VTM	Young's Modulus at 8% VTM
B (Coarse)	AC-20	-2.0	33.0	0.90	24.8	16.7
C (Medium)	AC-20	-1.6	31.0	0.94	24.6	18.2
D (Fine)	AC-20	-1.2	26.7	0.95	21.8	16.9

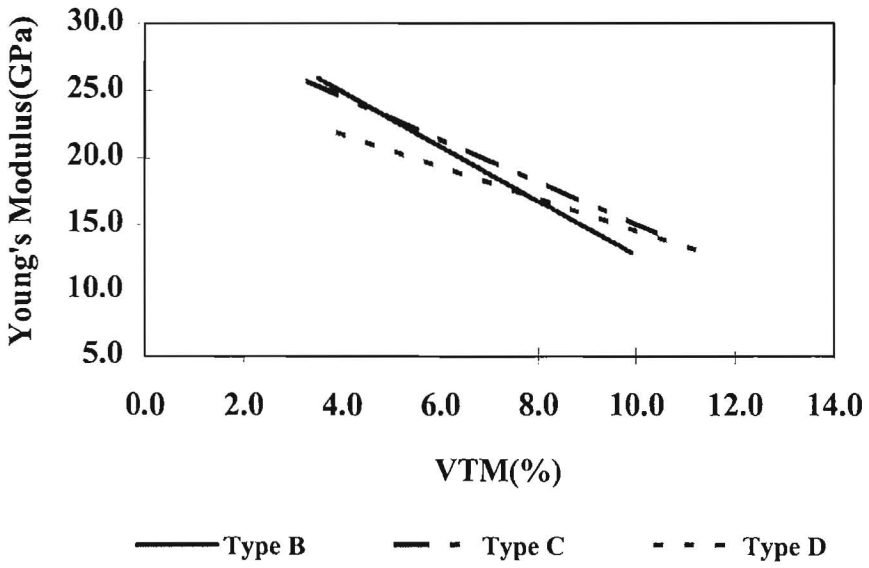

Figure 5.2-Variations in Modulus with VTM for Three Different Mixtures

The absolute value of the slope of the best-fit line also, typically, increases, as the mixture becomes coarser. For type B (coarse mix), the slope is about 2 GPa/percent VTM. For type D (fine mix), the slope is about 1.2 GPa/percent VTM. This trend indicates that the modulus decreases more significantly with increases in the VTM for the coarser mixtures.

The modulus values, at a nominal VTM of 4 percent (indicator of the design VTM of a mix) and 8 percent VTM (indicator of the laid-down VTM of the mat), are also shown in Table 5.1. At the VTM of 4 percent, the coarser mixtures generally exhibit higher moduli. This may occur because of the intimate grain-to-grain contact existing between the aggregates for coarser mixtures. However, at VTM of 8 percent the modulus from the coarser mixtures seems to be slightly lower. This may be an indicator of a less intimate structure of the coarser mixture in a looser state.

5.2.3 Impact of Viscosity

The impact of the binder viscosity on seismic modulus of the AC mixtures was similarly evaluated. The evaluation consisted of performing tests on briquettes with similar VTM's. Three different types of binder grades were used while the gradation was kept constant for the AC mixtures.

Typical variations in modulus with VTM for the three binder grades are shown in Figure 5.3. The trends indicate that the modulus is inversely proportional to the VTM. In addition, it may be observed that the modulus values are generally greater for the stiffer asphalt grades. As indicated in Table 5.2, the R^2-values are greater than 0.90, which indicates that the fitted line compares well with the measured data.

The intercepts of the lines, at a VTM of zero, become smaller as the binder grade (binder viscosity) decreases. For the mixtures with AC-30 binder, the intercept is about 30 GPa, whereas for AC-10 the intercept is about 24 GPa. At this level of VTM, all the voids are theoretically filled with binder, therefore it is reasonable to say that they significantly impact the modulus of the mixture.

As shown in Table 5.2, the absolute value of the slopes of the best fit lines decrease as the binder viscosity decreases. For AC-30 binder, the slope is about 1.4 GPa/percent VTM, and for AC-10 binder, it is about 1.1 GPa/percent VTM. This indicates that the effects of the VTM on modulus are more pronounced for stiffer binder than softer binders.

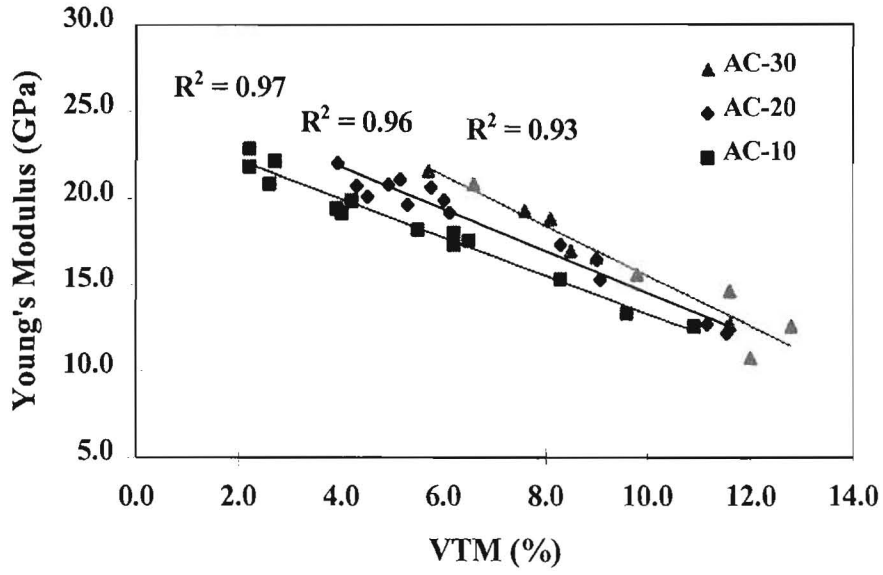

Figure 5.3-Typical Variation in Young's Modulus with VTM

Table 5.2-Variation in Modulus with VTM for Three Asphalt Grades

Mix Type	Binder Grade	Slope (GPa/%)	Intercept (GPa)	R^2	Young's Modulus at 4 % VTM	Young's Modulus at 8% VTM
D (Fine)	AC-30	-1.4	30.0	0.93	24.2	18.4
D (Fine)	AC-20	-1.2	26.7	0.96	21.8	16.9
D (Fine)	AC-10	-1.1	24.4	0.97	20.0	15.5

The predicted modulus values at 4 percent and 8 percent VTM are also listed in Table 5.2. At a 4 percent VTM, the modulus is greater for the stiffer binder grade. Although, these differences are not as pronounced at the intercept values (i.e., theoretical maximum density). This trend occurs because the binder becomes softer as the binder grade decreases. The modulus values are an indicator that a more rigid structure, between the binder and the aggregate, occurs for higher binder grades at room temperature. The modulus values ranged from about 24 GPa to about 20 GPa for AC-30 to AC-10, respectively.

At an 8 percent VTM, a similar trend in the tabulated modulus values can be observed. However, the modulus values are lower (impact of binder grade becomes less pronounced), when compared to values at a 4 percent VTM. This is due to a less intimate contact between the binder and aggregates. For an 8 percent VTM, the modulus values ranged from about 18 GPa to about 16 GPa for AC-30 to AC-10, respectively. This indicates that at higher VTM's the influence of binder viscosity on seismic modulus is not as significant.

5.3 Influence of Temperature

The objective of Phase II was to establish a relationship between the modulus of AC briquettes and temperature. Furthermore, the influence of changing the gradation and binder grade was also evaluated.

In order to establish a relationship, seventeen AC briquettes, about ten at a 4 percent VTM (nominal) and seven at an 8 percent VTM (nominal), were prepared for six AC mixtures. The briquettes were subjected to a sequence of temperatures ranging from -5°C to 45°C to –5°C; that is, the temperature was first increased from -5°C to 45°C and then deceased from 45°C to –5°C. However, for most AC briquettes the temperature was only increased from –5°C to 45°C. At the end of each temperature sequence, the AC briquette was tested.

Typical variations in modulus with temperature, at 4 and 8 percent VTM, are shown in Figure 5.4. In both cases, the modulus decreased with an increase in temperature. For briquettes prepared at a 4 % VTM, the moduli compared well for both cases (i.e., for a decrease as well as an increase in temperature). The moduli, from the briquette prepared at a 4 % VTM, for the cases when the temperature was increased compared reasonably well with those when the temperature decreased. The modulus values ranged from about 26 GPa to 45 GPa. However, for the briquette prepared at an 8 % VTM, some differences in the moduli can be observed when the temperature was increased as compared with when it was decreased. It is believed that experimental error is the cause of this trend. The modulus values for this case ranged from about 20 GPa to 12 GPa. In addition, one may observe from these trends that the measured modulus values decrease by a factor of about 3 when the temperature varied from –5°C to 45°C.

For both briquettes, a linear trend may also be observed between the modulus and temperature. A linear trend line, fitted to the data, is also shown for both cases. The correlation coefficient (R^2) value is greater than 0.91, which indicates that at the tested temperatures the relationship between modulus and temperature can be considered linear. The data associated with the –5°C were not included in the determination of the best-fit line, since performing QA/QC at temperatures below 5°C would be unlikely.

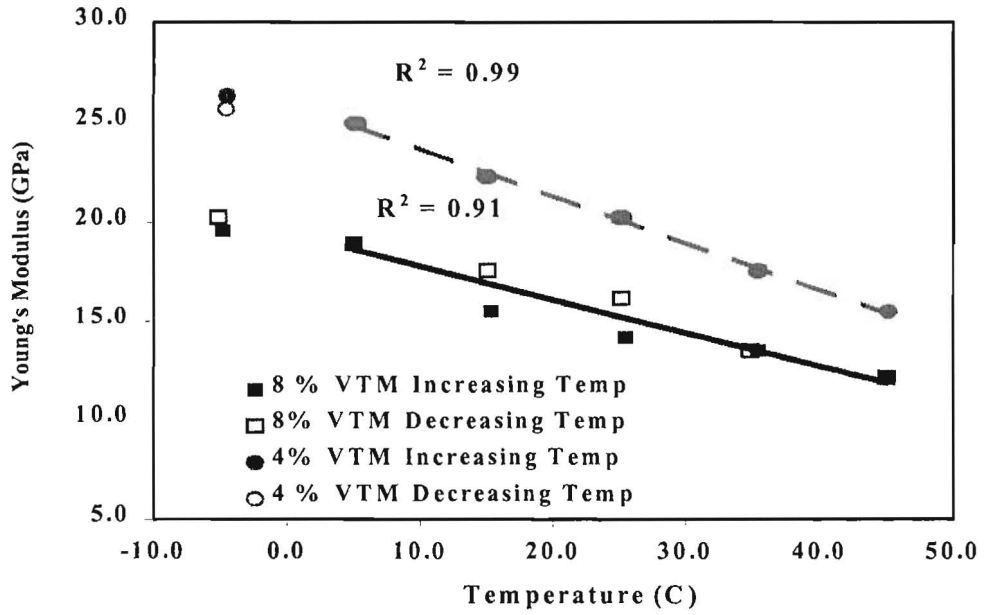

Figure 5.4-Variation in Young's Modulus with Temperature

5.3.1 Influence of Gradation

Using a similar analysis approach, the influence of gradation on temperature sensitivity of modulus was evaluated. The analysis results of the three mixes with different gradations at a 4 percent VTM are summarized in Table 5.3. The correlation coefficient (R^2) values are greater than 0.95, indicating that the fitted lines describe the data reasonably well. The rates of change in modulus with temperature for the mixtures are also shown in Table 5.3. The rates of change for the mixtures range from about 206 MPa/ °C to 216 MPa/ °C. The calculated average and standard deviation for the rates of change in modulus with temperature are also presented on Table 5.3.

Table 5.3- Impact of Gradation on Modulus-Temperature Relationship at 4% VTM

Mix Type	Asphalt Grade	Asphalt Content (%)	R^2	Rate of Change in Modulus (MPa/ °C)
B (Coarse)	AC-20	4.0	0.97	215
C[1] (Medium)	AC-20	4.5	0.97	206
D[2] (Fine)	AC-20	5.0	0.99	216
Average (Standard Deviation)				212 (6)

[1] Modulus-Temperature relationship is based on an average of two AC briquettes

[2] Modulus-Temperature relationship is based on an average of four AC briquettes

Table 5.4- Impact of Gradation on Modulus-Temperature Relationship at 8% VTM

Mix Type	Asphalt Grade	Asphalt Content (%)	R^2	Rate of Change in Modulus (MPa/ °C)
B (Coarse)	AC-20	4.0	0.99	188
C[1] (Medium)	AC-20	4.5	0.99	164
D[1] (Fine)	AC-20	5.0	0.97	160
Average (Standard Deviation)				171 (15)

[1] Modulus-Temperature relationship is based on an average of two AC briquettes

Similarly, the results for the same three mixtures at an 8 percent VTM are tabulated on Table 5.4. The R^2 values for the relationships are about 1.0, which again indicates that the fitted lines describe the data relatively well. The rates of change in modulus are also presented in Table 5.4 and range for about 160 MPa/ °C to 188 MPa/ °C. The calculated average and standard deviation for the rates of change in modulus were 171 MPa/ °C and 15 percent, respectively.

In general, the tabulated results, presented in Tables 5.3 and 5.4, indicate that the modulus-temperature relationships describe the fitted data for AC briquettes prepared at both levels of VTM. The rates of change in modulus with temperature are relatively higher for briquettes prepared at a 4 % VTM as compared with those prepared at 8%. This trend indicates that perhaps the rate of change in modulus is primarily dependent on the degree of compaction and relatively independent of the aggregate top size. The calculated standard deviation of AC briquettes prepared at 4 % VTM is less than 10 percent of the average. This result may implicate that the same modulus temperature relationship may be used for mixtures with relatively different gradation, but the same asphalt binder type.

5.3.2 Influence of Asphalt Viscosity

The impact of changing the asphalt viscosity (asphalt grade) on the modulus-temperature relationship was similarly investigated. The results for three mixes with different asphalt grades and constant gradation at a 4 % VTM and at an 8 % VTM are summarized in Table 5.5 and Table 5.6. In both cases of VTM, the R^2 values are about 1.0, indicating good agreement between the fitted and measured data.

The rates of change in modulus with temperature are also shown in the tables for both cases. The rates of change in modulus range from about 270 MPa/ °C to 214 MPa/ °C for AC briquettes prepared at a 4 % VTM. At an 8 % VTM, the rates of change in modulus range from about 217 MPa/ °C to 186 MPa/ °C. In general, for each case, the rate of change in modulus with temperature increases as the asphalt binder (asphalt grade) becomes stiffer, with the exception of AC-10 at 8% VTM. Besides possible experimental errors or variation in the asphalt consistency, the estimated value of the rate of change in modulus for AC-10 is unknown.

The calculated average and standard deviation for the rates of change in modulus for each case are also tabulated on Tables 5.5 and 5.6. In general the standard deviation in both cases is approximately 30 percent higher than the average. This result may indicate that a modulus temperature correction is influenced more by the asphalt binder type than by the gradation of the AC mix.

5.4 Results from Seismic Field Method

As mentioned before, in Phase III, the objective of the field study was to investigate the limitations and sensitivity of PSPA measurements in a controlled environment. In order to fulfill this objective, seismic tests were performed on six pavement models with different gradation, VTM, and thickness. The pavement models were cored after PSPA tests to compare the laboratory seismic moduli measured directly on cores with those determined with the PSPA.

Table 5.5- Impact of Viscosity on Modulus-Temperature Relationship at 4% VTM

Mix Type	Asphalt Grade	Asphalt Content (%)	R^2	Rate of Change in Modulus (MPa/ °C)
D (Fine)	AC-30	5.0	0.99	270
D[1] (Fine)	AC-20	5.0	0.99	216
D[2] (Fine)	AC-10	5.0	0.99	214
Average (Standard Deviation)				233 (32)

[1] Modulus-Temperature relationship is based on an average of four AC briquettes
[2] Modulus-Temperature relationship is based on an average of two AC briquettes

Table 5.6- Impact of Viscosity on Modulus-Temperature Relationship at 8% VTM

Mix Type	Asphalt Grade	Asphalt Content (%)	R^2	Rate of Change in Modulus (MPa/ °C)
D (Fine)	AC-30	5.0	0.99	217
D[1] (Fine)	AC-20	5.0	0.97	160
D[1] (Fine)	AC-10	5.0	0.99	186
Average (Standard Deviation)				188 (29)

[1] Modulus-Temperature relationship is based on an average of two AC briquettes

5.4.1 Influence of Gradation

The sensitivity of PSPA measurements to changes in gradation was evaluated by testing three pavement models with different mix types and a nominal constant thickness of 75 mm. The results are summarized in Table 5.7. The table shows the measured seismic moduli on cores in the lab and the measured seismic moduli on pavement models with the PSPA.

The average Poisson's ratio was estimated from the compression wave and the measured surface wave velocities of the AC layer. In general, the estimated Poisson's ratio ranged from 0.32 to 0.34 for the mixes.

From both the laboratory and PSPA results, the modulus increases, as the mixes become coarser. As before, this variation can be attributed to the change in gradation and to the relative increase in VTM as the mixes become coarser. The laboratory measured modulus varied from about 22 GPa to 15 GPa, and the PSPA modulus varied from about 21 GPa to 14 GPa.

In all three tested AC layers, the laboratory seismic modulus and the measured seismic modulus from the PSPA compared well. The comparisons between the laboratory and PSPA modulus resulted in a less than 10 percent difference in all three cases.

Table 5.7- Comparison of Field and Laboratory Tests Moduli

Mix Type	Average Core VTM (%)	Poisson's Ratio	Lab Young's Modulus (GPa)	PSPA Modulus (GPa)	Modulus Percentage Difference (%)
B (Coarse)	4.2	0.34	21.5[1] (6.2%)	20.7 (2.4%)	3.4
C (Medium)	10.0	0.32	16.5[2] (17.9%)	15.5 (4.7%)	6.1
D (Fine)	11.5	0.33	14.6 (1.6%)	14.1 (4.6%)	3.7

[1] Top number Corresponds to average and bottom number to coefficient of variation
[2] One Outlier was excluded from the average but included in the calculation of the coefficient of variation

In summary, the results indicate that the measurements made with the PSPA on the pavement models were sensitive to the changes in gradation and VTM content. In addition, approximately the same values are measured in the field and laboratory seismic tests.

5.4.2 Influence of Voids in Total Mix

The sensitivity of PSPA measurements to changes in VTM was evaluated by testing three pavement models with varied VTM and constant gradation. The ACP thickness varied from about 50 mm to 75 mm. The results are summarized in Table 5.8.

The VTM was measured from the cores taken from the pavement models. The measured VTM ranged from 11.5 percent to 5.5 percent. The estimated Poisson's ratio was about 0.33 for the three ACP models.

From Table 5.8, the measured laboratory and PSPA moduli decreased as the VTM increased. This variation was not observed between pavement models 1 and 2. This can perhaps be attributed to the fact that the specimens were fairly similar.

Similarly, in all ACP layers, the measured moduli, from the laboratory and from the PSPA, compared well. The comparisons between the laboratory and PSPA moduli indicate a less than 4 percent difference in moduli in all three cases.

Table 5.8- Comparison of Laboratory and Field Modulus Measured on Specimens with Different VTM's

Pavement Model No.	Mix Type	Average Core VTM (%)	Poisson's Ratio	Lab Young's Modulus (GPa)	PSPA Modulus (GPa)	Modulus Percentage Difference (%)
1	D (Fine)	5.6	0.33	18.9	18.7	1.1
2	D (Fine)	6.6	0.33	19.0	18.7	1.6
3	D (Fine)	11.5	0.33	14.6	14.1	3.7

Figure 5.5 shows the comparison of the predicted laboratory moduli determined from AC briquettes of the same mix with moduli measured with the PSPA on the three ACP models. A linear relationship between the measured PSPA modulus and the VTM is observed. The two relationships are fairly similar. The differences between the laboratory and PSPA modulus decreases as the VTM increases.

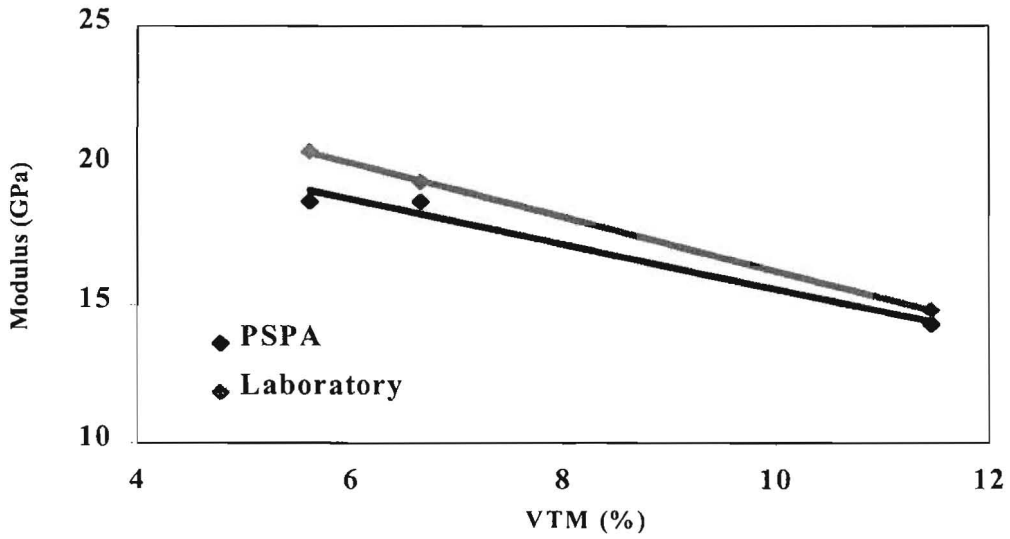

Figure 5.5-Variation in Measured and Predicted Modulus with VTM

5.4.3 Influence of AC Layer Properties

The impact of AC layer thickness on PSPA measurements was evaluated by testing two ACP models with a thickness of about 150 mm and 175 mm. The results are summarized in Table 5.9. The measured VTM was about 3.5 percent and 4.5 percent for the two models. At this VTM, the mixture is in a dense state, and an intimate grain to grain contact exists between the aggregates.

The measured Poisson's ratios were 0.35 and 0.38 for ACP models 1 and 2, respectively. At these values, the laboratory and field moduli are quite close. However, if the Poisson's ratios were assumed to be 0.33, the percentage difference in modulus for the laboratory and PSPA moduli would be approximately 11 percent and 25 percent. This matter demonstrates the importance of determining Poisson's ratio rather precisely.

The measured modulus values from PSPA tests and from laboratory tests on cores are also shown on Table 5.9. For each pavement model (1 and 2), the measured laboratory and PSPA moduli compared well. The comparisons between the laboratory and PSPA modulus resulted in a less than 2 percent difference for each ACP model. In general, the results demonstrate that the thickness of the ACP models did not influence the measured seismic modulus for each method.

Table 5.9- Comparison of Field and Laboratory Moduli on ACP Models with Different Thickness

Pavement Model No.	Mix Type	Average Core VTM (%)	Poisson's Ratio	Lab Young's Modulus (GPa)	PSPA Modulus (GPa)	Modulus Percentage Difference (%)
1	B (Coarse)	3.6	0.35	19.5	19.3	1.1
2	D (Fine)	4.6	0.38	10.1	10.4	-2.9

The relatively higher Poisson ratio value and lower modulus for pavement model 2, as compared with those measured in Table 5.8, were attributed to changes in the properties of the ACP layer. A typical AC core from ACP model 2 is shown in Figure 5.6. From this figure, one may observe that there is dissimilarity in the core texture and asphalt binder consistency. In order to verify these observations, each of the ACP model cores was split at the observed change in texture boundary and was tested individually with the V-Meter in the laboratory.

Figure 5.6-Typical ACP Model No. 2 Core

The measured seismic modulus values for each of the top and bottom cores (i.e., top half and bottom half of each individual core) for specific points on the pavement model are shown in Figure 5.7. From the figure, it may be observed that, generally, for the top 75 mm of ACP layer, the modulus values are greater than those of the bottom 75 mm. The average modulus values were about 12 GPa to 9.5 GPa for the top and bottom of the ACP layer, respectively. From these results, it may be concluded that seismic measurements were also sensitive to changes in the ACP model properties.

The measured PSPA and laboratory modulus values (i.e., for the tested 150-mm cores) for each point of the ACP model is also shown in Figure 5.7. From the figure it may be observed that, in general, the PSPA and laboratory modulus values are between the average top and bottom core modulus values, with the exception of points 3 and 7. Other than experimental error, the reason for this result is unknown.

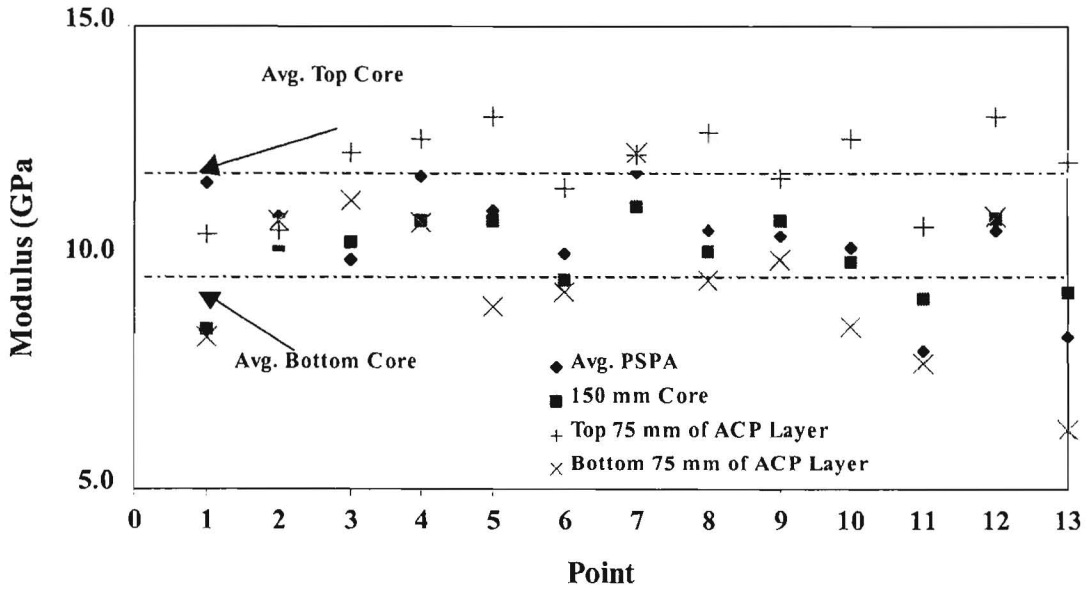

Figure 5.7-Variation in Modulus for ACP Model No. 2

These results indicate that an average property is typically measured by the seismic methods. However, it has been shown that the methods may be used to distinguish between changes in properties in ACP layers. The data of the seismic field study is presented in Appendix G.

5.5 Case Studies

The following two sections contain the results of two case studies performed in Texas. The case studies present the results of the field implementation of the seismic methods to determine the seismic modulus of two AC pavement roads.

5.5.1 El Paso Case Study

A 1.1-km section of Doniphan Road, which is a collector near IH-10, was tested with the seismic methods to compare the field and laboratory measured moduli of the ACP. The pavement section consisted of about 100 mm of Type B mix with an asphalt content of 3.9 percent and 3.0 percent of anti-stripping agent by weight. The pavement section was divided into four sublots, each about 0.28 km in length.

For QC/QA measures, two cores were taken at random locations within each sublot. The cores were tested in the laboratory using the V-meter to determine the modulus of the cores. The PSPA was then utilized near the coring locations to determine the seismic modulus of the ACP layer at each point. In addition, the pavement surface and air temperature was monitored during testing.

The results of the measurements are tabulated in Table 5.10. In general, the ACP surface temperature ranged from about 22 ^{0}C to 24 ^{0}C. The estimated Poisson's ratio varied from about 0.33 to 0.37, with an average of 0.35.

The measured laboratory modulus from cores and PSPA are also presented in Table 5.10. In general, it may be observed from the table that the laboratory and PSPA modulus compared fairly well, with a less than 10 percent difference. The average laboratory and PSPA moduli were about 17.5 GPa.

This preliminary study indicated that the measured values of the methodology in the field were fairly consistent with the results obtained in the laboratory on cores.

5.5.2 Odessa Case Study

The Odessa case study was a more comprehensive investigation utilizing the seismic methods. A 45-meter section of an access road of Highway 20 near Odessa was tested with the seismic methods. The pavement section consisted of 50 mm of AC over about 250 mm of base over subgrade. The AC mix was Type D (fine) with an asphalt content of about 5.4 percent. The gradation of the mix is presented in Appendix G.

Table 5.10-Comparison of Field and Laboratory Moduli for El Paso Case Study

Test Point	Mix Type	Measured ACP Surface Temperature (°C)	Estimated Poisson's Ratio	Average Lab Modulus (GPa)	Average PSPA Modulus (GPa)	Modulus Percentage Difference (%)
1	B (Coarse)	23	0.34	15.9	17.5	-10.0
2	B (Coarse)	23	0.37	17.8	16.4	7.8
3	B (Coarse)	22	0.33	19.3	18.5	4.1
4	B (Coarse)	24	0.34	16.8	18.0	7.1
Average			0.35	17.4	17.6	7.2

The first step of the study consisted of obtaining loose AC material to be used along the road. Subsequently, about fourteen briquettes were made using a SHRP gyratory compactor. As discussed before, the specimens were subjected to different numbers of gyration so those AC briquettes with different voids in total mix (VTM) could be prepared. The variation in seismic modulus with the VTM for these specimens is shown in Figure 5.8. A linear relationship between the modulus and the VTM can be observed. The least-squares best-fit line to the data yielded an R^2 of about 0.88, which indicated that the fitted line compared well with the measured data. From the figure, the compaction effort yielded VTMs between 5% and 10%, with associated modulus values ranging from about 17 GPa to 12 GPa.

The second step of the study consisted of performing field tests on the ACP sections. The measured variation in modulus of the ACP layer along the road, adjusted to a temperature of 25 ^{0}C, is shown in Figure 5.9. Since the composition of this mixture was close to El Paso District's Type D mixture, the modulus temperature correction from that

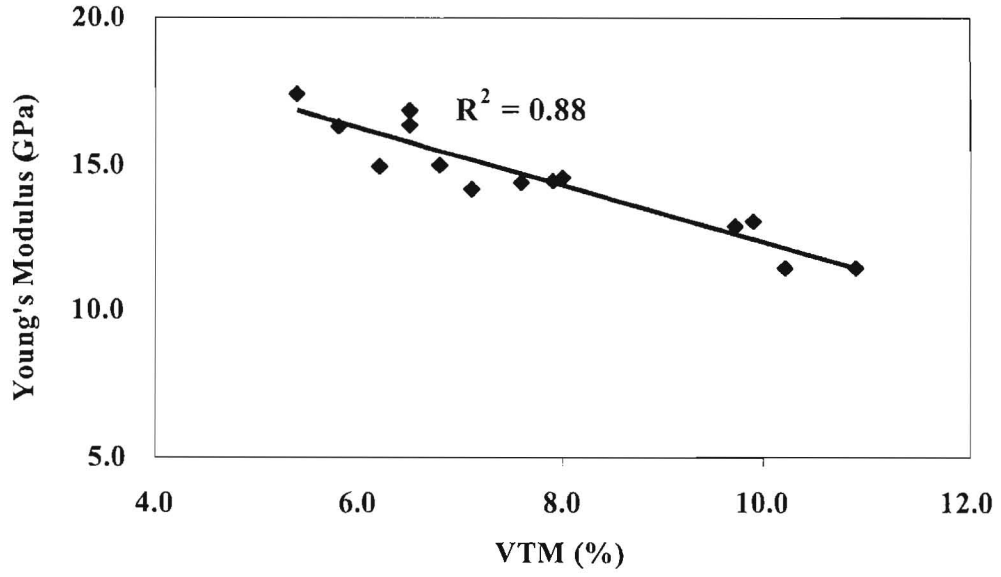

Figure 5.8-Variation in Young's Modulus with VTM for Odessa Material

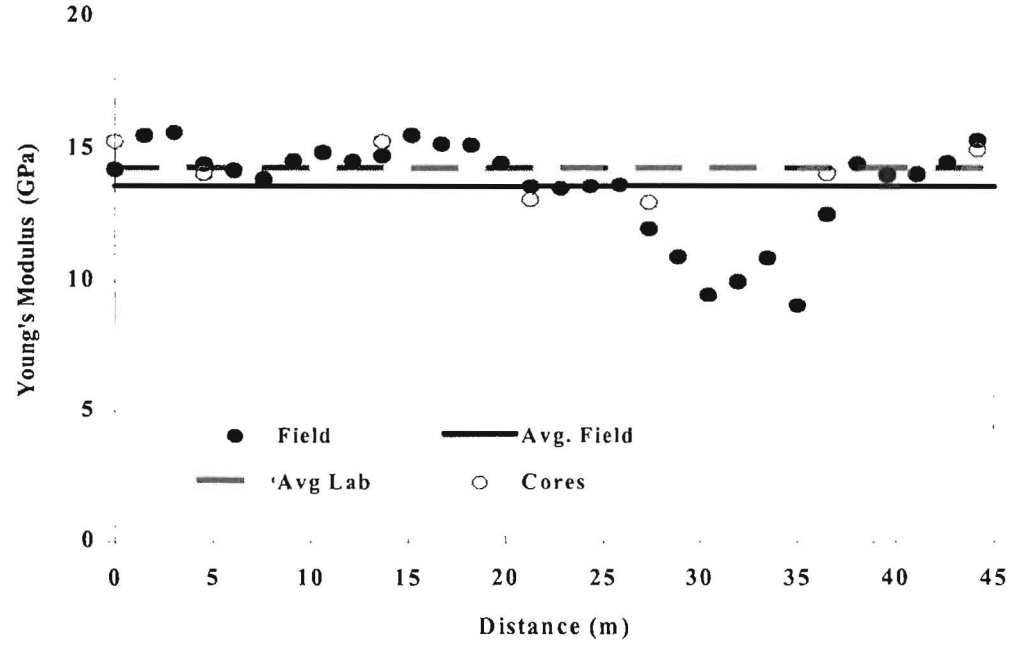

Figure 5.9 -Variation in Young's Moduli for Odessa ACP

material was adopted. The modulus values were fairly constant and were within the acceptable range of moduli, about 12 GPa and 17 GPa, except for an area between 27 m and 33 m. This area coincides with the entrance to a business where a new drainage pipe was installed. On an average, the modulus of the AC layer was about 13.8 GPa when all points were included and 14.9 GPa when the results from the area between 27 m and 33 m were ignored. Therefore, the area between 27 m and 33 m is substandard and should be considered for some type of improvement or penalty.

Seven cores, retrieved from the ACP at the site by TXDOT personnel, were also tested in the laboratory using the ultrasonic device. The average modulus from the laboratory tests, as shown in Figure 5.9, was about 14.3 GPa. The point by point comparison of moduli from the laboratory and from the field is also provided in Figure 5.9. The results from the two tests are quite close, with an average difference of about 4 percent and maximum difference of about 12 percent. The data and results of the case studies are presented in Appendix G.

After testing the cores, their VTM's were determined. The variation in modulus with VTM for the cores is demonstrated in Figure 5.10 along with the least-squares best-fit line through the data. In addition, the best-fit line, determined from the laboratory prepared AC briquettes shown in Figure 5.8, is also superimposed on Figure 5.10. The two best-fit curves are reasonably parallel but shifted. Such a systematic error (i.e., the shift) can perhaps be attributed to the differences in the compaction method, among other reasons. One can either use a different method of compaction that is more representative or perhaps use one or two field cores to calibrate the modulus-density relationship. This case study demonstrates the advantages of the proposed methodology, as well as some of the issues that have to be still addressed.

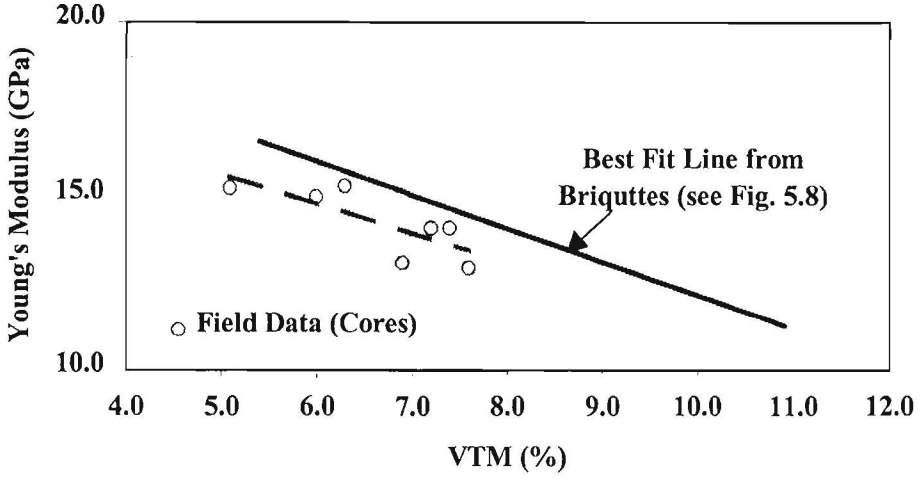

Figure 5.10 –Comparison of Modulus-VTM Relationship Obtained from Cores and AC Briquettes

Chapter 6

Conclusions and Recommendations

6.1 Conclusions

The main objective of this study was to present an economical quality management program based on seismic methods to determine the modulus of AC layers. More importantly, the goal was to understand the mixture parameters that affect the seismic modulus. The parameters investigated were the influence of the gradation, the viscosity of the asphalt, voids in total mix, and the temperature of the mixture. In the investigation, a seismic laboratory method and a field method using the PSPA were evaluated. The following conclusions may be drawn from this research:

1) AC seismic modulus is related to the void in total mix (VTM). The seismic modulus increases with a decrease in the VTM.

2) The gradation in AC mixtures affects the measured seismic moduli. Coarser mixtures are generally stiffer at a given VTM.

3) Seismic moduli are slightly affected by changes in binder viscosity (binder grade) of the AC mixtures. As the asphalt viscosity decreases, the seismic modulus decreases. However, the impact of the viscosity becomes less pronounced as the VTM increases.

4) The seismic modulus varied by a factor of 3 from temperatures of -5 to 45°C. In addition, a relationship dependent on VTM and on temperature may be developed easily in the laboratory to predict AC layer modulus.

5) The field study results indicated that PSPA measurements were sensitive to changes in mixture properties such as gradation, VTM, and changes in the quality of AC layers.

6) The ultrasonic surface wave and the ultrasonic body wave methods were effective in determining the modulus of AC layers.

7) Seismic moduli measured with the PSPA on pavement models and those measured on cores in the laboratory generally differed by less than 10%.

8) The presented case studies demonstrate that the PSPA may be equally and easily implemented in the field and that the seismic moduli measured on the ACP and cores compared very well.

In general, the seismic methods are feasible, would reduce the cost of a QA/QC program, and provide a fundamental material property that is related to the design parameters.

6.2 Recommendations for Future Research

1) A comprehensive evaluation of the seismic methods should be conducted to refine and optimize the protocol.

2) The influence of anti-stripping agents and additives like rubber on seismic modulus should be evaluated.

3) The seismic methods should be gradually implemented in the QA monitoring of AC pavements to better understand the unforeseen limitations.

References

1. AASHTO R 10-92 I (1992), "Definitions of Terms for Specifications and Procedures," Interim Specifications for Transportation Materials and Methods of Sampling and Testing, Part I Interim Specifications 1992, Washington, DC, AASHTO, pp. 67-70.
2. AASHTO (1996), "Quality Assurance Guide Specifications," AASHTO, Washington, DC, February.
3. Aouad, M. F., Stokoe, K. H., and Briggs, R. C. (1993), "Stiffness of Asphalt Concrete Surface Layer from Stress Wave Measurements," Transportation Research Board, No. 1384, Washington, DC, pp. 29-35.
4. Ayres, M. Jr. and Witczak, M. W. (1998), "AYMA-A Mechanistic Probabilistic System to Evaluate Flexible Pavement Performance," 77th Annual Transportation Research Board Meeting, Washington, DC.
5. Baker, M. R., Crain, K., and Nazarian, S. (1995), "Determination of Pavement Thickness with a New Ultrasonic Device," Research Report 1966-1, Center for Geotechnical and Highway Materials Research, The University of Texas at El Paso, Texas, August.
6. Baladi, G. Y. and Hanichandran, R. S. (1989), "Asphalt Mix Design and the Indirect Test: A New Horizon," Asphalt Mix Design: Development of More Rational Approaches, ASTM STP 1041, American Society for Testing and Materials, Philadelphia, Pennsylvania.
7. Benson, P. E. (1996), "Specifications of Asphalt Concrete Using Total Quality Management Principles," Transportation Research Record No. 1544, Transportation Research Board, National Research Council, Washington, DC, pp. 99-108.
8. Daniel, J. S., and Kim, Y. R. (1998), "Relationships Among Rate-Dependent Stiffness of Asphalt Concrete Using Laboratory and Field Test Methods," 77th Annual Transportation Research Board Meeting, Washington, DC.
9. Finn, F., Saraf, S., Kulkarini, R., Nair K., Smith W., and Abdullah A. (1977), "The Use of Distress Prediction Subsystems for the Design of Pavement Structures," Proceedings of the 4th International Conference on the Structural Design of Asphalt Pavements, pp. 3-37.

10. Kennedy, T. W., Haas, R., and Meyer, F. R. (1975), "Characterization of Pavement Materials for Fundamental Structural Analyses," Inter-American Conference on Materials Technology, Caracas, Venezuela.

11. Miller, G. F., and H. Pursey (1995), "On the Partition of Energy Between Elastic Waves in a Semi-Infinite Solid," Proceeding of the International Conference on Microzonation for Safer Construction: Research and Application, Society of Exploration Geophysicists, Seattle, WA, Vol. 2, pp. 545-558.

12. Naik, T. R., and Malhotra, V. M. (1991), Handbook on Nondestructive Testing of Concrete, CRC Press, Boca Raton, FL., pages 169-188.

13. Nazarian, S., and Stokoe, K. H. II (1986), "In Situ Determination of Elastic Moduli of Pavement Systems by Spectral-Analysis-of-Surface-Waves Methods (Practical Aspects)," Research Report No. 1123-1, Center for Transportation Research, The University of Texas at Austin, Austin, TX, 161 pages.

14. Nazarian, S., and Stokoe, K. H. II (1987), "In Situ Determination of Elastic Moduli of Pavements Systems by Spectral-Analysis-of-the-Surface-Waves Method: Theoretical Aspects," Research Report No. 437-2, Center for Transportation Research, The University of Texas at Austin, 114 pages.

15. Nazarian, S., and Desai, M. (1993), "Automated Surface Wave Testing: Field Testing," Journal of Geotechnical Engineering, American Society of Civil Engineers, New York, Vol. 119, No. 6, pp. 1094-1112.

16. Nazarian, S., Yuan, D., and Baker, M. (1995), "Rapid Determination of Pavement Moduli with Spectral-Analysis-of-Surface-Waves Method," Research Report No. 1243-1, The University of Texas at El Paso, 76 pages.

17. Nazarian, S., Yuan, D., and Baker, M. R. (1996), "Quality Control of Portland Cement Concrete Slabs with Wave Propagation Techniques," Transportation Research Record, No. 1544, Transportation Research Board, National Research Council, Washington, DC, pp. 91-98.

18. Nazarian S., Yuan, D., and Tandon, V. (1998), "Specifications for Tools Used in Structural Field Testing of Flexible Pavement Layers," TXDOT Report No. TX-981735-1, The University of Texas at El Paso, August.

19. Nazarian, S., Baker, M., and Crain, K. (1997), "Assessing Quality of Concrete with Wave Propagation Techniques," Materials Journal, American Concrete Institute, Farmington Hills, MI, Vol. 94, No. 4, pp. 296-306.

20. Press, F. and Siever, R. (1978), Earth, 2nd Edition, W. H. Freeman, San Francisco, CA.

21. Richard, J. E. Jr., Hall, J. R. Jr., and Woods, R. O. (1990), Vibrations of Soils and Foundations, Prentice-Hall Inc., Englewood Cliffs, New Jersey, 414 p.

22. Roberts, F. L., Kandhal, P. S., Brown, E. R., Lee, D. (1996), and Kennedy, T.W., Hot Mix Materials: Mixture Design and Construction, NAPA Education Foundation Lanham, Maryland.

23. Russell, J. S., Hanna, A. S., Bahia, H. U., Schmitt R.L., and Jung G.S. (1998), "Summary of Current QC/QA Practices for Hot-Mix Asphalt Construction," Proceedings of the 77th Annual Meeting of the Transportation Research Board, Washington, DC.

24. Schmitt, R. L., Hanna, A. S., Russell, J. S., and Nordheim, E. V. (1997), "Pavement Density Measurements Comparative Analysis Using Core and Nuclear Methods," Association of Asphalt Paving Technologies, Salt Lake City, Utah, Vol. 66, p. 379.

25. Shah, K. A. (1993), "Development of a New Laboratory Testing Procedure for Resilient Modulus of Asphalt Concrete", Master of Science Thesis, North Carolina State University, pp. 7-16.

26. Shook, J. F., Finn, F. N., Witczak, M. W., and Monismith, C. L. (1982), "Thickness Design of Asphalt Pavements – The Asphalt Institute Method," Proceedings of the 5th International Conference on the Structural Design of Asphalt Pavements.

27. Tangella, S. C. S. R., Craws, J., Deacon, J. A., and Monismith, C. L. (1990), "Summary Report on Fatigue Response of Asphalt Mixtures," TM-UCB-A-003A-89-3, Prepared for SHRP Project A-003, University of California at Berkeley, CA.

28. Willis, M. E., and Toksoz, M. N. (1990), "Automatic P- and S-Velocity Determination from Full Wave Form Digital Acoustic Logs," Geophysics, Vol. 48, No. 12, pp. 1631-44.

APPENDIX A

WAVE PROPAGATION THEORY

A.1 Wave Propagation Theory

A pavement section may be approximated by a layered half-space with reasonable accuracy. With this approximation, a pavement section is assumed to be homogeneous and to extend to infinity in the horizontal direction and to be heterogeneous in the vertical direction. This heterogeneity is often modeled by a number of layers, each having its own constant properties. In addition, it is assumed that the material in each layer is elastic and isotropic. The following sections present an overview of the wave propagation theory related to pavement engineering. The relationships between seismic modulus and wave velocities are also briefly discussed.

A.2 Seismic Body Waves

In a medium where stresses are not in equilibrium, a plain strain analysis may be used to derive the wave equation of motion for a stressed element in the media. The general form of the wave equation of motion may be written as follows:

$$\frac{1}{V^2}\frac{\partial^2 \varphi}{\partial_t^2} = \nabla^2 \varphi \qquad \text{(A.1)}$$

where ∇^2, is the Laplacian of φ. The φ term represents a disturbance in a medium that propagates form one point to another with velocity, V. Wave motion created by a disturbance within an ideal whole-space can be described by two kinds of waves: compression and shear waves. These waves are collectively called body waves, as they travel within the body of a medium. Compression and shear waves are distinguished by the direction of particle motion relative to the direction of wave propagation.

Compression waves (also called primary waves or P-waves) exhibit a push-pull motion. As a result, wave propagation and particle motion are in the same direction, as shown in Figure A.1a. Compression waves travel faster than other types of waves and, hence, appear first in a direct travel time record.

Shear waves (also called secondary waves or S-waves) generate a shearing motion, which causes particle motion to occur perpendicular to the direction of wave propagation, as shown in Figure A.1b. Shear waves can be polarized. If the directions of propagation and particle motion are contained in a vertical plane, the wave is said to be vertically polarized and is called an SV-wave. However, if the direction of particle motion is perpendicular to a vertical plane containing the direction of propagation, the wave is said to be horizontally polarized. This wave is termed a SH-wave. Shear waves travel slower than P-waves and, thus, appears as the second major wave type in a direct travel time record.

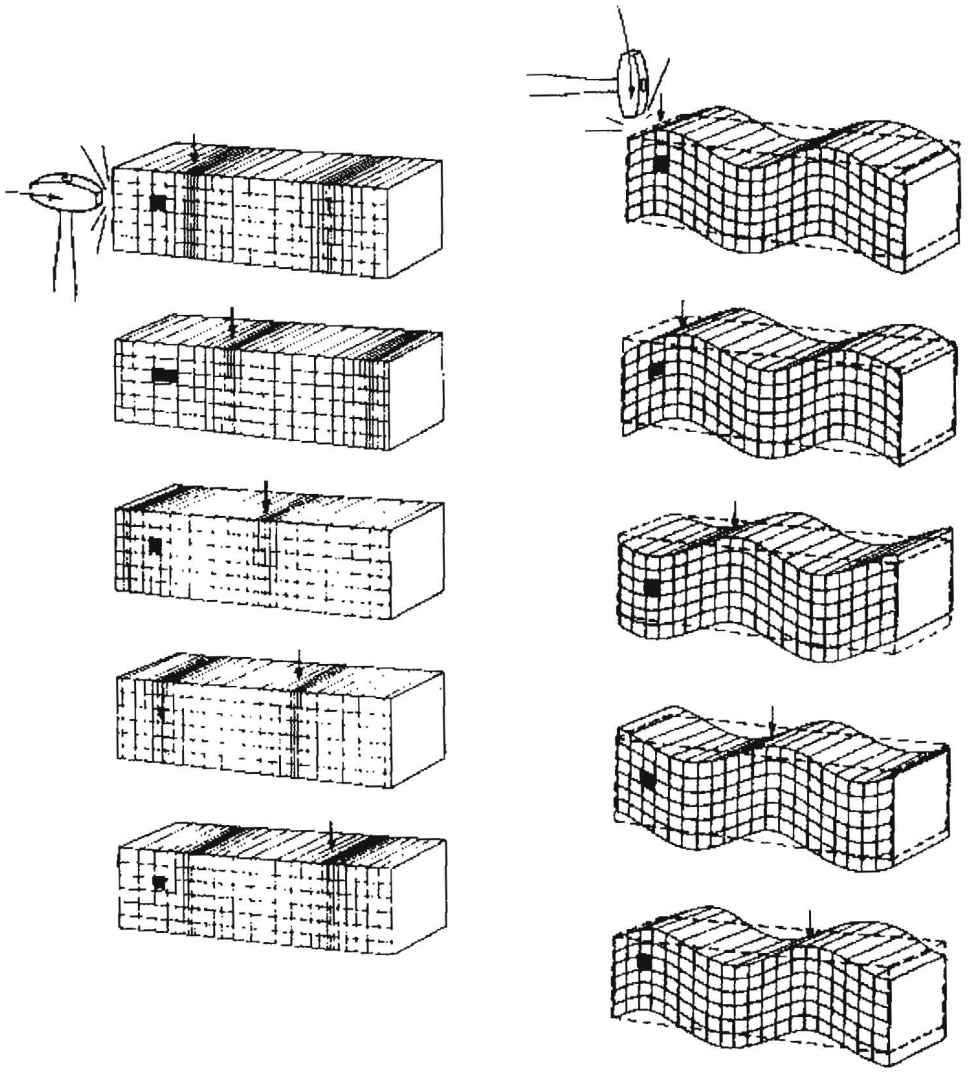

(a) P-wave (b) S-wave

Figure A.1 - Characteristic Motion of Body Waves(from Press and Siever, 1978)

A.3 Seismic Surface Waves

In a half-space, waves other than body waves are created. These waves are called surface waves; they are associated with near surface motion and diminish as they get farther from the surface. Many different types of surface waves have been identified and described. The main type of surface waves are Rayleigh waves. Rayleigh waves (R-waves) propagate at a speed of approximately 90 percent of S-waves. Particle motion associated with R-waves is composed of both vertical and horizontal components which, when combined, form a retrograde ellipse close to the surface, as shown in Figure A.2. However, with depth, R-wave particle motion changes to

purely vertical and, finally, to a prograde ellipse, as illustrated in Figure A.2. The amplitude of motion attenuates quite rapidly with depth.

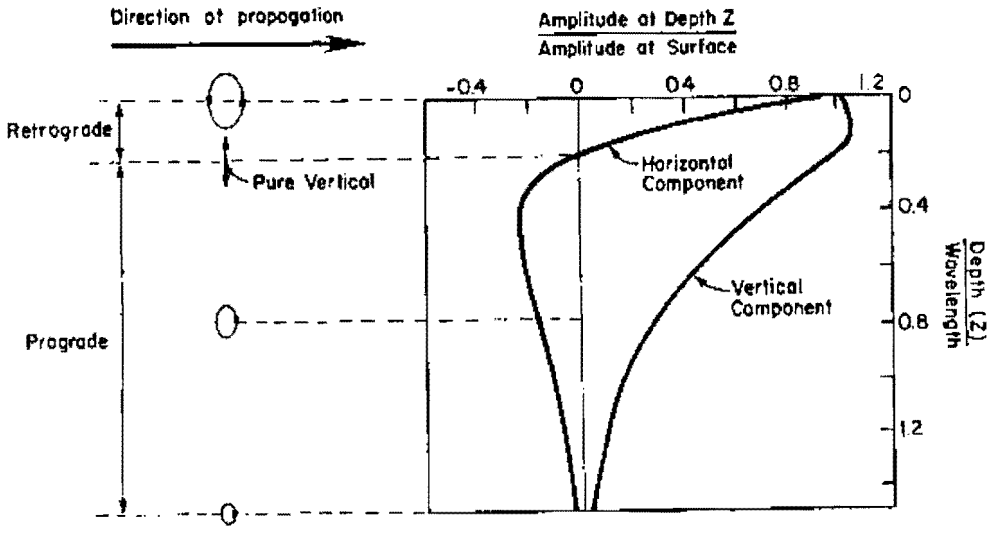

Figure A.2 - Particle Motion Distribution with Depth for Rayleigh Waves

At a depth equal to about 1.5 times the wavelength, the vertical component of the amplitude is approximately equal to 10% of the original amplitude at the ground surface.

The propagation of body waves and surface waves (Rayleigh waves) away from a vertically vibrating circular source at the surface of a homogeneous, isotropic, elastic half-space is shown in Figure A.3. Miller and Pursey (1955) found that, for the situation shown in Figure A.3, approximately 67 percent of the input energy propagates in the form of R-waves. Shear and compression waves carry 26 and 7 percent of the energy, respectively and propagate radically outward from the source. R-waves propagate along a cylindrical wavefront near the surface. Although body waves travel faster than surface waves, body waves attenuate in proportion to $1/r^2$, where r is the distance from the source. Surface wave amplitude decreases in proportion to $1/r^{0.5}$.

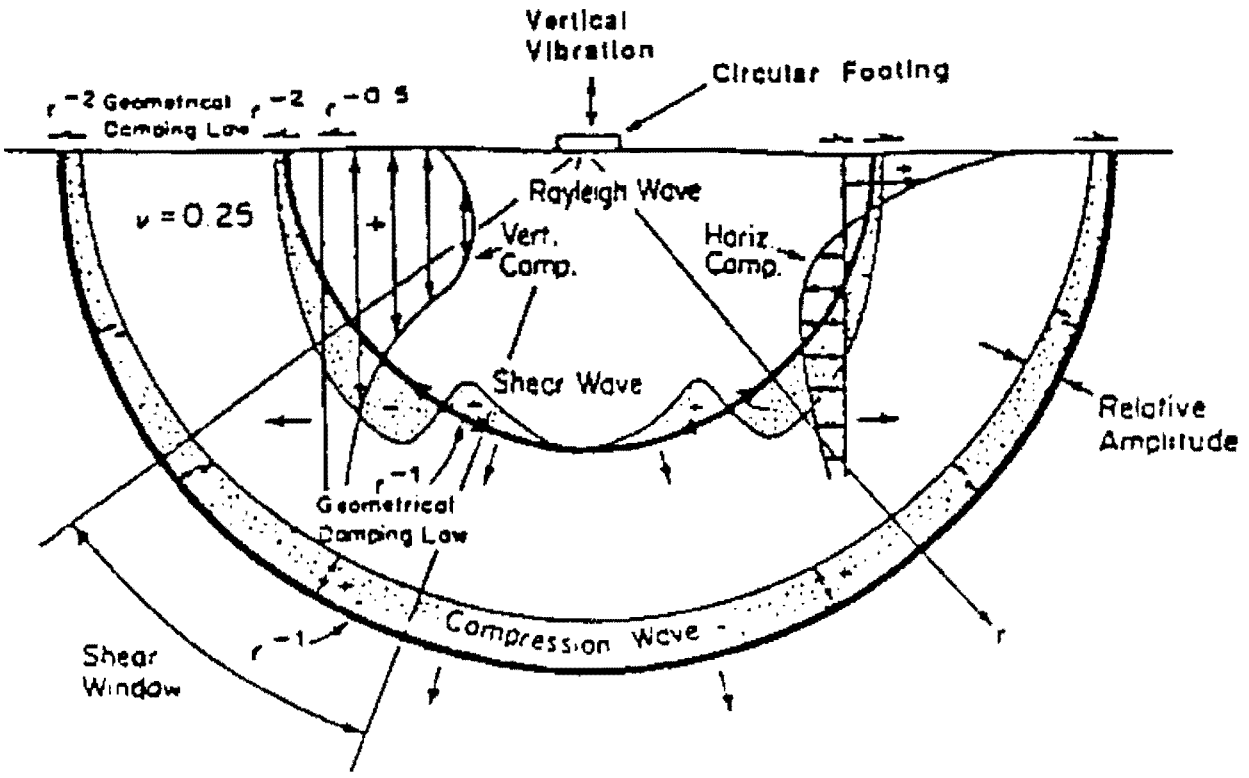

Figure A.3 - Distribution of Rayleigh, Shear, and Compression Wave Displacements (from Richard et al, 1970)

A.4 Seismic Wave Velocities and Elastic Constants

Seismic wave velocity is defined as the rate at which a wave propagates in a medium. Wave velocity is a direct indication of the stiffness of the material; higher wave velocities are associated with higher stiffness. By employing the elastic theory, compression wave velocity can be defined as

$$V_p = \sqrt{\frac{\lambda + 2G}{\rho}}, \tag{A.2}$$

where

V_p = compression wave velocity,
λ = Lame's constant,
G = shear modulus, and
ρ = mass density.

Shear wave velocity, V_s, is equal to

$$V_S = \sqrt{\frac{G}{\rho}}. \tag{A.3}$$

Compression and shear wave velocities are theoretically interrelated by Poisson's ratio. The relation can be expressed as

$$\frac{V_s}{V_p} = \sqrt{\frac{0.5 - \nu}{1 - \nu}}, \tag{A.4}$$

where ν is the Poisson's ratio. A graphic illustration of Eq. A.4 is shown in Figure A.4. For a constant shear wave velocity, compression wave velocity increases with an increase in Poisson's ratio. For a ν of zero, the ratio of V_p to V_s is equal to 1.4; for a ν of 0.5 (an incompressible material), the ratio is equal to infinity.

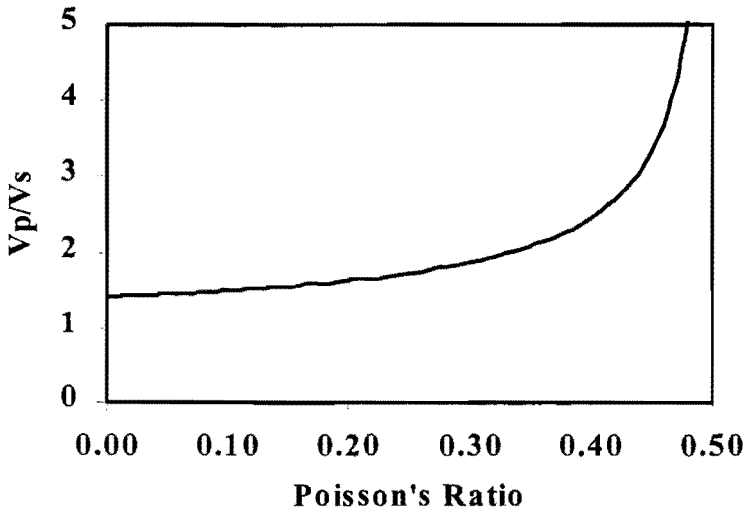

Figure A.4 – Theoretical Elastic Relationship Between Poisson's Ratio and the Ratio of Compression to Shear Wave Velocity

For a layer with constant properties, R-wave velocity and shear wave velocity is related by Poisson's ratio as well. Although the ratio of R-wave to S-wave velocities increases as Poisson's ratio increases, its change is not significant, as shown in Figure A.5.

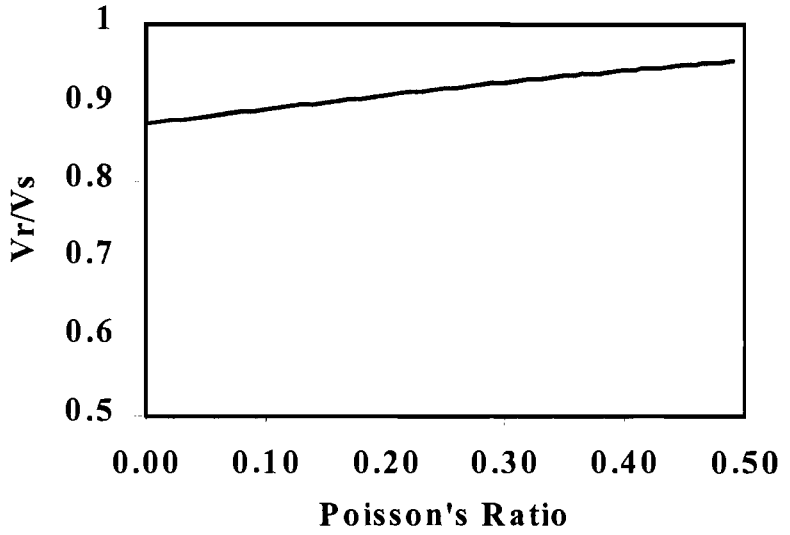

Figure A.5 Theoretical Elastic Relationship Between Poisson's Ratio and the Ratio of Rayleigh to Shear Wave Velocity

For Poisson's ratios of zero and 0.5, this ratio changes from approximately 0.86 to 0.95, respectively. Therefore, it can be assumed that, without introducing an error larger than about five percent, the ratio is equal to 0.90. Equation A.4 can be rewritten as

$$\nu = \frac{0.5 - \left(\frac{V_s}{V_p}\right)^2}{1 - \left(\frac{V_s}{V_p}\right)^2}. \qquad \text{(A.5)}$$

The R-wave velocity and compression wave velocity is related by Poisson's ratio similarly as Vs/Vp ratio as well. The ratio of R-wave to P-wave velocities decreases as Poisson's ratio increases, as shown in Figure A.6. For Poisson's ratios of zero and 0.5, this ratio changes from approximately 0.62 to zero, respectively.

A.5 Elastic Constants

In pavement engineering, the Young's moduli of different layers should be measured. Calculation of elastic moduli from propagation velocities is, thus, important. The compression wave's velocity travels faster than any other type of seismic wave and is detected first on seismic

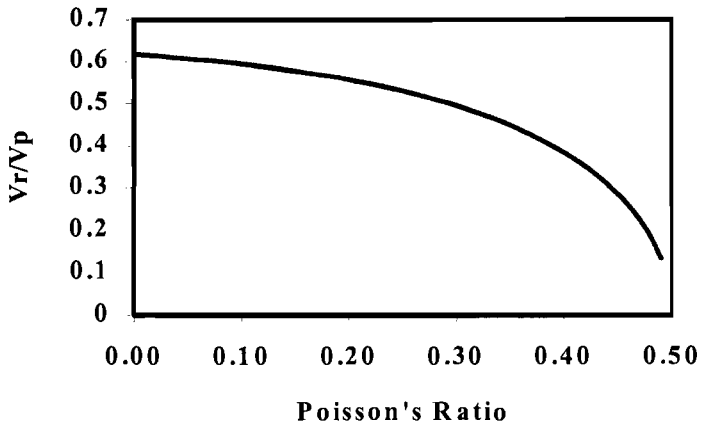

Figure A.6 - Theoretical Elastic Relationship Between Poisson's Ratio and the Ratio of Rayleigh to Compression Wave Velocity

records. The in a medium where the material is restricted from deformation in two lateral directions, the ratio of axial stress to axial strain is called constrained modulus. Constrained modulus, M, is defined as

$$M = \rho V_p^2 \tag{A.6}$$

where ρ is the mass density. The constrained modulus may also be expressed in terms of R-wave velocity as follows;

$$M = \rho(CV_R)^2 \tag{A.7}$$

where V_R is the surface wave velocity and C is the inverse of the V_R/V_P ratio, which is dependent

on Poisson's ratio. In terms of Young's modulus and Poisson's ratio:

$$M = \frac{(1-\nu)E}{[1+\nu)(1-2\nu)]}. \tag{A.8}$$

The shear wave velocity, V_s, is used to calculate shear modulus, G, by

$$G = \rho V_s^2, \tag{A.9}$$

where ρ is the mass density.

If Poisson's ratio (or compression wave velocity) is known, other moduli can be calculated for given V_s. Young's and shear moduli are related by

$$E = 2G(1+\nu) \tag{A.10}$$

or

$$E = 2\rho V_s^2(1+\nu). \tag{A.11}$$

Bulk modulus, B, is the ratio of hydrostatic stress to volumetric strain and can be determined by:

$$B = M - 4/3G. \tag{A.12}$$

where M, is the constrained modulus and G is the shear modulus.

APPENDIX B

MIX DESIGNS

Table B.1: Job Mix Gradation Formula for Type B

Sieve Number	Sieve Opening (mm)	Weight Retained (gm)	Percent Retained (%)	Cumulative % Retained (%)	(% Passing) (Org. Soil) (%)
5/8"	15.875	92.4	11.00	11.00	87.6
3/8"	9.525	168.80	20.10	31.10	79.90
No. 4	4.760	156.20	18.60	49.69	50.31
No. 10	2.000	143.64	17.10	66.80	33.20
No. 40	0.420	150.40	17.91	84.70	15.30
No. 80	0.180	78.10	9.30	94.00	6.00
No. 200	0.074	21.80	2.60	96.60	3.40
Pan	....	28.60	3.41	100.00	0.00
Total		839.94			
Optimum Asphalt Content			4%		

Table B.2: Job Mix Gradation Formula for Type C

Sieve Number	Sieve Opening (mm)	Weight Retained (gm)	Percent Retained (%)	Cumulative % Retained (%)	(% Passing) (Org. Soil) (%)
5/8"	15.875	33.2	4.00	4	96
3/8"	9.525	145.40	17.50	21.50	82.50
No. 4	4.760	212.70	25.60	47.10	52.90
No. 10	2.000	144.60	17.40	64.50	35.50
No. 40	0.420	157.90	19.00	83.50	16.50
No. 80	0.180	79.80	9.60	93.11	6.89
No. 200	0.074	24.10	2.90	96.01	3.99
Pan	....	33.20	4.00	100.00	0.00
Total		830.90			
Optimum Asphalt Content			4.5%		

Table B.3: Job Mix Gradation Formula for Type D

Sieve Number	Sieve Opening (mm)	Weight Retained (gm)	Percent Retained (%)	Cumulative % Retained (%)	(% Passing) (Org. Soil) (%)
3/8"	9.525	74.80	9.00	9.00	91.00
No. 4	4.760	257.70	31.00	40.00	60.00
No. 10	2.000	158.80	19.10	59.10	40.90
No. 40	0.420	185.70	22.34	81.44	18.56
No. 80	0.180	81.90	9.85	91.29	8.71
No. 200	0.074	36.30	4.37	95.66	4.34
Pan	....	35.90	4.32	99.98	0.02
Total		831.10			
Optimum Asphalt Content			5%		

APPENDIX C

QUALITY ASSURANCE LABORATORY/FIELD TESTING PROCEDURES

Preliminary Protocol for QA of AC Pavements

1. Implementation Statement:

The following document describes the preliminary protocol for monitoring the quality of laid-down AC pavements with seismic methods presented in this study. A gradual implementation of the seismic methods in QC/QA programs is recommended to state DOT's. In order to establish criteria for AC pavement quality based on seismic measurements, the methodology should be combined with field observations of the pavement conditions. As a result, a managed data base should be kept in order to develop performance-based specifications, which will allow for tolerances or limits to be set on measured seismic modulus or predicted voids in total mix.

2. Scope:

The following test methods determine the seismic modulus for AC pavements. The test methods consist of a laboratory and of a field procedure.

3. Referenced Documents:

3.1 TXDOT Testing Methods

- Tex-222-F Methods for Sampling Bituminous Mixtures
- Tex-221-F Sampling Aggregates for Bituminous Mixtures, Surface Treatments and Limestone Rock Asphalt
- Tex-225-F Random Selection of Bituminous Mixture Samples
- Tex-206-F Mixtures Method of Compacting Test Specimens of Bituminous Mixtures
- Tex-205-F Laboratory Method of Mixing Bituminous Mixtures
- Tex-223-F Preparation of Control Charts for Asphaltic Concrete Paving Projects
- Tex-207-F Determination of Density of Compacted Bituminous Mixtures
- Tex-227-F Theoretical Maximum Specific Gravity of Bituminous Mixtures

3.2 AASHTO Documents

- T40 Methods for Sampling Bituminous Materials
- T2 Methods for Sampling Aggregate
- T168 Methods for Sampling Bituminous Paving Mixtures
- TP4 Practice for Preparation of Asphalt Concrete Specimens by Means of the SHRP Gyratory Compactor
- PP2 Practice for Short and Long Term Aging of Hot-Mix Asphalt (HMA)

- QC/QA Quality Control/Quality Assurance Specifications and Implementation Guide

3.3 ASTM Documents

- D 3203 Standard Method for Percent Air Voids in compacted Dense and Open Bituminous Paving Mixtures
- D 2041 Standard Methods for Theoretical Maximum Specific Gravity and Density of Bituminous Paving Mixtures
- D 3549 Methods for Thickness or Height of Compacted Bituminous Paving Mixture Specimens

4. Terminology:

The terminology relevant to the seismic methods may be found in Chapter Three of this study. Definitions for the terms pertaining to asphalt may be found in ASTM D8 and MP1.

5. Summary of Test Methods

The following test method presents a laboratory testing procedure using the V-Meter to determine the modulus of AC briquettes and cores. In the field, the Portable Seismic Pavement Analyzer (PSPA) is utilized to monitor the quality of laid-down AC layer based on modulus.

6. Significance and Use:

The described protocol may be used to monitor the quality of AC layers based on seismic measurements. The seismic methods may be used to detect changes in quality of AC layers based on the measured seismic modulus.

7. Testing Procedures:

1) Laboratory Briquette Preparation

a) The aggregate should be proportioned and graded according to the Agency mix design for the AC mix type.

b) The aggregate used to prepare the required gradation for the briquettes is kept in the oven, at a temperature of at least 150°C, for 24 hours prior to making the bowls for mixing.

c) Place the aggregate with its correct gradation in a steel bowl and place it in the oven, which is set with a temperature of 150°C °± 1°C. Each specimen requires two bowls.

d) Place two asphalt cement cups with the correct asphalt grade for the mixture into an oven, which has a maintained temperature of 154°C to 160°C, for 1 hour. At the same time, place two aggregate bowls in the oven, along with the asphalt cement.

e) Place the mixing bowl (including whip) into the oven for at least 30 minutes so that the mix temperature may be maintained during mixing.

f) Five minutes before the asphalt cement reaches its 1-hour period, take one bowl of aggregate and the mixing bowl out of the oven. Then, place the aggregate into the mixing bowl and make a small hole in the middle of the aggregate. Next, place the mixing bowl on a balance scale and rezero the scale.

g) Take one asphalt cement cup out of the oven and pour it into the mixing bowl. The amount of asphalt poured into the mixing bowl should be specified by the mix design specifications.

h) Place the whip into the mixing bowl and mix the hot mix asphalt in the mixer for 50 seconds, making sure that all the aggregate particles are coated with asphalt.

i) Next, place the hot asphalt mix in a bowl and, then, into an oven, which has a maintained temperature of 135°C.

j) Repeat steps f-h, and place the hot mix asphalt into the same bowl of step (i) (each briquette requires two bowls and two asphalt cups)

k) Cure the hot mix asphalt for a period of four hours at a temperature of 135°C. The hot asphalt mix should be mixed every hour during the curing period.

l) Place the gyratory mold and base plate in an oven with a temperature of 142° C to 148°C, 1 hour before the end of the curing period.

m) At the end of the curing period, place the hot mix asphalt into the oven with the gyratory mold for 30 minutes so that the mixture temperature may decrease to the compaction temperature of 142°C to 148°C.

n) Five minutes before the hot mix asphalt reaches a period of 30 minutes, take the gyratory out of the oven and place in on the gyratory compaction machine. Before placing the hot mix asphalt into the mold, spray light oil on the mold to prevent sticking.

o) Place the hot mix asphalt into the gyratory mold and compact it to the desired compacting effort.

p) Take the briquettes out of the mold and let it cool at room temperature for 24 hours before performing any tests on the briquette.

2) Preparation of AC Briquettes Sampled from Plant Feed

The preparation of AC briquettes is the same as described in section 1, with the exception that the process begins at (c), skips to (k), and, then, continues as before.

3) V-Meter Test

a) Measure the diameter and length of each briquette. The average of three measurements for each briquette, of the diameter and of the length, should be taken.

b) Calibrate the V-Meter using the calibration rod and place the couplet on the transducer and receiver. A constant pressure should be placed on the rod during calibration.

c) Place the briquette between the receiver and the transducer on the metal pedestal.

d) Place a constant pressure on the briquette, then turn on the V-Meter and record the travel time after 30 seconds, or until the time stabilizes. This process step should be repeated two more times to obtain an average travel time.

e) The final two steps are to perform VTM and Rice specific gravity on each briquette in accordance with ASTM D 3203-91 and ASTM D 2041-91, respectively.

8. Temperature Correction for Field Measured Modulus:

If measured pavement surface temperatures are greater than 25°C, an appropriate temperature correction factor should be applied to the averaged measured modulus. The temperature correction factors may be obtained using the methodology presented in section 4.2.4. A correction factor may be calculated by determining the modulus at 25°C from a temperature dependent linear model and by dividing this value by a calculated modulus at the measured temperature in the field.

9. Calculations and Procedures

The necessary calculations related to the methodology are described in Chapter 3 of this report.

APPENDIX D

PHASE I LABORATORY STUDY DATA

Material: El Paso **Mix Type:** B
Asphalt Grade: AC-20 **Asphalt Content:** 4%

Table D.1: Results of Seismic Tests on AC Briquettes

Briquette	Gyrations	Avg. Diam. (mm)	Avg. Length (mm)	Air Voids (%)	V-Meter		
					Travel Time (micro-sec.)	Velocity (m/s)	Young's Modulus (GPa)
Briquette Set 1							
1	5	101	103	9.80	33.6	3078	13.5
2	10	101	100	7.80	29.4	3398	17.1
3	15	100	97	6.20	27.7	3512	18.8
4	20	100	97	6.20	27.3	3567	19.3
5	25	100	95	4.70	25.2	3753	22.0
6	30	100	94	4.50	24.2	3893	24.0
7	35	100	94	4.40	25.0	3745	22.4
Briquette Set 2							
1	5	101	102	9.90	32.3	3171	14.2
2	10	101	101	7.70	30.6	3290	15.8
3	15	100	97	5.80	24.9	3912	23.4
4	20	100	96	5.40	25.7	3753	21.8
5	25	100	96	5.30	25.4	3782	22.3
6	30	100	95	3.50	22.7	4183	27.5
7	35	100	96	3.90	23.1	4139	26.8

Material: El Paso **Mix Type:** C
Asphalt Grade: AC-20 **Asphalt Content:** 4.5%

Table D.2: Results of Seismic Tests on AC Briquettes

Briquette	Gyrations	Avg. Diam. (mm)	Avg. Length (mm)	Air Voids (%)	V-Meter		
					Travel Time (micro-sec.)	Velocity (m/s)	Young's Modulus (GPa)
Briquette Set 1							
1	5	100	100	8.50	30.0	3344	16.5
2	10	100	100	7.90	29.1	3420	17.3
3	15	100	98	6.20	26.3	3724	20.9
4	20	100	96	5.10	24.7	3901	23.2
5	25	100	96	4.80	24.3	3944	24.0
6	30	100	95	3.70	23.8	3978	24.7
7	35	100	95	3.50	23.8	3981	24.9
Briquette Set 2							
1	5	101	103	10.40	30.6	3363	16.0
2	10	101	100	7.60	28.3	3523	18.4
3	15	100	98	5.70	26.5	3694	20.7
4	20	100	96	5.30	25.2	3824	22.5
5	25	100	96	4.20	23.5	4075	25.7
6	30	100	96	3.70	23.8	4020	25.1
7	35	100	95	3.30	23.2	4077	26.1

Material: El Paso **Mix Type:** D
Asphalt Grade: AC-30 **Asphalt Content:** 5%

Table D.3: Results of Seismic Tests on AC Briquettes

Briquette	Gyrations	Avg. Diam. (mm)	Avg. Length (mm)	Air Voids (%)	V-Meter		
					Travel Time (micro-sec.)	Velocity (m/s)	Young's Modulus (GPa)
Briquette Set 1							
1	5	101	107	12.8	35.2	3028	12.6
2	10	101	103	11.6	32.3	3203	14.6
3	15	100	100	9.00	29.8	3339	16.6
4	20	100	99	8.50	29.4	3366	17.0
5	25	100	99	8.10	27.9	3536	18.8
6	30	100	97	6.60	26.4	3679	20.9
7	35	100	96	5.70	25.7	3727	21.6
Briquette Set 2							
1	5	101	105	12.0	37.3	2814	10.7
2	10	101	104	11.6	34.7	2989	12.7
3	15	100	101	9.80	31.0	3255	15.6
4	20	100	101	10.1	28.3	3556	18.7
5	25	100	97	7.60	27.4	3550	19.3
6	30	100	98	7.70	25.6	3829	22.3
7	35	100	98	7.70	26.0	3767	21.5

Material: El Paso **Mix Type:** D
Asphalt Grade: AC-20 **Asphalt Content:** 5%

Table D.4: Results of Seismic Tests on AC Briquettes

Briquette	Gyrations	Avg. Diam. (mm)	Avg. Length (mm)	Air Voids (%)	V-Meter		
					Travel Time (micro-sec.)	Velocity (m/s)	Young's Modulus (GPa)
Briquette Set 1							
1	5	102	103	11.5	34.8	2954	12.2
2	10	101	99	9.01	29.8	3327	16.4
3	15	100	97	6.01	26.9	3588	19.9
4	20	100	96	5.75	26.3	3661	20.6
5	25	100	96	4.92	26.2	3653	20.8
6	30	100	94	4.30	26.1	3618	20.7
7	35	100	94	3.92	25.2	3725	22.0
Briquette Set 2							
1	5	101	102	11.2	34.3	2976	12.7
2	10	100	100	9.07	31.1	3207	15.2
3	15	100	99	8.30	29.1	3407	17.3
4	20	100	97	6.12	27.5	3539	19.1
5	25	100	96	5.15	26.1	3680	21.1
6	30	100	95	5.30	26.7	3548	19.6
7	35	100	95	4.50	26.4	3592	20.1

Material:	El Paso	**Mix Type:**	D
Asphalt Grade:	AC-10	**Asphalt Content:**	5%

Table D.5: Results of Seismic Tests on AC Briquettes

Briquette	Gyrations	Avg. Diam. (mm)	Avg. Length (mm)	Air Voids (%)	V-Meter		
					Travel Time (micro-sec.)	Velocity (m/s)	Young's Modulus (GPa)
Briquette Set 1							
1	5	101	104	10.9	34.8	2979	12.5
2	10	101	101	8.3	31.2	3224	15.3
3	15	100	99	6.2	28.6	3455	18.0
4	20	100	98	5.5	28.3	3460	18.2
5	25	100	96	4.2	26.8	3586	19.9
6	30	100	95	2.7	25.2	3752	22.1
7	35	100	94	2.2	24.8	3800	22.9
Briquette Set 2							
1	5	101	102	9.6	33.6	3041	13.3
2	10	100	99	6.5	29.0	3419	17.5
3	15	100	99	6.2	29.2	3394	17.3
4	20	100	96	4.0	27.3	3512	19.2
5	25	100	96	3.9	27.2	3541	19.4
6	30	100	95	2.6	26.0	3636	20.8
7	35	100	95	2.2	25.4	3726	21.8

APPENDIX E

PHASE II LABORATORY TEMPERATURE STUDY DATA

Table E.1: Variation in Modulus with Temperature for Type B -AC 20

Project:	1735	**Air Voids:**	7.7 %
Briquette:	1	**Gyrations :**	10
Material:	El Paso		
Mix Type:	B	**Avg. Diam.**	101 mm
Asphalt Grad	AC-20	**Avg. Length**	99 mm
Asphalt Cont	4.0 %	**Mass Density**	2204 kg/m^3

Target Temperatur (C°)	Briquette Temperatur (C°)	V-Meter		
		Travel Time (micro-sec.)	Velocity (m/s)	Young's Modulus (GPa)
-5	-4.3	27.2	3627	19
5	5.8	27.4	3600	19
15	15.4	29.2	3378	17
25	25.4	30.6	3224	15
35	36.2	33.3	2962	13
45	44.7	34.8	2835	12

Table E2: Variation in Modulus with Temperature for Type B -AC 20

Project:	1735	**Air Voids:**	3.9 %
Briquette:	2	**Gyrations :**	35
Material:	El Paso		
Mix Type:	B	**Avg. Diam.**	100 mm
Asphalt Grad	AC-20	**Avg. Length**	94 mm
Asphalt Cont	4.0 %	**Mass Density**	2334 kg/m^3

Target Temperatur (C°)	Briquette Temperatur (C°)	V-Meter		
		Travel Time (micro-sec.)	Velocity (m/s)	Young's Modulus (GPa)
-5	-5.7	22.5	4186	27.2
5	5.1	22.8	4131	26.5
15	15.3	23.1	4077	25.8
25	25.0	24.7	3813	22.5
35	34.9	25.7	3665	20.8
45	45.2	27.1	3476	18.7

Table E.3: Variation in Modulus with Temperature for Type C -AC 20

Project:	1735	**Air Voids:**	8.9 %
Briquette:	1	**Gyrations :**	10
Material:	El Paso		
Mix Type:	C	**Avg. Diam.**	100 mm
Asphalt Grad	AC-20	**Avg. Length**	101 mm
Asphalt Cont	4.5 %	**Mass Density**	2163 kg/m^3

Target Temperatur (C°)	Briquette Temperatur (C°)	V-Meter		
		Travel Time (micro-sec.)	Velocity (m/s)	Young's Modulus (GPa)
-5	-4.6	27.2	3724	20
5	4.9	27.8	3643	19
15	15.4	29.0	3493	18
25	25.2	30.4	3332	16
35	35.5	32.3	3136	14
45	45.5	35.3	2869	12

Table E.4: Variation in Modulus with Temperature for Type C -AC 20

Project:	1735	**Air Voids:**	7.2 %
Briquette:	2	**Gyrations :**	15
Material:	El Paso		
Mix Type:	C	**Avg. Diam.**	100 mm
Asphalt Grad	AC-20	**Avg. Length**	99 mm
Asphalt Cont	4.5 %	**Mass Density**	2213 kg/m^3

Target Temperatur (C°)	Briquette Temperatur (C°)	V-Meter		
		Travel Time (micro-sec.)	Velocity (m/s)	Young's Modulus (GPa)
-5	-4.6	26.3	3774	21
5	4.9	26.8	3704	20
15	15.4	27.6	3596	19
25	25.2	28.7	3459	18
35	35.5	30.3	3276	16
45	45.5	32.3	3073	14

Table E.5: Variation in Modulus with Temperature for Type C -AC 20

Project:	1735	**Air Voids:**	4.2 %
Briquette:	3	**Gyrations :**	30
Material:	El Paso		
Mix Type:	C	**Avg. Diam.**	100 mm
Asphalt Grad	AC-20	**Avg. Length**	96 mm
Asphalt Cont	4.5 %	**Mass Density**	2298 kg/m^3

Target Temperatur (C°)	Briquette Temperatur (C°)	V-Meter		
		Travel Time (micro-sec.)	Velocity (m/s)	Young's Modulus (GPa)
-5	-4.3	24.7	3867	23
5	5.2	25.6	3731	21
15	15.5	26.9	3551	19
25	25.3	27.2	3512	19
35	35.2	29.0	3294	17
45	45.4	30.6	3122	15

Table E.6: Variation in Modulus in Temperature with Type C -AC 20

Project:	1735	**Air Voids:**	3.8 %
Briquette:	4	**Gyrations :**	30
Material:	El Paso		
Mix Type:	C	**Avg. Diam.**	100 mm
Asphalt Grad	AC-20	**Avg. Length**	96 mm
Asphalt Cont	4.5 %	**Mass Density**	2291 kg/m^3

Target Temperatur (C°)	Briquette Temperatur (C°)	V-Meter		
		Travel Time (micro-sec.)	Velocity (m/s)	Young's Modulus (GPa)
-5	-4.3	22.7	4208	27
5	5.2	23.2	4117	26
15	15.5	25.3	3776	22
25	25.3	25.9	3688	21
35	35.2	28.7	3328	17
45	45.4	29.4	3249	16

Table E.7: Variation in Modulus with Temperature for Type D -AC 30

Project:	1735	**Air Voids:**	8 %
Briquette:	1	**Gyrations :**	10
Material:	El Paso		
Mix Type:	D	**Avg. Diam.**	100 mm
Asphalt Grad	AC-30	**Avg. Length**	97 mm
Asphalt Cont	5 %	**Mass Density**	2241 kg/m^3

Target Temperatur (C°)	Briquette Temperatur (C°)	V-Meter		
		Travel Time (micro-sec.)	Velocity (m/s)	Young's Modulus (GPa)
-5	-4.4	25.2	3868	22
5	5.1	25.8	3778	21
15	15.8	27.3	3570	19
25	24.9	28.8	3384	17
35	35.3	31.3	3114	14
45	45.6	33.2	2936	13

Table E.8: Variation in Modulus with Temperature for Type D -AC 30

Project:	1735	**Air Voids:**	3.9 %
Briquette:	2	**Gyrations :**	35
Material:	El Paso		
Mix Type:	D	**Avg. Diam.**	100 mm
Asphalt Grad	AC-30	**Avg. Length**	93 mm
Asphalt Cont	5 %	**Mass Density**	2358 kg/m^3

Target Temperatur (C°)	Briquette Temperatur (C°)	V-Meter		
		Travel Time (micro-sec.)	Velocity (m/s)	Young's Modulus (GPa)
-5	-4.3	21.7	4290	29
5	5.1	22.0	4231	28
15	15.2	23.2	4012	25
25	25.0	24.0	3878	24
35	34.6	25.8	3608	20
45	45.8	27.7	3360	18

Table E.9: Variation in Modulus with Temperature for Type D -AC 10

Project:	1735	**Air Voids:**	7.8 %
Briquette:	1	**Gyrations :**	10
Material:	El Paso		
Mix Type:	D	**Avg. Diam.**	100 mm
Asphalt Grad	AC-10	**Avg. Length**	101 mm
Asphalt Cont	5 %	**Mass Density**	2190 kg/m^3

Target Temperatur (C°)	Briquette Temperatur (C°)	V-Meter		
		Travel Time (micro-sec.)	Velocity (m/s)	Young's Modulus (GPa)
-5	-4.6	27.2	3698	20
5	4.8	27.9	3605	19
15	15.2	29.3	3433	17
25	24.9	31.3	3213	15
35	35.4	33.3	3020	13
45	45.3	36.2	2778	11

Table E.10: Variation in Modulus with Temperature for Type D -AC 10

Project:	1735	**Air Voids:**	4.5 %
Briquette:	2	**Gyrations :**	15
Material:	El Paso		
Mix Type:	D	**Avg. Diam.**	100 mm
Asphalt Grad	AC-10	**Avg. Length**	96 mm
Asphalt Cont	5 %	**Mass Density**	2290 kg/m^3

Target Temperatur (C°)	Briquette Temperatur (C°)	V-Meter		
		Travel Time (micro-sec.)	Velocity (m/s)	Young's Modulus (GPa)
-5	-4.6	24.0	4019	25
5	4.8	25.3	3813	22
15	15.2	25.9	3725	21
25	24.9	27.4	3521	19
35	35.4	28.7	3361	17
45	45.3	31.3	3082	14

Table E.11: Variation in Modulus with Temperature for Type D-AC-10

Project:	1735	**Air Voids:**	3 %
Briquette:	3	**Gyrations :**	30
Material:	El Paso		
Mix Type:	D	**Avg. Diam.**	100 mm
Asphalt Grad	AC-10	**Avg. Length**	95 mm
Asphalt Cont	5 %	**Mass Density**	2329 kg/m^3

Target Temperatur (C^0)	Briquette Temperatur (C^0)	V-Meter		
		Travel Time (micro-sec.)	Velocity (m/s)	Young's Modulus (GPa)
-5	-4.7	23.3	4077	26
5	5.9	23.7	4008	25
15	14.5	25.5	3725	21
25	24.4	26.3	3612	20
35	34.8	27.6	3442	18
45	45.6	30.3	3135	15

Table E.12: Variation in Modulus with Temperature for Type D-AC-20

Project:	1735	**Air Voids:**	8.4 %
Briquette:	1	**Gyrations :**	10
Material:	El Paso		
Mix Type:	D	**Avg. Diam.**	101 mm
Asphalt Grad	AC-20	**Avg. Length**	100 mm
Asphalt Cont	5.0 %	**Mass Density**	2195 kg/m^3

Target Temperatur (C°)	Briquette Temperatur (C°)	V-Meter		
		Travel Time (micro-sec.)	Velocity (m/s)	Young's Modulus (GPa)
-5	-4.8	28.2	3542	18
5	5.1	28.6	3493	18
15	15.4	29.6	3375	17
25	25.5	31.7	3151	14
35	35.4	32.8	3046	14
45	45.0	35.4	2822	12
35	34.8	33.2	3009	13
25	25.2	31.0	3223	15
15	15.1	29.3	3409	17
5	5.0	28.3	3530	18
-5	-5.1	27.2	3673	20

Table E.13: Variation in Modulus with Temperature for Type D-AC-20

Project:	1735	**Air Voids:**	8.0 %
Briquette:	2	**Gyrations :**	15
Material:	El Paso		
Mix Type:	D	**Avg. Diam.**	100 mm
Asphalt Grad	AC-20	**Avg. Length**	99 mm
Asphalt Cont	5.0 %	**Mass Density**	2220 kg/m^3

Target Temperatur (C°)	Briquette Temperatur (C°)	V-Meter		
		Travel Time (micro-sec.)	Velocity (m/s)	Young's Modulus (GPa)
-5	-4.8	27.6	3596	19
5	5.1	27.9	3557	19
15	15.4	31.1	3191	15
25	25.5	32.3	3072	14
35	35.4	33.1	2998	13
45	45.0	35.3	2811	12
35	34.8	33.3	2980	13
25	25.2	30.0	3308	16
15	15.1	28.8	3446	18
5	5.0	28.1	3532	18
-5	-5.1	27.2	3648	20

Table E.14: Variation in Modulus with Temperature for Type D-AC-20

Project:	1735	**Air Voids:**	4.1 %
Briquette:	1	**Gyrations :**	30
Material:	El Paso		
Mix Type:	D	**Avg. Diam.**	100 mm
Asphalt Grad	AC-20	**Avg. Length**	95 mm
Asphalt Cont	5.0 %	**Mass Density**	2342 kg/m^3

Target Temperatur (C°)	Briquette Temperatur (C°)	V-Meter		
		Travel Time (micro-sec.)	Velocity (m/s)	Young's Modulus (GPa)
-5	-4.4	23.0	4121	26
5	5.0	23.6	4017	25
15	15.2	24.9	3807	23
25	25.1	26.0	3646	21
35	35.4	27.6	3435	18
45	45.2	29.1	3257	16
35	35.5	27.3	3472	19
25	25.4	25.7	3688	21
15	15.0	24.6	3853	23
5	5.4	23.7	4000	25
-5	-4.5	23.1	4104	26

Table E.15: Variation in Modulus with Temperature for Type D-AC-20

Project:	1735	**Air Voids:**	4.0 %
Briquette:	2	**Gyrations :**	30
Material:	El Paso		
Mix Type:	D	**Avg. Diam.**	100 mm
Asphalt Grad	AC-20	**Avg. Length**	95 mm
Asphalt Cont	5.0 %	**Mass Density**	2328 kg/m^3

Target Temperatur (C°)	Briquette Temperatur (C°)	V-Meter		
		Travel Time (micro-sec.)	Velocity (m/s)	Young's Modulus (GPa)
-5	-4.4	23.3	4084	26
5	5.0	23.8	3998	25
15	15.2	25.1	3791	22
25	25.1	26.6	3577	20
35	35.4	28.3	3363	17
45	45.2	30.1	3161	15
35	35.5	28.3	3363	17
25	25.4	26.3	3618	20
15	15.0	25.2	3776	22
5	5.4	24.0	3965	24
-5	-4.5	23.4	4067	26

Table E.16: Variation in Modulus with Temperature for Type D-AC-20

Project:	1735	**Air Voids:**	3.5 %
Briquette:	1	**Gyrations :**	35
Material:	El Paso		
Mix Type:	D	**Avg. Diam.**	100 mm
Asphalt Grad	AC-20	**Avg. Length**	94 mm
Asphalt Cont	5.0 %	**Mass Density**	2348 kg/m^3

Target Temperatur (C°)	Briquette Temperatur (C°)	V-Meter		
		Travel Time (micro-sec.)	Velocity (m/s)	Young's Modulus (GPa)
-5	-4.4	22.9	4112	26
5	5.0	23.5	4007	25
15	15.2	24.1	3907	24
25	25.1	25.6	3678	21
35	35.4	26.7	3527	19
45	45.2	28.9	3258	17
35	35.5	26.4	3567	20
25	25.4	25.5	3693	21
15	15.0	24.3	3875	23
5	5.4	23.2	4059	26
-5	-4.5	23.3	4041	25

Table E.17: Variation in Modulus with Temperature for Type D-AC-20

Project:	1735	**Air Voids:**	3.3 %
Briquette:	2	**Gyrations :**	35
Material:	El Paso		
Mix Type:	D	**Avg. Diam.**	100 mm
Asphalt Grad	AC-20	**Avg. Length**	94 mm
Asphalt Cont	5.0 %	**Mass Density**	2353 kg/m^3

Target Temperatur (C°)	Briquette Temperatur (C°)	V-Meter		
		Travel Time (micro-sec.)	Velocity (m/s)	Young's Modulus (GPa)
-5	-4.4	22.3	4217	28
5	5.0	23.0	4089	26
15	15.2	23.5	4002	25
25	25.1	24.7	3807	23
35	35.4	26.4	3562	20
45	45.2	27.8	3383	18
35	35.5	26.3	3576	20
25	25.4	24.7	3807	23
15	15.0	23.3	4036	25
5	5.4	22.9	4107	26
-5	-4.5	22.3	4217	28

APPENDIX F

PAVEMENT MODEL/FEILD STUDY DATA

F1) PSPA DATA

F2) LABORATORY CORE DATA

F3) CASE STUDY DATA

F1) PAVEMENT MODEL- PSPA DATA

Table F1.1: ACP Model data - Mix Type D

Test Point	Avg. Mass Density (kg/m^3)	Avg. Surface Wave[1] Velocity (m/s)	PSPA Modulus (GPa)
1	2177	1415	13.2
1	2177	1484	14.5
1	2177	1495	14.7
1	2177	1483	14.5
2	2177	1534	15.5
2	2177	1481	14.4
2	2177	1375	12.4
3	2177	1473	14.3
3	2177	1464	14.1
3	2177	1463	14.1
4	2177	1462	14.0
4	2177	1461	14.0
4	2177	1466	14.1
5	2177	1462	14.0
5	2177	1464	14.1
5	2177	1448	13.8
	Avg.:	**1464**	**14.1**

(1) Based on Frequency Domain Records

Table F1.2: ACP Model data- Mix Type C

Test Point	Avg. Mass Density (kg/m^3)	Avg. Surface Wave[1] Velocity (m/s)	PSPA Modulus (GPa)
1	2215	1550	15.4
1	2215	1558	15.6
1	2215	1548	15.4
2	2215	1615	16.8
2	2215	1624	16.9
3	2215	1557	15.6
3	2215	1545	15.3
3	2215	1542	15.3
3	2215	1549	15.4
4	2215	1485	14.2
4	2215	1491	14.3
4	2215	1504	14.5
5	2215	1567	15.8
5	2215	1565	15.7
5	2215	1564	15.7
5	2215	1570	15.8
	Avg.:	**1552**	**15.5**

(1) Based on Frequency Domain Records

Table F1.3: ACP Model - Mix Type D

Test Point	Avg. Mass Density (kg/m^3)	Avg. Surface Wave[1] Velocity (m/s)	PSPA Modulus (GPa)
1	2331	1630	19.0
1	2331	1639	19.2
1	2331	1638	19.1
2	2331	1698	20.6
2	2331	1637	19.1
2	2331	1632	19.0
3	2331	1629	18.9
3	2331	1638	19.1
3	2331	1640	19.2
4	2331	1572	17.6
4	2331	1576	17.7
5	2331	1606	18.4
5	2331	1608	18.4
5	2331	1609	18.5
6	2331	1583	17.9
6	2331	1578	17.8
	Avg.:	**1620**	**18.7**

(1) Based on Frequency Domain Records

Table F1.4: ACP Model data - Mix Type D

Test Point	Avg. Mass Density (kg/m^3)	Avg. Surface Wave[1] Velocity (m/s)	PSPA Modulus (GPa)
1	2291	1646	19.0
1	2291	1649	19.1
1	2291	1648	19.0
2	2291	1591	17.7
2	2291	1600	17.9
2	2291	1621	18.4
3	2291	1657	19.2
3	2291	1677	19.7
4	2291	1627	18.6
4	2291	1648	19.0
4	2291	1598	17.9
4	2291	1589	17.7
5	2291	1645	19.0
5	2291	1659	19.3
5	2291	1640	18.9
5	2291	1613	18.2
	Avg.:	**1632**	**18.7**

(1) Based on Frequency Domain Records

Table F1.5: ACP Model data- Mix Type B

Test Point	Avg. Mass Density (kg/m^3)	Avg. Surface Wave[1] Velocity (m/s)	PSPA Modulus (GPa)
1	2308	1570	17.6
1	2308	1567	17.6
1	2308	1568	17.6
1	2308	1557	17.3
2	2353	1604	18.8
2	2353	1602	18.7
2	2353	1597	18.6
2	2353	1598	18.6
3	2375	1636	19.7
3	2375	1631	19.6
3	2375	1637	19.7
3	2375	1641	19.8
4	2376	1723	21.9
4	2376	1712	21.6
4	2376	1707	21.5
4	2376	1706	21.4
5	2341	1687	20.7
5	2341	1686	20.6
5	2341	1696	20.9
5	2341	1697	20.9
6	2369	1736	22.1
6	2369	1727	21.9
6	2369	1730	22.0
6	2369	1729	22.0
Avg.:		**1656**	**20.0**

(1) Based on Frequency Domain Records

Table F1.6: ACP Model data- Mix Type B

Test Point	Avg. Mass Density (kg/m^3)	Avg. Surface Wave[1] Velocity (m/s)	PSPA Modulus (GPa)
7	2371	1705	21.4
7	2371	1703	21.3
7	2371	1708	21.4
7	2371	1709	21.5
8	2371	1697	21.2
8	2371	1686	20.9
8	2371	1711	21.5
8	2371	1710	21.5
9	2374	1723	21.8
9	2374	1725	21.9
9	2374	1728	22.0
9	2374	1735	22.2
10	2375	1691	21.1
10	2375	1694	21.1
10	2375	1689	21.0
10	2375	1692	21.1
11	2375	1662	20.3
11	2375	1671	20.6
11	2375	1674	20.6
11	2375	1673	20.6
Avg.:		**1699**	**21.2**

(1) Based on Frequency Domain Records

Table F1.7: ACP Model data- Mix Type B (Layer Thickness 170 mm)

Test Point	Avg. Mass Density (kg/m^3)	Avg. Surface Wave[1] Velocity (m/s)	PSPA Modulus (GPa)
1	2308	1490	15.8
1	2308	1488	15.7
1	2308	1501	16.0
1	2308	1496	15.9
2	2353	1697	20.9
2	2353	1695	20.8
2	2353	1711	21.2
2	2353	1712	21.2
3	2375	1606	18.9
3	2375	1601	18.7
3	2375	1610	19.0
3	2375	1617	19.1
4	2376	1640	19.7
4	2376	1631	19.5
4	2376	1643	19.8
4	2376	1637	19.6
5	2341	1582	18.0
5	2341	1582	18.0
5	2341	1581	18.0
5	2341	1587	18.2
6	2369	1657	20.0
6	2369	1664	20.2
6	2369	1651	19.9
6	2369	1650	19.9
Avg.:		**1614**	**18.9**

(1) Based on Frequency Domain Records

Table F1.8: ACP Model data- Mix Type B (Layer Thickness 170 mm)

Test Point	Avg. Mass Density (kg/m^3)	Avg. Surface Wave[1] Velocity (m/s)	PSPA Modulus (GPa)
7	2371	1673	20.4
7	2371	1662	20.2
7	2371	1699	21.1
7	2371	1667	20.3
8	2371	1661	20.1
8	2371	1674	20.5
8	2371	1669	20.3
8	2371	1674	20.5
9	2374	1532	17.2
9	2374	1503	16.5
9	2374	1519	16.9
9	2374	1542	17.4
10	2375	1653	20.0
10	2375	1673	20.5
10	2375	1692	20.9
10	2375	1666	20.3
11	2375	1678	20.6
11	2375	1686	20.8
11	2375	1674	20.5
11	2375	1670	20.4
Avg.:		**1643**	**19.8**

(1) Based on Frequency Domain Records

Table F1.9: ACP Model data- Mix Type D (Layer Thickness 150 mm)

Test Point	Avg. Mass Density (kg/m^3)	Avg. Surface Wave[1] Velocity (m/s)	PSPA Modulus (GPa)
1	2211	1326	12.1
1	2211	1342	12.4
1	2211	1320	12.0
1	2211	1292	11.5
1	2211	1277	11.2
1	2211	1254	10.8
1	2211	1283	11.4
2	2212	1251	10.8
2	2212	1252	10.8
2	2212	1251	10.8
2	2212	1304	11.7
2	2212	1239	10.6
2	2212	1243	10.7
2	2212	1244	10.7
3	2176	1346	12.3
3	2176	1201	9.8
3	2176	1208	9.9
3	2176	1211	10.0
3	2176	1201	9.8
3	2176	1201	9.8
3	2176	1142	8.9
3	2176	1180	9.5
4	2206	1307	11.8
4	2206	1301	11.6
4	2206	1309	11.8
4	2206	1307	11.8
5	2239	1253	11.0
5	2239	1260	11.1
5	2239	1233	10.6
5	2239	1278	11.4
5	2239	1253	11.0
5	2239	1247	10.9
5	2239	1267	11.2
6	2163	1234	10.3
6	2163	1246	10.5
6	2163	1246	10.5
6	2163	1246	10.5
6	2163	1214	9.9
6	2163	1176	9.3
6	2163	1184	9.5
Avg.:		**1253**	**10.8**

(1) Based on Frequency Domain Records

Table F1.10: ACP Model data- Mix Type D (Layer Thickness 150 mm)

Test Point	Avg. Mass Density (kg/m^3)	Avg. Surface Wave[1] Velocity (m/s)	PSPA Modulus (GPa)
7	2203	1244	10.6
7	2203	1283	11.3
7	2203	1279	11.2
7	2203	1277	11.2
7	2203	1278	11.2
7	2203	1232	10.4
7	2203	1182	9.6
7	2203	1189	9.7
7	2203	1187	9.7
7	2203	1191	9.7
7	2203	1293	11.5
7	2203	1284	11.3
7	2203	1288	11.4
7	2203	1292	11.5
7	2203	1298	11.6
7	2203	1308	11.8
7	2203	1308	11.8
7	2203	1331	12.2
7	2203	1293	11.5
7	2203	1253	10.8
7	2203	1254	10.8
7	2203	1266	11.0
7	2203	1285	11.3
7	2203	1256	10.8
7	2203	1258	10.9
7	2203	1261	10.9
7	2203	1258	10.9
Avg.:		**1264**	**11.0**

(1) Based on Frequency Domain Records

Table F1.11: ACP Model data- Mix Type D (Layer Thickness 150 mm)

Test Point	Avg. Mass Density (kg/m^3)	Avg. Surface Wave[1] Velocity (m/s)	PSPA Modulus (GPa)
8	2171	1259	10.7
8	2171	1254	10.7
8	2171	1245	10.5
8	2171	1246	10.5
9	2198	1309	11.8
9	2198	1297	11.5
9	2198	1237	10.5
9	2198	1230	10.4
9	2198	1160	9.2
9	2198	1176	9.5
10	2209	1217	10.2
10	2209	1218	10.2
10	2209	1214	10.2
10	2209	1215	10.2
11	2160	1113	8.3
11	2160	1109	8.3
11	2160	1068	7.7
11	2160	1068	7.7
12	2198	1187	9.7
12	2198	1188	9.7
12	2198	1187	9.7
12	2198	1209	10.0
12	2198	1259	10.9
12	2198	1246	10.6
12	2198	1233	10.4
12	2198	1268	11.0
12	2198	1280	11.2
12	2198	1280	11.2
12	2198	1281	11.3
12	2198	1280	11.2
13	2155	1025	7.1
13	2155	1024	7.1
13	2155	1146	8.8
13	2155	1153	8.9
13	2155	1153	8.9
13	2155	1154	9.0
Avg.:		**1200**	**9.9**

(1) Based on Frequency Domain Records

F2) Pavement Model Core Data

Table F2.1: ACP Model Core data

Material El Paso **Mix Type:** **D**

Core No.	Avg. Diam. (mm)	Avg. Length (mm)	Mass Density (kg/m^3)	Air Voids (%)	V-Meter		
					Travel Time (micro-sec.)	Velocity (m/s)	Young's Modulus (GPa)
1	97	73	2124	12.4	22.6	3211	14.8
2	97	69	2209	10.0	21.8	3172	15.0
3	79	70	2171	11.6	22.0	3184	14.8
4	79	73	2195	11.2	23.5	3121	14.4
5	79	69	2183	12.1	23.8	2886	12.3

Table F2.2: ACP Model Core data

Material El Paso **Mix Type:** **C**

Core No.	Avg. Diam. (mm)	Avg. Length (mm)	Mass Density (kg/m^3)	Air Voids (%)	V-Meter		
					Travel Time (micro-sec.)	Velocity (m/s)	Young's Modulus (GPa)
1	97	66	2229	9.0	18.3	3629	20.5
2	97	69	2205	9.5	19.4	3554	19.4
3	79	59	2254	10.1	19.0	3104	15.2
4	79	66	2214	9.8	21.8	3032	14.2
5	79	68	2172	11.8	24.0	2838	12.2

Table F2.3: ACP Model Core data

Material El Paso **Mix Type:** **D**

Core No.	Avg. Diam. (mm)	Avg. Length (mm)	Mass Density (kg/m^3)	Air Voids (%)	V-Meter		
					Travel Time (micro-sec.)	Velocity (m/s)	Young's Modulus (GPa)
1	97	68	2314	5.8	19.0	3573	19.9
2	97	65	2315	6.0	18.8	3482	18.9
3	97	67	2281	6.3	19.3	3455	18.4
4	79	69	2367	5.5	21.1	3290	17.3
5	79	66	2340	5.4	18.5	3591	20.3
6	79	69	2369	4.7	20.0	3453	19.0

Table F2.4: ACP Model Core data

Material El Paso **Mix Type** **D**

Core No.	Avg. Diam. (mm)	Avg. Length (mm)	Mass Density (kg/m^3)	Air Voids (%)	V-Meter		
					Travel Time (micro-sec.)	Velocity (m/s)	Young's Modulus (GPa)
1	97	46	2438	6.3	13.0	3565	20.9
2	97	50	2168	5.6	13.6	3645	19.4
3	79	51	2274	7.4	14.2	3582	19.7
4	79	55	2289	7.0	16.0	3436	18.2
5	79	56	2283	7.0	16.8	3321	17.0

Table F2.5: ACP Model Core data

Material El Paso **Mix Type** **B**

Core No.	Avg. Diam. (mm)	Avg. Length (mm)	Mass Density (kg/m^3)	Air Voids (%)	V-Meter		
					Travel Time (micro-sec.)	Velocity (m/s)	Young's Modulus (GPa)
1	79	174	2308	4.8	52.2	3333	16.0
2	79	174	2353	3.88	51.7	3356	16.5
3	79	173	2375	3.19	50.6	3419	17.3
4	79	170	2376	3.36	48.6	3502	18.2
5	79	180	2341	3.92	50.3	3569	18.6
6	79	177	2369	3.43	52.6	3365	16.7
7	79	175	2371	3.54	50.3	3469	17.8
8	79	174	2371	3.23	49.8	3494	18.0
9	79	178	2374	3.50	52.1	3407	17.2
10	79	175	2375	3.28	50.5	3455	17.7
11	79	174	2375	3.71	49.4	3512	18.2

Table F2.6: ACP Model Core data

Material El Paso **Mix Type** **D**

Core No.	Avg. Diam. (mm)	Avg. Length (mm)	Mass Density (kg/m^3)	Air Voids (%)	V-Meter		
					Travel Time (micro-sec.)	Velocity (m/s)	Young's Modulus (GPa)
1	79	143	2211	4.9	53.6	2660	8.4
2	79	156	2212	4.10	53.0	2943	10.2
3	79	135	2176	4.80	45.4	2978	10.3
4	79	155	2206	4.60	51.2	3027	10.8
5	79	140	2239	3.30	46.6	3004	10.8
6	79	160	2163	5.90	55.8	2867	9.5
7	79	164	2203	4.40	53.4	3071	11.1
8	79	147	2171	5.10	49.8	2952	10.1
9	79	144	2198	4.70	47.3	3034	10.8
10	79	144	2209	4.40	49.7	2897	9.9
11	79	144	2160	5.00	51.1	2808	9.1
12	79	150	2198	4.70	49.3	3043	10.9
13	79	141	2155	4.70	49.6	2833	9.2

Table F2.7: ACP Model Core data (Top and Bottom Cores)

Material El Paso **Mix Type** **D**

Core No.	Avg. Diam. (mm)	Avg. Length (mm)	Mass Density (kg/m^3)	Air Voids (%)	V-Meter		
					Travel Time (micro-sec.)	Velocity (m/s)	Young's Modulus (GPa)
1B[(1)]	79	60	2203	4.37	22.6	2654	8.3
2B	79	77	2220	3.61	25.4	3016	10.8
3B	79	64	2155	6.18	20.5	3124	11.2
4B	79	72	2209	4.53	23.7	3021	10.8
5B	79	66	2237	3.91	24.1	2735	8.9
6B	79	61	2141	6.15	21.6	2840	9.2
7B	79	78	2225	3.97	24.3	3214	12.3
8B	79	65	2148	5.68	22.7	2877	9.5
9B	79	60	2208	5.16	20.7	2902	9.9
10B	79	67	2193	4.76	25.0	2694	8.5
11B	79	67	2124	6.70	25.7	2607	7.7
12B	79	66	2175	4.69	21.6	3061	10.9
13B	79	65	2132	6.08	27.6	2351	6.3
1T[(2)]	79	81	2177	5.92	26.9	3002	10.5
2T	79	76	2187	6.26	25.3	3011	10.6
3T	79	67	2184	5.94	20.8	3244	12.3
4T	79	81	2180	5.36	24.5	3287	12.6
5T	79	71	2224	4.71	21.3	3313	13.0
6T	79	96	2156	6.62	30.4	3159	11.5
7T	79	83	2166	6.58	25.4	3249	12.2
8T	79	79	2183	5.76	23.9	3299	12.7
9T	79	80	2177	7.17	25.3	3174	11.7
10T	79	74	2186	5.24	22.6	3280	12.6
11T	79	73	2189	5.74	24.2	3020	10.7
12T	79	81	2207	5.74	24.3	3325	13.0
13T	79	72	2191	5.85	22.4	3208	12.0

(1) Bottom Core
(2) Top Core

F3) Case Study Data

Table F3.1: Doniphan ACP Core data

Core No.	Avg. Diam. (mm)	Avg. Length (mm)	Mass Density (kg/m^3)	Air Voids (%)	V-Meter		
					Travel Time (micro-sec.)	Velocity (m/s)	Young's Modulus (GPa)
1A	108	85	2178	10.1	24.7	3441	16.7
1B	108	88	2193	9.7	27.0	3259	15.1
2A	108	71	2255	8.0	19.4	3660	17.1
2B	108	68	2282	7.7	17.9	3799	18.6
3A	108	78	2245	9.1	21.6	3611	19.8
3B	108	83	2209	9.8	23.4	3547	18.8
4A	108	52	2122	7.9	15.2	3421	16.1
4B	108	68	2179	9.2	19.4	3505	17.4

Table F3.2: Doniphan Road-PSPA data

Test Point	Surface Temp (C^0)	Air Temp (C^0)	Avg. Density (kg/m^3)	Average Surface Wave Velocity (m/s)	PSPA Modulus (GPa)
1	23	19	2186	1574	16.6
1	23	19	2186	1637	18.0
1	23	19	2186	1625	17.7
1	23	19	2186	1618	17.6
2	23	18	2269	1529	16.5
2	23	18	2269	1526	16.5
2	23	18	2269	1512	16.1
3	22	15	2227	1663	18.9
3	22	15	2227	1656	18.7
3	22	15	2227	1628	18.1
4	24	19	2151	1617	17.3
4	24	19	2151	1628	17.5
4	24	19	2151	1663	18.3
4	24	19	2151	1677	18.6

(1) Based on Frequency Domain Records

Table F3.3: Odessa Mix Gradation

Sieve Number	Sieve Opening (mm)	Weight Retaine (gm)	Percent Retained (%)	Cumulativ % Retaine (%)	(% Passing) (Org. Soil) (%)
1/2"	12.700	3.50	0.40	0.40	99.60
3/8"	9.525	85.75	9.80	10.20	89.80
No. 4	4.760	248.50	28.40	38.60	61.40
No. 10	2.000	228.38	26.10	64.70	35.30
No. 40	0.420	126.00	14.40	79.10	20.90
No. 80	0.180	71.75	8.20	87.30	12.70
No. 200	0.074	70.88	8.10	95.40	4.60
Pan	....	40.25	4.60	100.00	0.00
Total		875.01			
Optimum Asphalt Content					5.4%

Figure F3.1: Odessa Mix Design Gradation

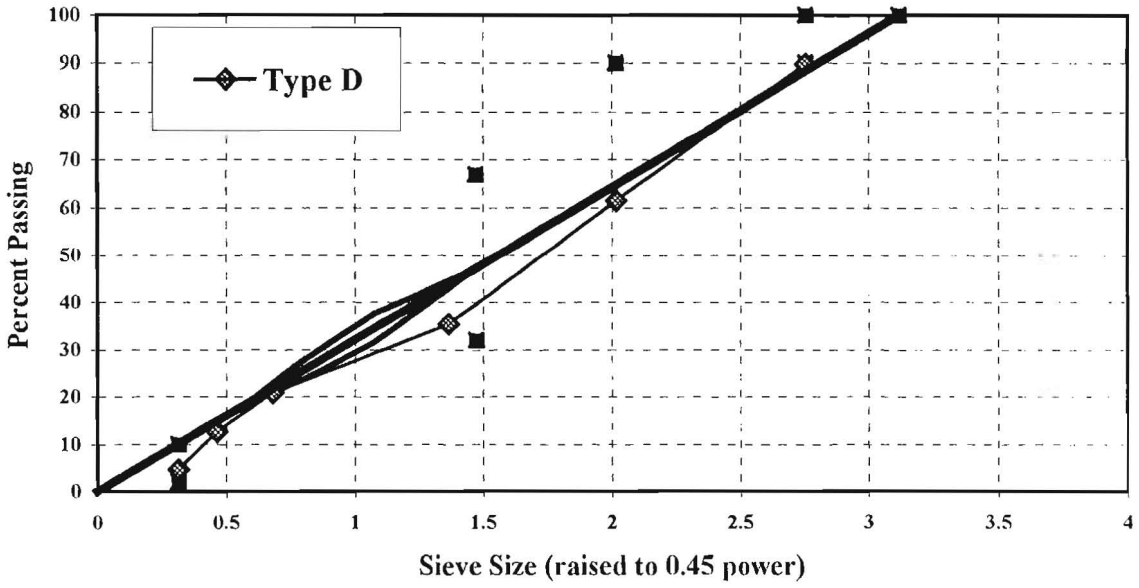

Table F3.4: Variation in Modulus with VTM for Odessa Mix

Material	Odessa			Mix Type:	D			
						V-Meter		
Briquette No.	Gyrations	Avg. Diam. (mm)	Avg. Length (mm)	Mass Density (kg/m^3)	Air Voids (%)	Travel Time (micro-sec.)	Velocity (m/s)	Young's Modulus (GPa)
1	5	100	112	1991	10.9	38.3	2921	11.5
2	5	100	113	1964	10.2	38.4	2942	11.5
3	10	100	111	2014	9.9	35.7	3096	13.0
4	10	100	110	2016	9.7	35.8	3084	12.9
5	15	100	107	2071	7.6	33.5	3207	14.4
6	15	100	109	2051	7.9	33.6	3229	14.4
7	20	100	107	2086	7.1	33.7	3167	14.1
8	20	100	107	2082	8.0	33.2	3219	14.6
9	25	100	105	2120	6.2	32.5	3231	14.9
10	25	100	106	2097	6.8	32.6	3257	15.0
11	30	100	106	2100	6.5	30.8	3444	16.8
12	30	100	106	2107	5.8	31.2	3385	16.3
13	35	100	104	2140	5.4	30.0	3470	17.4
14	35	100	105	2120	6.5	31.0	3382	16.4

Table F3.5: Odessa Cores data

Material	Odessa			Mix Type:	D		
					V-Meter		
Test Point	Avg. Diam. (mm)	Avg. Length (mm)	Mass Density (kg/m^3)	Air Voids (%)	Travel Time (micro-sec.)	Velocity (m/s)	Young's Modulus (GPa)
1	97	50	2103	6.30	14.6	3390	16.3
5	97	46	2125	7.40	14.3	3238	15.0
10	97	54	2146	5.10	16.1	3354	16.3
15	97	51	2109	6.90	16.4	3130	13.9
20	97	52	2063	7.60	16.5	3152	13.8
25	97	48	2149	7.20	14.9	3221	15.1
30	97	50	2160	6.00	15.1	3311	16.0

Table F3.6: Odessa Road PSPA data

Test Point	Distance (meters)	Surface Temp. Co	Average Density (kg/m3)	Surface Wave Velocity (m/sec)	PSPA Modulus (GPa)
1	0.0	11.7	2200	1577	14.3
2	1.5	11.7	2200	1646	15.5
3	3.0	11.7	2200	1652	15.6
4	4.6	11.7	2200	1588	14.5
5	6.1	11.7	2200	1576	14.2
6	7.6	11.7	2200	1557	13.9
7	9.1	11.7	2200	1595	14.6
8	10.7	11.7	2200	1612	14.9
9	12.2	11.7	2200	1594	14.6
10	13.7	11.7	2200	1605	14.8
11	15.2	11.7	2200	1647	15.5
12	16.8	11.7	2200	1629	15.2
13	18.3	12.2	2200	1622	15.2
14	19.8	12.2	2200	1585	14.5
15	21.3	12.2	2200	1537	13.6
16	22.9	12.2	2200	1532	13.5
17	24.4	12.2	2200	1537	13.6
18	25.9	12.2	2200	1540	13.7
19	27.4	12.2	2200	1442	12.0
20	29.0	12.8	2200	1372	10.9
21	30.5	12.8	2200	1278	9.5
22	32.0	12.8	2200	1312	10.0
23	33.5	12.8	2200	1368	10.9
24	35.1	12.8	2200	1250	9.1
25	36.6	12.8	2200	1469	12.5
26	38.1	10.0	2200	1605	14.5
27	39.6	10.0	2200	1581	14.0
28	41.1	9.4	2200	1588	14.1
29	42.7	9.4	2200	1612	14.5
30	44.2	8.9	2200	1663	15.3